Charles University

Faculty of Science

Immunology

Mgr. Barbora Tomalová

Anti-tumor activity and toxicity of HPMA-copolymer conjugates bearing cytostatic drug

Protinádorová aktivita a toxicita konjugátů na bázi HPMA kopolymerů nesoucí cytostatikum

Doctoral Thesis

Supervisor: RNDr. Marek Kovář, PhD.

Prague, 2018

Prohlášení

Prohlašuji, že jsem závěrečnou práci zpracovala samostatně a že jsem uvedla všechny použité informační zdroje a literaturu. Táto práce ani žádná její podstatná část nebyla předložena k získání jiného nebo stejného akademického titulu.

V Praze.....

Podpis

Declaration

I declare that I prepared this thesis solely on my own with all information sources and literature cited. I did not use either this thesis or its substantial part as a background to obtain another or equivalent academic degree.

Prague.....

Signature

I would like to express my gratitude to my supervisor RNDr. Marek Kovář, PhD. for help and advice he offered during my PhD studies. My sincere thanks belong to my colleagues Pavlína Jungrová and Helena Mišurcová from Laboratory of Tumor Immunology at the Institute of Microbiology for their help and support. Special thanks to my husband RNDr. Jakub Tomala, PhD., for reading the manuscript. This work would not be possible without his endless support, encouragement and advice.

Last but not least, I would like to thank my colleagues from the Laboratory of Biomedicinal Polymers at the Institute of Macromolecular Chemistry, whose cooperation, development of polymer prodrug structures and professional expertise were essential for realization of this study.

TABLE OF CONTENTS

LIST OF ABBREVIATIONS

38C13	muse B-cell lymphoma
B16-F10	mouse skin melanoma
BCL1	mouse B-cell leukemia
DOX	doxorubicin
DOX^{AM}-PHPMA	HPMA copolymer-bound conjugate bearing DOX bound via amide bond
DOX^{AM}-PHPMA-galactosamine	HPMA copolymer-bound conjugate bearing DOX bound via amide bond and containing galactosamine
DOX^{HYD}-PHPMA	HPMA copolymer-bound conjugate bearing DOX bound via hydrazone bond
DTX	docetaxel
EKE	$(VAALEKE)_4$
EL4	mouse T-cell lymphoma cell line
EPR	Enhanced Permeability and Retention
ESE	$(IAALESE)_2$-IAALESKIAALESE
GFLG	glycine-phenylalanine-leucine-glycine
HMW	high-molecular weight
HPMA	*N*-(2-hydroxypropyl)methacrylamide
HSA	human serum albumin
HuIg	human immunoglobulin
KEK	$(VAALKEK)_4$
KSK	IAALKSKIAALKSE-$(IAALKSK)_2$
L-1210	murine skin lymphocytic leukemia
LMW	low-molecular weight
M5076	mouse ovarian reticulosarcoma
mAb	monoclonal antibody
MDR	multidrug resistance
MRI	magnetic resonance imaging
MTD	maximum tolerated dose
M_w	molecular weight
NK	natural killer

NSCLC ..... non-small cell lung carcinoma
OA-3 ..... ovarian carcinoma antigen
OVCAR-3 ..... human ovarian cancer cell line
P388 ..... mouse monocyte/macrophage lymphoma
PAMAM ..... polyamidoamine
PBS ..... phosphate buffered saline
PHPMA ..... polyHPMA
PK ..... Prague-Kiel
PNA ..... peanut agglutinin
R_h ..... hydrodynamic radius
scFv ..... single chain fragment variable
Treg ..... regulatory T
VEGF ..... vascular endothelial growth factor
WGA ..... wheat germ agglutinin

ABSTRACT

In this study, we addressed the biological activity and pharmacological features of selected HPMA copolymer-based drug conjugates. We determined their cytostatic activity *in vitro* as well as toxicity *in vivo* and therapeutic effcicacy in mouse tumor models. Assessment of maximum tolerated dose (MTD) of two structurally different HPMA copolymer-based conjugates bearing doxorubicin (DOX) attached via pH-sensitive hydrazon bond (HPMA-DOX^{HYD}) showed that high molecular weight non-degradable star HPMA-DOX^{HYD} conjugate possesses relatively low MTD ~22.5 mg DOX/kg, while linear HPMA-DOX^{HYD} has MTD ~85 mg DOX/kg. Thus, MTD of linear conjugate is 3.7 times higher than that of the star conjugate. Subsequently, we reported that linear conjugate proved to be more efficient in case of treatment of solid tumor EL4 lymphoma and star conjugate to be superior in case of BCL1 leukemia treatment. We also compared biological activity of star and linear HPMA copolymer-based conjugates bearing docetaxel (DTX) attached via pH-sensitive hydrazon bond (HPMA-DTX^{HYD}). MTD of star conjugate (~160 mg DTX/kg) was proved to be 4 times higher than MTD od free DTX (40 mg/kg). We were not able to determine MTD of linear conjugate as it exceeded 200 mg DTX/kg (the highest soluble dose we were able to administer as a bolus). Anti-tumor activity of both conjugates was tested in EL4 lymphoma and they proved to be superior to free DTX given at the same dose, with star conjugate to be more potent than the linear one.

Further, we have investigated binding and therapeutic activity of targeted conjugate composed of HPMA copolymer bearing pirarubicin and recombinant scFv fragment derived from BCL1 leukemia-specific B1 mAb non-covalently attached to conjugate via coiled-coil interaction of two complementary peptides $(VAALKEK)_4$/$(VAALEKE)_4$ or IAALKSKIAALKSE-$(IAALKSK)_2$/$(IAALESE)_2$-IAALESKIAALESE (abbreviated KEK/EKE or KSK/ESE, respectively). We proved that targeted conjugate exerts higher anti-tumor efficacy than non-targeted conjugate or free pirarubicin. Moreover, we compared two different pairs of complementary peptides and we showed that conjugate containing KSK and ESE peptides exerts 4 times better binding activity and 2 times higher cytotoxicity *in vitro* compared to conjugate containing KEK and EKE peptides.

In conclusion, our findings shed a light on relationship of HPMA copolymer-based drug conjugates structure and their biological and pharmacological activities. These findings might be useful in design of novel anti-cancer HMW therapeutics not only those based on HPMA copolymer.

ABSTRAKT

V této studii jsme se zaměřili na testování biologické aktivity a farmakologických vlastností vybraných konjugátů na bázi HPMA kopolymerů nesoucí léčivo. Určili jsme jejich cytostatickou aktivitu *in vitro*, toxicitu *in vivo* a terapeutický efekt v myších nádorových modelech. Porovnáním maximální tolerované dávky (MTD) dvou strukturně odlišných konjugátů na bázi HPMA kopolymerů nesoucích doxorubicin (DOX) vázaný pH senzitivní hydrazonovou vazbou (HPMA-DOX^{HYD}) jsme prokázali, že vysokomolekulární nedegradovatelný hvězdicový HPMA-DOX^{HYD} konjugát má relativně nízkou MTD, přibližně 22,5 mg DOX/kg, zatímco lineární HPMA-DOX^{HYD} konjugát má MTD okolo 85 mg DOX/kg. Lineární konjugát má tedy 3,7krát vyšší MTD než hvězdicový. Následně jsme také ukázali, že lineární konjugát je účinnější při léčbě solidního EL4 lymfomu zatímco hvězdicový konjugát jej předčil v léčbě BCL1 leukémie. Porovnali jsme také biologickou aktivitu hvězdicového a lineárního HPMA kopolymeru nesoucího docetaxel (DTX) vázaný pH senzitivní hydrazonovou vazbou (HPMA-DTX^{HYD}). MTD hvězdicového (~160 mg DOX/kg) byla 4krát vyšší než MTD volného DTX (40 mg/kg). MTD lineárního HPMA-DTX^{HYD} konjugátu jsme nebyli schopni určit, jelikož převyšovala dávku 200 mg DTX/kg, což bylo nejvyšší množství, které jsme byli schopni podat jako bolus. Protinádorovou aktivitu jsme testovali na modelu lymfomu EL4 a oba konjugáty byly účinnější než volné léčivo s tím, že hvězdicový konjugát předčil konjugát lineární.

Mimoto jsme se také zabývali výzkumem vazebné a terapeutické aktivity směrovaného konjugátu skládajícího se z HPMA kopolymeru nesoucího pirarubicin a rekombinantní scFv fragment B1 protilátky rozpoznávající buňky BCL1 leukemie nekovalentně navázaného na konjugát prostřednictvím interakce mezi dvěma komplementárními peptidy $(VAALKEK)_4$/$(VAALEKE)_4$ nebo IAALKSKIAALKSE-$(IAALKSK)_2$/$(IAALESE)_2$-IAALESKIAALESE (zkráceně KSK/ESE nebo KEK/EKE). Prokázali jsme, že směrovaný konjugát vykazuje vyšší protinádorovou aktivitu než nesměrovaný konjugát, respektive volný pirarubicin. Porovnali jsme dva odlišné páry komplementárních peptidů a zjistili jsme, že konjugát nesoucí KSK a ESE peptidy vykazuje 4krát lepší vazebnou aktivitu a 2krát vyšší cytotoxicitu *in vitro* než konjugát obsahující KEK a EKE peptidy.

Naše výsledky objasňují vztah struktury, biologických a farmakologických vlastností konjugátů na bázi HPMA kopolymeru a mohou být aplikované pro další výzkum a vývoj nových protinádorových vysokomolekulárních léčiv nejen na bázi HPMA kopolymeru.

I. INTRODUCTION

There have always been serious restrictions and limitations when it comes to classical tumor treatment via chemotherapy. This is mainly due to the severe side-effects and toxicity associated with high doses of low-molecular weight (LMW) drugs used during the standard chemotherapy [1, 2]. Another problem is their profound immunosupressivity that affects patient's immune system, leaving it hampered and unable to respond to subsequent immunotherapeutic interventions. Last, but not least, variety of cancers, e.g. ovarian, lung or breast cancers, is able to develop multidrug resistance (MDR) to LMW therapeutics.

The idea of site-specific targeting of therapeutic agent to the site of pathology originates from Paul Erlich´s "Magic bullet" idea [3]. Later on, Helmut Ringsdorf proposed an idea to use polymers either of synthetic or natural origin as carriers of biologically active compounds [4]. The agent is transported in its inactive form right into the tumor site where it is released in its pharmaceutically active form. This strategy seems to be very promising and there have been many delivery systems designed ever since. Such high-molecular weight (HMW) drug conjugates possess anti-tumor activity of the selected drug usually with significantly lowered side-toxicity together with markedly improved pharmacokinetics over the respective free drug [1, 5]. There are various drug delivery systems, however, those based on *N*-(2-hydroxypropyl)methacrylamide (HPMA) copolymer are among most intensively studied ones, since they possess extremely favorable properties including bio- and immunocompatibily, and therefore present one of the most promising drug carriers [2, 6-8].

I.1. LOW-MOLECULAR WEIGHT DRUGS IN CANCER TREATMENT

LMW drugs have been used in clinical practice for many years [9]. They are of quite different type and origin and their mechanism of action is diverse – they can inhibit cell proliferation, induce apoptosis or hamper tumor neoangiogenesis. Nevertheless, their use is accompanied by adverse effects since the LMW drugs have quite narrow therapeutic window and their mechanism of action leads to destruction of rapidly dividing cells. This covers not only tumor cells but also cells of common origin, such as hair follicles or bone marrow cells. Immunosuppressivity of many LMW drugs is another downside that needed to be dealt with.

Moreover, mostly hydrophobic character of LMW drugs makes their administration and bioavailability very diffucult. It is not unusual for them to be administered in special solutions on the oil basis employing emulsifiers that exert severe adverse side-effects (e.g. combination of ethanol and Cremophor EL) [10, 11]. These solvents can not only cause additional normal tissue damage but also hamper the drug effectivity.

All these issues led to an investigation of how to modify LMW drugs in order to improve their pharmacokinetics, solubility, stability, pharmacodistribution, or to establish stimulus-controlled long-term release. Many various drug delivery systems have been designed, employing encapsulation of the drug into bio- and immunocompatible structures or covalent or physical attachment of the drug to the specifically developed HMW carrier. Immunomodulants, proteins, anti-inflammatory drugs, multidrug resistance inhibitors and cytostatic drugs can all be found among frequently used molecules for attachment to HMW carrier, some of which are listed in Table 1.

Load	Mechanism of action	Examples	Toxicity
Anthracycline antibiotics	DNA intercalation, interaction with DNA-binding proteins, induction of apoptosis	doxorubicin, daunorubicin, epirubicin	cardiomyopathy, febrile neutropenia
Taxanes	interference with microtubule disassembly (inhibition of cell division, induction of cell death), anti-angiogenic effects	paclitaxel, docetaxel	neurotoxicity, neuropathy, neutropenia, alopecia, hypersensitivity reactions, arthralgia, myalgia
Vinca alkaloids	microtubule disrupting agents (inhibition of cell division, induction of cell death), anti-angiogenic effects	vinblastine, vinorelbine, vincristine, vindesine	neurotoxicity, bone marrow suppression, gastrointestinal toxicity
Alkylating agents	cell-cycle non-specific agents, bind negatively charged residues in DNA and disrupt DNA replication	nitrogen mustards (e.g. cyclophosphamide), alkyl sulfonates, triazines, nitrosoureas, ethylenimines, platinates (e.g. *cis*-platin, oxaliplatin)	carcinogenesis, cause permanent infertility, hematotoxicity, immunosuppression
Antimetabolites	intereference with nucleid acid synthesis	pyrimidine compounds (e.g. 5-fluorouracil), purine compounds (e.g.fludarabine), folate antagonists (e.g.methotrexate and its derivatives)	myelosuppression, mucositis, dermatitis, renal dysfunction
Topoisomerase I inhibitors	block actions of topoisomerase I – DNA cleavage stimulation, generation of DNA lesions	camptothecin	myelosuppression, neutropenia, gastrointestinal toxicity
Topoisomerase II inhibitors	block actions of topoisomerase II- DNA cleavage stimulation	etoposide	myelosuppression, gastrointestinal toxicity, cardiotoxicity, carcinogenesis

Table 1: Selected LMW drugs frequently attached to HMW carriers and their properties.

I.2. MACROMOLECULAR THERAPEUTICS

Nanotherapeutics, macromolecular carrier-drug conjugates with hydrodynamic radius (R_h) ranging from 1 to 100 nm, have been developed in an attempt to overcome obstacles and disadvantages of LMW drugs characterized, apart from other things, by poor water solubility, short circulation half-life and severe side-toxicities [12].

Variety of different drugs were bound to these carriers and exploited for diverse applications including diagnostics, magnetic resonance imaging (MRI) or therapy [13-20]. However, the most intensive research is focused on their use as platforms for anti-cancer therapeutics. Drugs can be attached either by covalent bond, or non-covalent interaction with HMW macromolecular carrier's surface, or entrapped inside the carrier's cavities. Conjugation of anti-cancer drug and HMW carrier enables drug's transport right into the tumor site in an inactive form without damaging normal cells and tissues due to the Enhanced Permeability and Retention effect (see I.2.1). There are many kinds of HMW drug delivery systems, some of which are depicted in Figure 1.

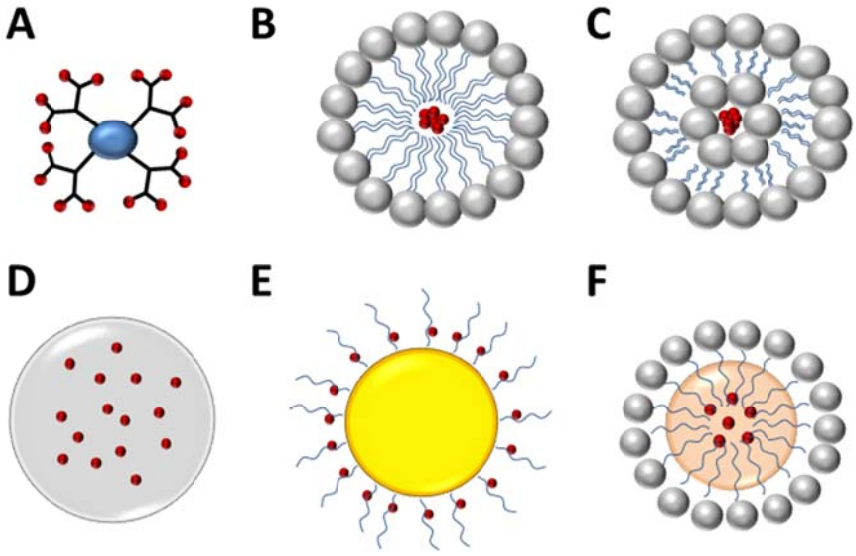

Figure 1: Simplified structures of the most frequent HMW drug delivery systems. A) Dendrimers, B) Micelles, C) Liposomes, D) Nanogels, E) Magnetic nanoparticles, F) Emulsions.

Attached drug is protected from rapid clearance, binding to serum proteins, enzymes and scavengers present in the circulation and thus its blood half-life is significantly prolonged. It allows administration of lower doses of drug and lead to significantly wider therapeutic window while resulting side-toxicity of HMW carrier-bound anti-cancer drug is significantly

reduced compared to the free drug [5]. The drug should remain bound to the carrier with minimal release in circulation during its transport. Only when the delivery system reaches specific destination and conditions, drug is released into its pharmacologicaly active form. This could be either in tumor extracellular microenvironment or directly inside the tumor cell. Drug release is controlled by various stimuli of internal (e.g. difference in pH or reduction potential between normal and tumor tissue) or external origin (e.g. hyperthermia, magnetic field, electric pulses or light) [21]. Drug release from the carrier is not necessary in applications like MRI or radiotherapy [22].

Multidrug resistance (MDR) is another disadvantage that is at least partially overcome by attachment of the drug to HMW carrier [23]. MDR is developed by variety of cancers and is based on adenosine triphosphate-dependent pump-mediated efflux of xenobiotics out of cancer cells. Normally, LMW drugs are rapidly pumped out of the MDR tumor cell since they enter the cell directly through the plasma membrane. HMW carrier-bound anti-cancer drug conjugates, on the contrary, enter the cell via endocytosis and possible elimination of the drug from the cell is therefore more complicated.

Two general mechanisms could be employed to deliver HMW conjugates into the tumor. Abnormal vascular architecture (i.e. “leaky endothelium”) of tumor tissue and its compromised lymphatic drainage enables extravasation from the bloodstream and retention of large macromolecules (up to several dozens of nm) in the tumor mass (see I.2.1.). The second mechanism relies on the use of specific targeting moieties selectively recognizing various cancer cell surface markers which enable site-specific drug delivery (see I.2.2.). For comparison of LMW drugs with HMW carrier-bound drugs see Table 2.

Feature	LMW drug	HMW carrier-bound drug	Advantages of HMW carrier-bound drug
Size	small	large	passive accumulation in tumor (see I.3.1)
Cell entry	direct, uncontrolled diffusion	facilitated endocytosis	partial bypass of multidrug resistance
Dosage	high, frequent	low	wider therapeutic window
Toxicity	high	low	wider therapeutic window
Half-life	short (<hours)	long (>hours, days)	better drug availability, lesser dosage
Solubility	mostly hydrophobic	hydrophilic	better drug availability and administration
Administration	special dissolving solution	dissolved in simple solutions like PBS	no admnistration-related toxicities

Table 2: Comparison of LMW drugs with HMW carrier bound drugs.

I.2.1. Passive accumulation of HMW drug delivery systems

HMW and considerable R_h of macromolecular carriers significantly influence biodistribution of attached drug(s) and allow HMW carrier-drug conjugate to exploit abnormal architecture of tumor tissue and passively accumulate in solid tumors [24, 25].

Rapidly growing tumors require increased amount of nutrients and oxygen [26, 27]. In order to compensate for that, tumors produce high levels of vascular endothelial growth factor (VEGF) and other angiogenic factors. Therefore, considerable angiogenesis takes place at tumor site, but the neovasculature of generated blood vessels is significantly different compared to normal tissues. The endothelial layer is defected, fenestrated with large pores up to several hundreds of nm [28, 29]. Tumor vessels can even lack small muscle cell layer usually formed around them [30]. Such discontinuous endothelium allows macromolecules (molecular weight ≥40kDa, R_h ~100 nm), which normally stay inside the circulation and cannot pass through normal vessels' endothelium, to extravasate into tumor site. It was proved that R_{hyd} of administered macromolecules should not exceed 30 nm since tumor tissue penetration by bigger particles is significantly lower [31]. Furthermore, tumor lymphatic system is very limited or even not present at all [32]. This leads to hampered clearance of accumulated macromolecules from tumor intersticium.

Thus, variety of HMW drug delivery systems can travel via blood stream without damaging normal tissues and due to the leaky endothelium of tumor vessels and poor

lymphatic drainage, they can accumulate inside the tumor and release here their anti-cancer drugs.

This generaly recognized phenomenon is called Enhanced Permeability and Retention (EPR; [24, 25]) effect and is valid for macromolecules, HMW drug conjugates or even particles up to the size of bacteria. However, it is highly variable and depends on size, rate of growth and type of solid tumor (e.g. experimental vs. spontaneous), presence of angiogenic regulators (e.g. nitric oxide) and other naturally occurring factors [33]. Level of EPR effect can vary even inside a single tumor mass as the architecture of vasculature in different areas of tumor is quite diverse. It was reported that EPR-mediated tumor accumulation of macromolecules is possitively correlated with the degree of tumor vascularization [31].

General principles of LMW drug biodistribution and EPR effect of macromolecules are shown in Figure 2.

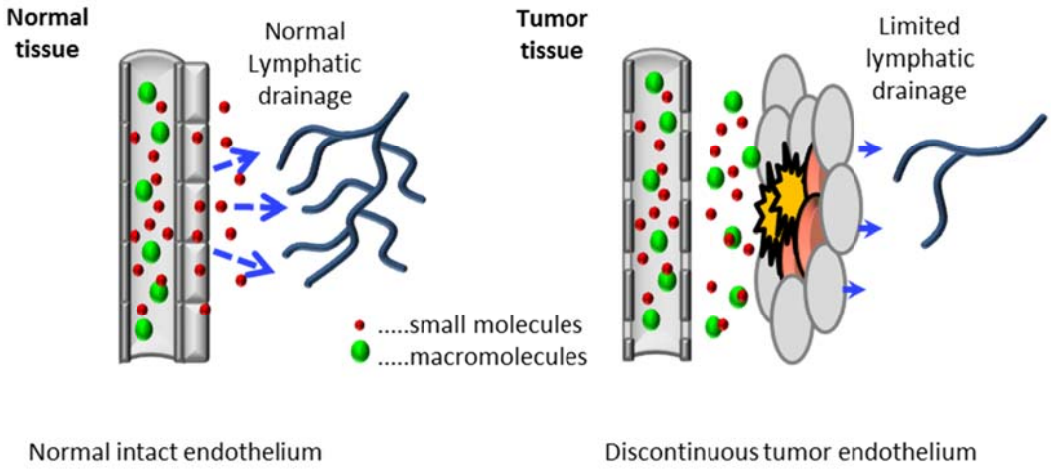

Figure 2: Schematic depiction of EPR effect. Comparison of macromolecule and small molecule penetreation through normal (left) and tumor (right) endothelium.

I.2.2. Active targeting of HMW drug delivery systems

In addition to passive accumulation of HMW drug delivery systems in tumors via EPR effect, these nanotherapeutics can be actively targeted to the tumor site by attachment of targeting moiety (Figure 3) specific for particular surface markers expressed solely or in very high density on cancer cells [34]. The most important in ligand-targeted therapy is precise selection of targeted surface structure, relevant high affinity targeting moiety and effective anti-cancer agent. Targeted structure should not be present as a soluble molecule in circulation or tumor environment in order to avoid its competition for targeting moiety with its surface counterpart. Moreover, the subsequent fate of generated ligand-targeting moiety complex and its relevance to the therapy should be considered, e.g. whether it needs to be

internalized or just stay on the cell surface to exert its anti-tumor actions. Drug requirements depend on selected model and also on the amount of molecules attached to the HMW carrier – the fewer molecules the higher anti-tumor activity of the drug is needed for effective therapy.

The most efficient and intensively studied targeting moieties are antibodies (mostly of IgG class) and their scFv fragments, since they exert high affinity and specificity for their ligands [35-37]. Unfortunately, there are very few tumor-specific antigens expressed solely on cancer cells and only some, that are overexpressed on tumors compared to normal cells so they can be used for antibody-mediated targeting of HMW drug delivery systems. There are also several non-antibody ligands (e.g. aptamers, transferrin or folate) whose targets are not exclusively expressed on cancer cell surface and are generally present on normal cells and in bloodstream as well which may cause unwanted side effects [38-40].

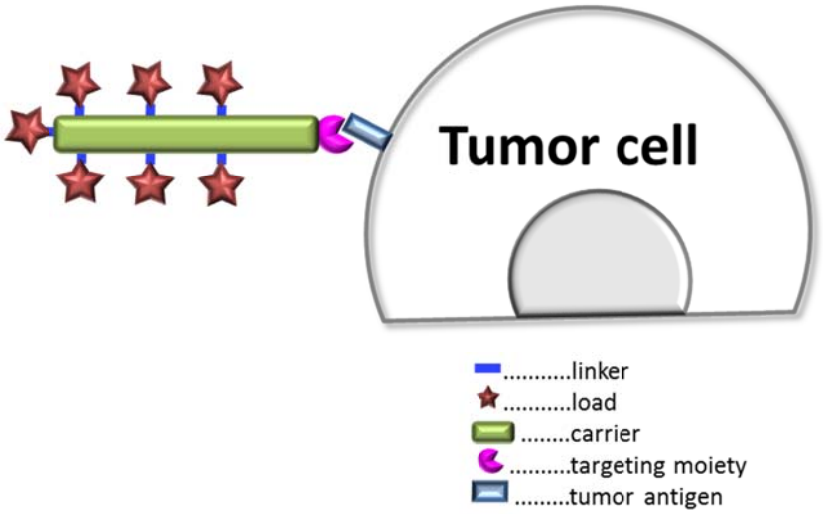

Figure 3: Schematic depiction of actively targeted HMW drug delivery system.

I.3. HPMA COPOLYMER-BASED DRUG DELIVERY SYSTEM

I.3.1. HPMA copolymer carrier

Polymers based on *N*-(2-hydroxypropyl)methacrylamide (HPMA) are almost ideal water-soluble polymeric drug carriers originaly developed in Prague in 1970s [41]. They have been widely exploited for attachment of various molecules including LMW cytostatic drugs, enzymes, hormones, antimicrobial agents, immunomodulants and many others. HPMA homopolymer is biocompatible, non-immunogenic and does not exert any toxicity up to dose of 30 g/kg. However, poly(HPMA) as a homopolymer (Figure 4) lacked reactive functional groups that could be modified to attach biologically active moities; therefore HPMA copolymers composed of repetitive HPMA monomers and containing suitable functional groups were designed [42].

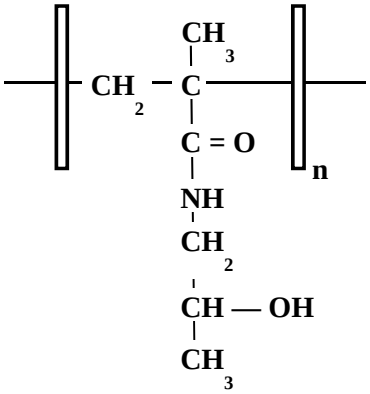

Figure 4: Structure of HPMA homopolymer.

HPMA copolymers are composed of linear chains of molecular weight (M_w) usually around 25 kDa. The polymer backbone can carry multiple pendant groups due to the presence of several modifiable functional groups, however it is not biodegradable – one of a few downsides of HPMA carrier [2, 6-8]. Nevertheless, polymer chains smaller than 40-45 kDa can be excreted via renal filtration; therefore, HPMA copolymer-based drug delivery systems contain enzymatically degradable spacers (e.g. GlyPheLeuGly), disulfide bridges or combination of both which ensure disintegration of the polymeric backbone under certain conditions [43, 44].

There are various HPMA copolymer structures of different biological properties, shapes and Mw, such as small linear HPMA chains, large star-like HPMA systems with dendrimer core with multiple HPMA copolymer side-chains or graft polymers with multivalent HPMA copolymer grafted with semitelechelic HPMA homopolymer side-chains [43, 44]. Moreover,

linear HPMA copolymers of Mw ~25 kDa can form HMW supramolecular micellar structures upon attachment of hydrophobic molecules to the polymer (e.g. cholesterol). As stated in I.2.1., there is a positive correlation between the size of a drug delivery system and tumor accumulation, nevertheless, design of robust HPMA copolymer carriers is limited by maximum size of a particle that can effectively penetrate through tumor mass and difficulty of synthesis of well-defined complex systems with low polydispersity and fair reproducibility.

I.3.2. Biocompatibility and immunocompatibility of HPMA copolymers

As stated in I.3.1., HPMA homopolymer is biocompatible and non-immunogenic structure – features quite important for drug delivery systems since the triggering of immune response could hamper the therapy and lead to critical damage of patient's organism. Whilst HPMA homopolymer do not induce any immune reactions of humoral or cellular type or even activate complement pathways [45], HPMA copolymer containing oligopeptide sequences trigger weak immune response depending on Mw of the polymer [46-48]. The immune response include mainly IgM production; nevertheless, resulting antibody titers are 4 orders of magnitude lower compared to titers elicited by reference immunogenic protein (e.g. albumin). Moreover, HPMA copolymers have no effect on macrophages, B or T cells, or complement pathways [47, 49].

There are no documented signs of possible side toxicity elicited by HPMA homo- or copolymers up to the dose of 30 g/kg and attachment of biologically active agent results in lowered toxicity of that agent as well [2, 48, 49]. If the agent is a protein, the resulting HPMA copolymer-bound protein conjugate induce about 250-fold lower antibody titers compared to unmodified free protein [2, 8]. This observation was proved in many HPMA copolymer-bound protein conjugates such as HPMA-immunoglobulin, HPMA-transferrin or HPMA-HSA (human serum albumin) [2, 7, 8].

Even though HPMA copolymers are not biodegradable they do not form long-term deposits in organism and their circulation half-life depends on their Mw [2, 7, 8].

I.3.3. Controlled drug release

Among many advantages of HPMA copolymer-based drug delivery systems is stimulus-controlled release of the attached drug that provides better efficacy and lowers the negative side-effects. The system itself behave as a prodrug, it travels via circulation and exploit its prolonged half-life to reach the final destination through fenestrated endothelium of

tumor vasculature. Inside the tumor, the drug is released from its carrier either extracellularly or intracellularly depending on HPMA copolymer-drug conjugate design. The bond between the carrier and anti-tumor drug can be either pH-sensitive or enzymatically degradable and upon its breakage the drug usually becomes biologically active [50, 51].

Actively targeted HPMA copolymer-based drug delivery systems are taken up by tumor cells via receptor-mediated endocytosis, whereas non-targeted passively accumulated systems enter the cell through pinocytosis [52-54]. Upon the structure's engulfment, enzymatically degradable bond covalently attaching the drug to the carrier is cleaved by enzymes of endosome/lysosome compartment which are consequently activated by decreased pH (from pH 7.2-7.4 typical to extracellular environment to pH 4.5-5 present in lysosomes) [54].

Acidic environment of endosome/lysosome compartment can also promote hydrolysis of pH-sensitive bond between drug and carrier which is stable in normal conditions and degradable in acidic environment [54]. Moreover, tumor tissue is characterized by its hypoxic, mildly acidic environment with pH 0.5-1 lower than in normal tissue [55, 56]. This feature allows extracellular cleavage of pH-sensitive bond connecting drug to polymer carrier and release of the drug outside the cell. The carrier itself can be degradable if it contains biodegradable linkers in its backbone. Among the most utilized pH-sensitive linkages belong hydrazon bond and *cis*-aconityl spacer.

I.3.4. HPMA copolymer-bound drug conjugates

Attachment of selected biologically active agent(s) to the HPMA copolymer-based carrier creates HPMA copolymer-bound drug conjugate with superior anti-cancer activity, lower hematotoxicity and immunosupression in comparison to the free drug. Many reports show complete cure of various mouse tumor models *in vivo* together with successful establishment of long-term anti-tumor immune memory in cured mice which bestows them with resistance to the original tumor [57, 58].

Selected biologically active moiety is bound to the side chain of HPMA copolymer carrier either via pH-sensitive linkages (e.g. hydrazone bond, *cis*-aconityl spacer) [59, 60], or by attachment to enzymatically degradable oligopeptide spacer (e.g. tetrapeptide GlyPheLeuGly; GFLG) [50] via amide bond. Release of the drug could be therefore realized by extracellular or intracellular enzyme activity or pH-controlled hydrolysis. Load that do not need to be released from the carrier to exert its pharmacological activity (e.g. radionuclides or

photosensitizers) can be attached via non-degradable diglycin or single amino acid spacer [61].

The ideal oligopeptide spacer between HPMA copolymer carrier and drug should be stable in blood stream and degradable in presence of lysosomal enzymes. The best properties has GFLG spacer (Figure 5A) that is most frequently used in HPMA copolymer-based drug conjugates [62-64]. In case of pH-sensitive spacers, those containing hydrazon bond (Figure 5B) have become most exploited ones due to their fair stability in body fluids (pH 7.4) and degradability in lower pH at tumor site or intracellularly. HPMA copolymer- bound doxorubicin (DOX) conjugates with hydrazon bond were proved to have higher loading of the carrier with unchanged solubility in comparison to conjugates containing GFLG spacer and amide bond [65, 66]. On top of that, conjugates with hydrazon bond are less difficult to synthesize and they exert better anti-tumor activity *in vivo*.

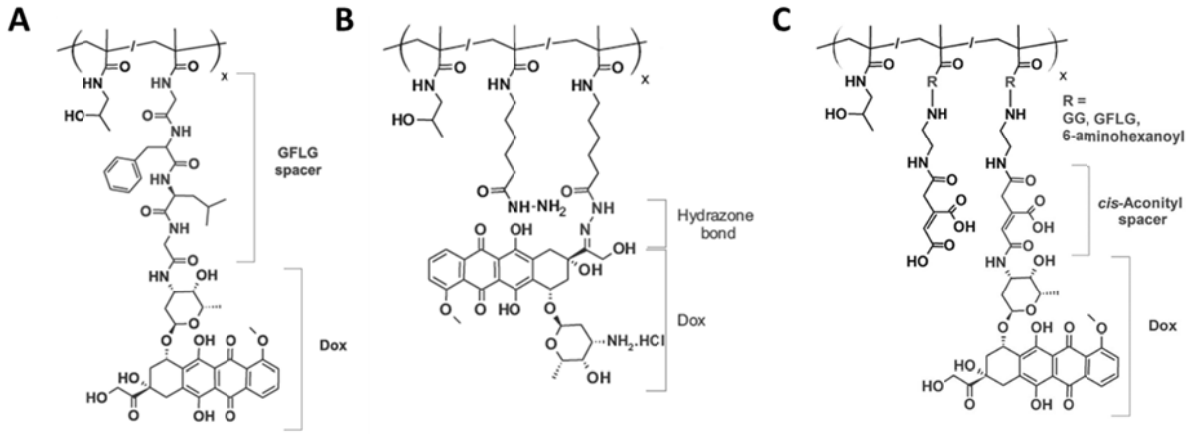

Figure 5: Different drug attachment to HPMA carrier. Attachment via oligepeptide spacer GFLG and amide bond (A), attachment via pH-sensitive hydrazon bond (B) or cis-aconityl spacer (C). Adopted from Chytil 2017.

Apart from above mentioned spacers, there are also other types of linkage used for generation of polymer-drug conjugates, e.g. disulfide-containing spacers sensitive to reductive environment of cell cytoplasm or non-covalent interactions like pH-sensitive coiled-coil peptide binding motifs [67, 68].

HPMA copolymer carrier is hydrophilic and provides water solubility to the attached drug even if they are highly hydrophobic (e.g. taxanes); moreover, it improves drug's pharmacokinetics and tumor accumulation, lowers toxicity and helps to at least partially overcome MDR. Water solubility of polymeric conjugates has another advantage in comparison to free drugs – the HPMA copolymer-bound drug conjugates can be

administrated without the need of special solutions (e.g. dimethylsulfoxide, Cremophor EL in combination with ethanol) which often cause adverse or unexpected side effects.

Improved pharmacokinetics of HPMA copolymer-bound drug conjugates provides wider therapeutic window and in combination with passive accumulation in tumors via EPR effect, it results in significantly improved anti-tumor activity. Passive accumulation of HPMA copolymer-bound drug conjugates is ensured by their structure and high Mw. Moreover, in addition to passive accumulation, HPMA copolymer-bound drug conjugates can be also actively targeted via attachment of targeting moiety.

Some HPMA copolymer-based conjugates have entered preclinical studies, e.g. conjugates containing DOX, camptothecin, platinum or taxanes [69]. Clinical trials proved their safety, prolonged circulation half-life, improved pharmacokinetics, tumor accumulation and immunostimulatory effects. However, none of them have been approved for application in clinical practice since there are several problems that need to be adressed, such as difficult synthesis.

I.3.4.1. HPMA copolymer-bound DOX conjugates

Over the years, variety of drugs with different properties, structure and biological activities have been attached to HPMA copolymer carrier. Nevertheless, anthracycline antibiotic DOX became one of the most often used drugs in development of effective HPMA copolymer-based drug conjugates. It can be bound onto the polymeric carrier as a single anti-cancer agent or even in combination with other biologically active molecules (e.g. mesochlorin e6 monoethylenediamine, dexamethasone, mitomycin C) [70-73] for simultaneous delivery. Such bifunctional conjugates exert synergistic effects of attached drugs, long-term survival of experimental animals and superior anti-tumor activity in comparison to conjugates bearing only one drug. Moreover, it is possible to design the linkers connecting drugs to the carrier so that the drug release could be of different rates. Mixtures of single drug conjugates usually do not show synergistic effects observed during therapy with bifunctional conjugates. Moreover, conjugates can even combine block of HPMA copolymer bearing amide-bound DOX and block of HPMA copolymer bearing hydrazon-bound DOX [74]. It was proved they have increased anti-tumor activity employing induction of apoptosis (hydrazon-bound DOX) and necrosis (amide-bound DOX) of tumor cells [54]. Interestingly, conjugates bearing randomly distributed DOX bound via amide and hydrazon bond are less effective than combination of a HPMA copolymer-bound DOX-bearing conjugate containing

amide bond and HPMA copolymer-bound DOX-bearing conjugate containing hydrazone bond [74].

I.3.4.1.1. Non-targeted HPMA copolymer-bound DOX conjugates

The first HPMA copolymer-bound conjugate bearing DOX consisted of linear carrier, oligopeptide GLFG spacer and DOX bound via amide bond (DOX^{AM}-PHPMA, "Prague-Kiel", PK1; Figure 6) [75]. It was proved inactive in plasma serum and enzymatically degradable by range of enzymes such as chymotrypsin, lysosomal proteases or various bovine cathepsins [76].

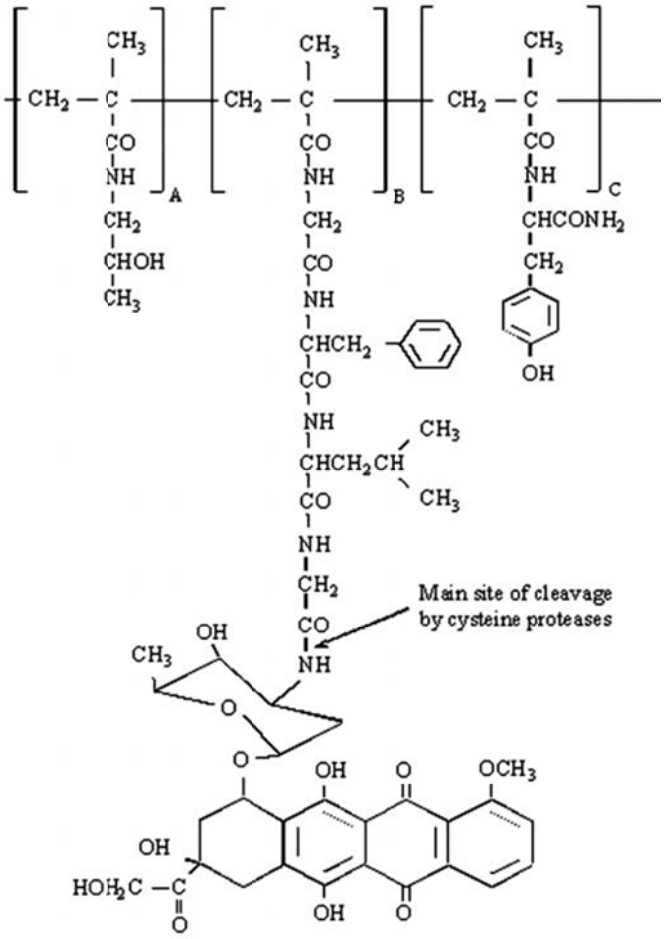

Figure 6: structure of PK1 (adopted from Seymour et al., 2009).

Several tumor cell lines of mouse, rat and human origin used for *in vitro* and *in vivo* studies proved to be sensitive to PK1 [77-79], e.g. murine skin lymphocytic leukemia (L-1210), murine monocyte/macrophage lymphoma (P388), murine ovarian reticulosarcoma (M5076), murine skin melanoma (B16-F10), rat Walker sarcoma or human colorectal carcinoma xenografts. Effectivity in human solid tumor models led to investigation of its

possible clinical application. PK1 was tested in phase I/II [76, 79] and it was proved to have prolonged circulation half-life, to be able to passively accumulate into tumor tissue, 5-times lower side toxicity than free DOX with maximum tolerated dose (MTD) 320 mg/m^2 of DOX equivalent. Anti-tumor activity and biological properties of PK1 were tested on DOX-naïve patients with non-small cell lung carcinoma (NSCLC), colorectal cancer and breast cancer. No patient with colorectal carcinoma responded to the therapy; however, 6 of 62 patients in phase II showed partial response (PR) to the therapy – 3 with NSCLC, 3 with breast cancer. Collected data proved that PK1 has superior anti-tumor activity and potential for NSCLC and breast cancer therapy. Nevertheless, there have been no further studies after phase II clinical trial so far.

Aside from PK1, number of linear HPMA copolymer-bound DOX conjugates employing pH-sensitive bond connecting polymer side chain with biologically active agent, were designed and tested for their anti-tumor activity which was subsequently proved in several tumor cells lines both *in vitro* [60] and *in vivo* [80]. *Cis*-aconytil residue was one of the first linkers used for DOX attachment to the polymer carrier and was effective against human ovarian cancer [81]. Subsequently, linear conjugates with DOX linked through hydrazon bond (DOX^{HYD}-PHPMA) and exerting significant *in vitro* and *in vivo* anti-tumor activity were designed [59].

Linear HPMA copolymer-bound DOX conjugates were later on replaced by conjugates containing grafted polymer backbone or dendrimer core, which showed superior tumor accumulation and anti-tumor efficacy *in vivo* [43, 44].

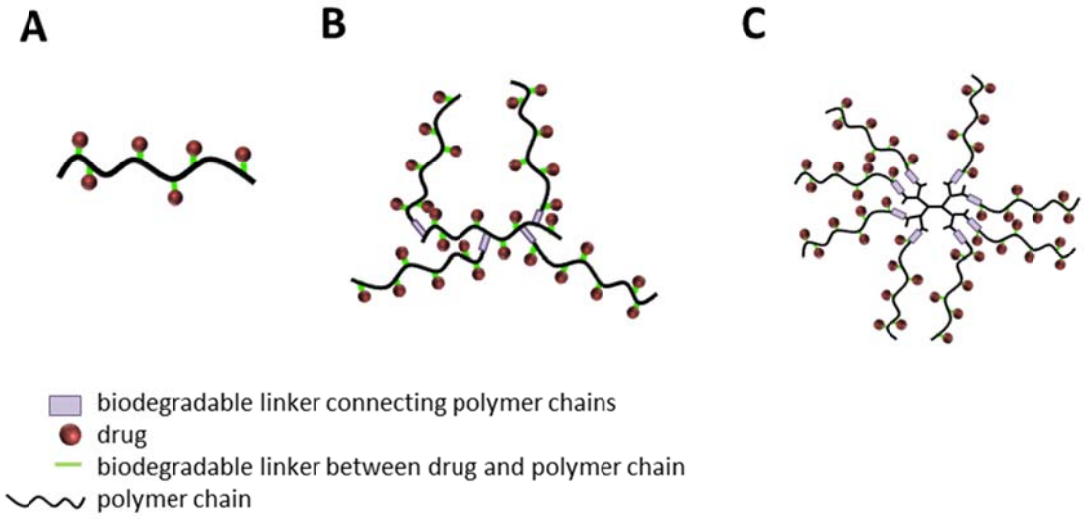

Figure 7: Schematic depiction of linear conjugate (A), grafted conjugate (B) and conjugate containing dendrimer core (C).

I.3.4.1.2. Actively targeted HPMA copolymer-bound DOX conjugates

Several functional groups along HPMA copolymer chain allow attachment of biologically active anti-tumor agents as well as targeting moieties of various types and origins. Antibodies, lectins, peptides or hormones recognizing molecular markers expressed on the tumor cell surface can be utilized as targeting moieties. Tumor antigens could be either rare and exclusive for tumor cells (tumor-specific antigens) [82], or markers that are present on normal and tumor cells alike, however on tumor cells are of aberrant expression (tumor-associated antigens) [83]. These markers can be recognized by immune cells leading to cancer cell elimination. It has been proved that T cells, natural killer (NK) cells or macrophages can be found inside the tumor mass or within draining lymph nodes [84-86].

HPMA copolymer-bound drug conjugates specifically targeted to tumor antigens combine EPR effect and active targeting. Moreover, they can be also exploited in therapy of disseminated tumors that do not form solid tissues like leukemias. They enter tumor cells via receptor-mediated endocytosis. Among the first specifically targeted HPMA copolymer-based conjugates belong PK2 (DOX^{AM}-PHPMA-galactosamine, FCE28069; Figure 8) [87, 88].

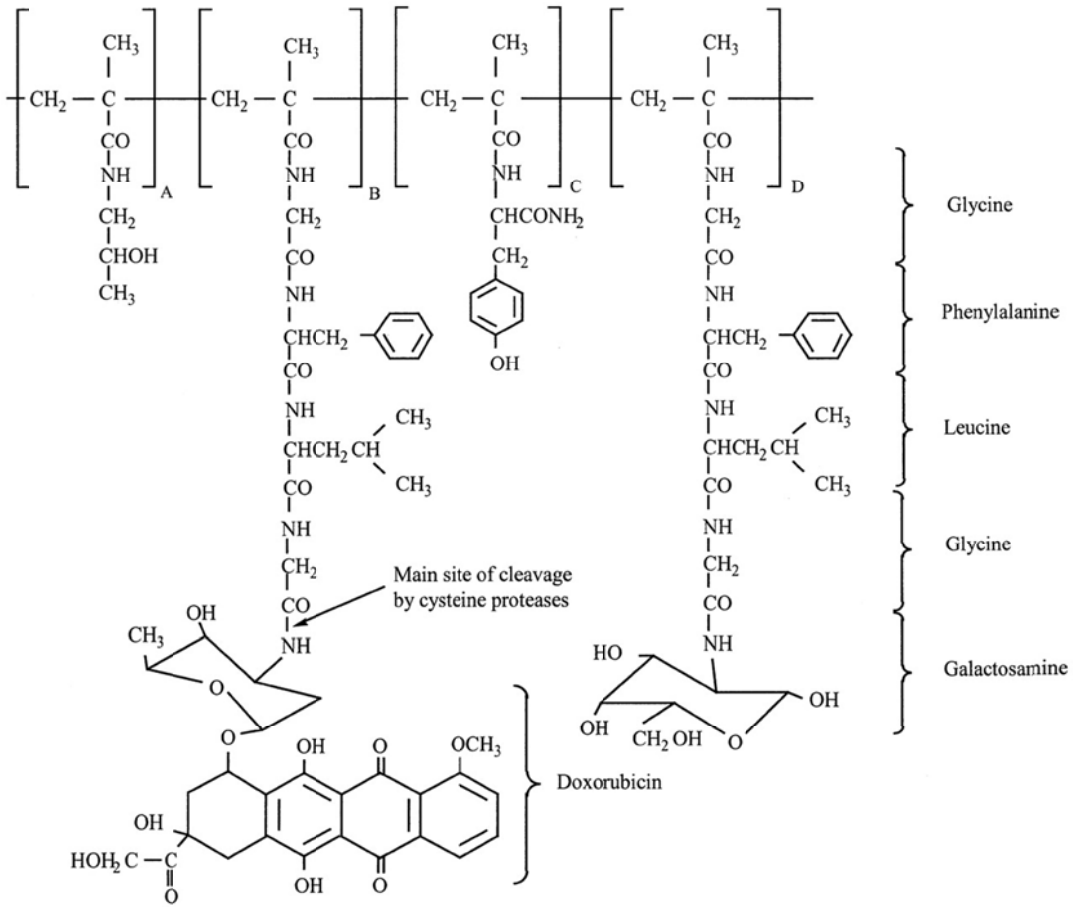

Figure 8: Structure of PK2 adopted from Seymour et al. 2002[88].

It is linear HPMA copolymer-bound DOX conjugate containing galactosamine as the targeting moiety, which bind to the asialoglycoprotein receptor overexpressed on hepatocellular carcinoma cells. PK2 showed lowered cardiotoxicity and long-term circulation half-life in comparison with free DOX. Upon entering phase I/II studies [88], PK2 showed higher liver accumulation and lower MTD (160 mg/m^2 DOX eq.) than PK1. Even though partial response to therapy with PK2 in few patients with hepatocellular carcinoma was documented, further clinical testing was abandoned since there was no difference in accumulation rate between malignant and normal liver due to the presence of asialoglycoprotein receptor on the surface of normal hepatocytes, though on a lower level than on tumor cells.

Altered glycosylation pattern of tumor cells led to use of lectins as targeting moieties such as peanut agglutinin (PNA) or wheat germ agglutinin (WGA), however, the efficacy of such targeted conjugates was not sufficient [89, 90]. In 2000, Kunath *et al.* [91] focused on investigation of HPMA copolymer bearing adriamycin attached via GFLG spacer and monoclonal antibody OV-TL16 recognizing OA-3 surface antigen (CD47) overexpressed on surface of human ovarian carcinoma cell line (OVCAR-3) and its effect on expression of MDR-related genes. They proved difference in cell entry of free drug (diffusion), non targeted conjugate (fluidphase pinocytosis) and targeted conjugate (receptor-mediated endocytosis) together with different effect on expression of P-glycoprotein and other multidrug resistance-associated protein efflux pumps. In 2002, Kovar *et al.* [51] evaluated *in vitro* and *in vivo* HPMA copolymer-bound DOX^{AM} conjugate targeted with transferrin or anti-CD71 mAb to transferrin receptor (CD71) expressed on mouse 38C13 B-cell lymphoma cell line. Both conjugates caused significant reduction of tumor growth, prolonged survival and even completely cured some experimental animals, however, anti-CD71 mAb-targeted one was more effective than transferrin-targeted or non-targeted conjugates.

Number of studies led to overall conclusion that the most potent and defined targeting moieties are antibodies and they have been intensively studied over the years. Two types of antibody-targeted HPMA copolymer-drug conjugates were designed: conjugates of classical structure and star structure (Figure 9).

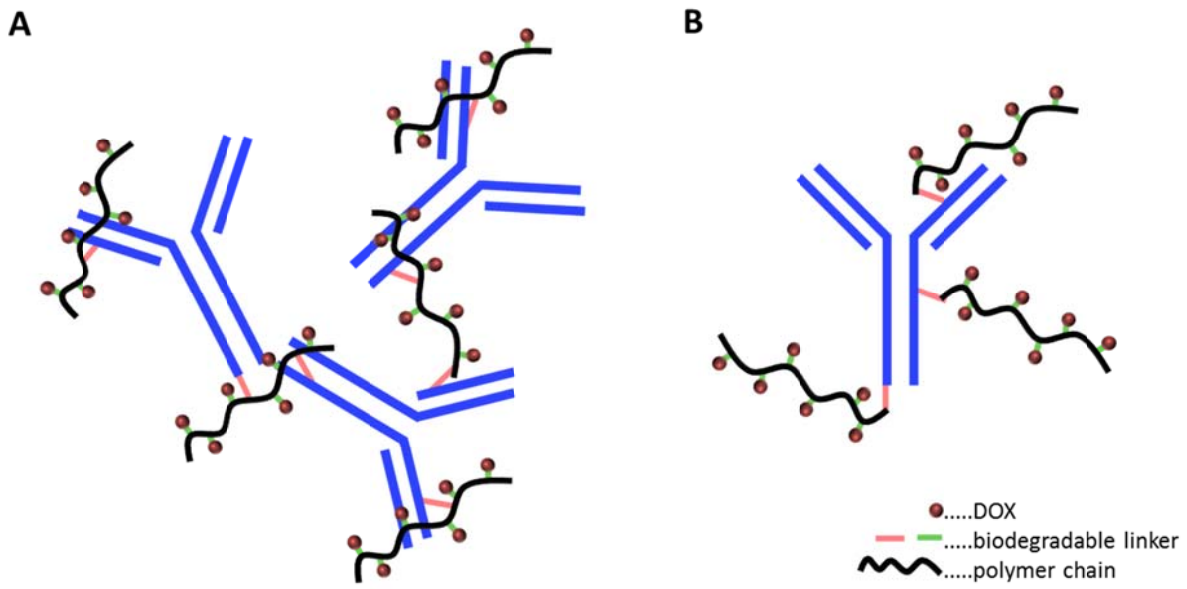

Figure 9: Classical (A) and Star (B) antibody targeted HPMA copolymer-bound DOX conjugate.

Conjugates of classical structure were developed first. They contained random covalent bonds between copolymer chains and primary amino groups of antibody's molecule which could hamper the antibody's binding activity. Moreover, these conjugates had wide Mw distribution caused by branching effect of multivalent HPMA copolymer chains. Conjugates of star structure, however, were more potent both *in vitro* and *in vivo* [51, 92, 93]. Selected antibody is situated in the center of the conjugate. It is attached to the activated terminal carboxyl groups of 30-40 semitelechelic HPMA copolymer chains with DOX bound via amide bond and enzymatically degradable GFLG spacer or pH-sensitive hydrazon bond. They have quite narrow Mw and since semitelechelic HPMA copolymer chains are monovalent, these star structures are better defined because there is no possibility of branching.

Study comparing anti-tumor efficacy of targeted HPMA copolymer-bound drug conjugate of star or classical structure was performed in 2002 [94]. Mice inoculated with BLC1 leukemia were treated either with star or classical DOX^{AM}-PHPMA conjugates targeted with B1 monoclonal antibody specific for idiotype of surface IgM on BCL1 cells. Significantly higher anti-tumor acitivity of targeted star and classic conjugate compared to non-targeted one was observed. Both targeted conjugates were able to completely cure mice with established BCL1 leukemia. Moreover, cured mice developed tumor-specific resistance to BCL1 leukemia and this phenomenon was later on described also for EL4 mouse model of T-cell lymphoma and 38C13 lymphoma mouse tumor models, therefore it appears to be valid for variety of mouse tumor models [57, 94]. Surprisingly, it was proved that the more effictive the treatment was, the weaker the tumor-specific resistance in cured mice was established

[78]. In 2008, study performed on BCL1-leukemia bearing mice described the mechanism of the phenomenon of tumor resistance. It was proved, that even though establishment of the resistance is mediated by both $CD4^+$ and $CD8^+$ T cells, its maintenance is dependend only on $CD8^+$ T cells. Moreover, study also presents the first direct evidence that Treg cells promote progression of tumor growth and significantly influence therapeutic outcome.

DOX^{AM}-PHPMA conjugate containing human immunoglobulin (HuIg) entered pilot clinical studies and was tested on patients with generalized breast carcinoma that were non-responsive to other clinical treatment [95]. Stability in the bloodstream and increased numbers of $CD16^+CD56^+$ and $CD4^+$ cells together with activation of NK and lymphokine-activated killer cells was observed in all patients together with disease stabilization up to several months. Unfortunately, no further clinical studies were performed ever since. Mice study focusing on treatment of EL4 lymphoma proved complete cure of experimental animals when treated with DOX^{AM}-PHPMA-HuIg conjugate. Establishment of anti-tumor resistance to the original tumor in cured animals was also reported and it was proved to be tumor-specific since mice transplanted with other type of tumor (i.e. B16-F10 melanoma) developed the dissease regardless to previous successfull cure. Moreover, transfer of splenocytes or $CD8^+$ T cells from cured mice to naïve mice bestowed them with tumor-specific resistance as well which demonstrated that the phenomenon of tumor protection is indeed mediated and transferable by T lymphocytes.

II. AIMS OF THE THESIS

The general aim of this study was to evaluate biological activity of novel HPMA copolymer-bound drug conjugates and to address their anti-tumor efficacy. These aims can be divided into following fields of interest:

1. Investigation of HPMA copolymer-bound drug conjugate toxicity.

2. Determination of maximum tolerated doses of star non-degradable HPMA copolymer-bound drug conjugate and linear HPMA copolymer-bound drug conjugate.

3. Investigation of HPMA copolymer-bound drug conjugate efficacy in treatment of solid tumors.

4. Investigation of HPMA copolymer-bound drug conjugate efficacy in treatment of leukemia.

5. Invetigation of BCL1 targeted HPMA copolymer-bound drug conjugate therapeutic efficacy.

6. Comparison of binding activity and anti-tumor efficacy of BCL1 targeted HPMA copolymer-bound drug conjugates containing different pairs of complementary peptides.

III. PUBLICATIONS

The thesis was prepared on the basis of these publications:

Etrych T., Strohalm J., Sirova M., Tomalova B., Rossmann P., Rihova B., Ulbrich K. and Kovar M.: High-molecular weight star conjugates containing docetaxel with high anti-tumor activity and low systemic toxicity *in vivo*. Polym. Chem. 6: 160-170, **2015**.

IF = 5,52

Tomalova B., Sirova M., Rossmann P., Pola R., Strohalm J., Chytil P., Cerny V., Tomala J., Kabesova M., Rihova B., Ulbrich K., Etrych T. and Kovar M.: The structure-dependent toxicity, pharmacokinetics and anti-tumour activity of HPMA copolymer conjugates in the treatment of solid tumours and leukaemia. JCR 223: 1-10, **2016**.

IF = 7,44

Pechar M., Pola R., Janouškova O., Sieglova I., Kral V., Fabry M., Tomalova B. and Kovar M.: Polymer Cancerostatics Targeted with an Antibody Fragment Bound via a Coiled Coil Motif: *In Vivo* Therapeutic Efficacy against Murine BCL1 Leukemia. Macromol. Biosci. Published online, ahead of print, **2017**.

IF = 3,23

OTHER PUBLICATIONS

Tomala J., Kovarova J., Kabesova M., Votavova P., Chmelova H., Dvorakova B., Rihova B. and Kovar M.: Chimera of IL‑2 Linked to Light Chain of anti-IL‑2 mAb Mimics IL-2/anti-IL‑2 mAb Complexes Both Structurally and Functionally. ACS Chem. Biol. **2013**.

IF = 5,356

Skopova K., Tomalova B., Kanchev I., Rossmann P., Svedova M., Adkins I., Bibova I., Tomala J., Masin J., Guiso N., Osicka R., Sedlacek R., Kovar M. and Sebo P.: Cyclic AMP-Elevating Capacity of Adenylate Cyclase Toxin-Hemolysin Is Sufficient for Lung Infection but Not for Full Virulence of *Bordetella pertussis.* Infection and Immunity 85 (6): e00937-16, **2017**

IF = 3,593

Polymer Chemistry

PAPER

Cite this: *Polym. Chem.*, 2015, **6**, 160

High-molecular weight star conjugates containing docetaxel with high anti-tumor activity and low systemic toxicity *in vivo*

T. Etrych,*[a] J. Strohalm,[a] M. Šírová,[b] B. Tomalová,[b] P. Rossmann,[b] B. Říhová,[b] K. Ulbrich[a] and M. Kovář[b]

Received 14th August 2014,
Accepted 9th September 2014

DOI: 10.1039/c4py01120a

www.rsc.org/polymers

Here we present the polymer conjugates where the core formed by poly(amido amine) dendrimers was grafted with semitelechelic *N*-(2-hydroxypropyl)methacrylamide (HPMA) copolymers containing docetaxel (DTX) attached by a pH-sensitive hydrazone bond. DTX was derivatized with three different keto acids prior to attachment to the polymer carrier to introduce reactive keto groups into the drug. The therapeutic efficacy of such high-molecular-weight star conjugates is based on: (a) the enhanced permeability and retention (EPR) effect facilitating selective accumulation within solid tumors; (b) pH-controlled release of the drug, thus ensuring faster DTX release in the mildly acidic tumor microenvironment. The star DTX conjugate had a remarkably higher maximum tolerated dose in comparison with free DTX when administered as a single i.v. injection (~160 mg kg^{-1} *vs.* 40 mg kg^{-1} of DTX) in C57BL/6 mice. The star DTX conjugate showed significantly higher antitumor activity than free drug in the EL4 T cell lymphoma growing in syngeneic C57BL/6 mice even when given at the same dose (20 mg kg^{-1} of DTX eq.). Thus, the star DTX conjugates exert a much higher therapeutic activity and yet a lower systemic toxicity than free DTX.

Introduction

In designing an efficient drug delivery system, proper selection of the polymer carrier and the spacer between the drug and its carrier is crucial.[1,2] The tumor-accumulation principle of the enhanced permeability and retention (EPR) effect of macromolecules in solid tumors was originally described in 1986 by Matsumura and Maeda.[3] The EPR effect takes advantage of (i) the aberrant architecture of tumor blood vessels, (ii) the higher production of vascular permeability factors and (iii) the lack of functional lymphatic drainage in tumor tissue.[3–5] These tumor-specific features lead to the accumulation of biocompatible macromolecular drugs in tumor tissue, which results in their superior anti-tumor activity and decreased adverse effects. Recent progress in designing nanomedicines with anti-tumor activity has utilized the EPR effect as the prime principle of tumor targeting.[6,7] Among synthetic polymer drug carriers, the water-soluble HPMA copolymers[8–10] represent one of the most intensively studied and most promising systems for enabling actively or passively targeted drug delivery.[11–13] HPMA copolymers are nontoxic and nonimmunogenic drug carriers enabling easy control of drug loading. High-molecular-weight (HMW) HPMA copolymers (M_w > 50 g mol^{-1}) circulate longer and preferentially accumulate in tumor tissue *via* the EPR effect.[14] The effect of EPR on accumulation of poly(HPMA) polymers in sarcoma[15] and HPMA copolymers (PHPMA) in lymphoma[16] and other tumors[17] has been demonstrated in mice. Furthermore, the proper selection of the spacer between the drug and the carrier is a crucial step for obtaining a tumor- or tumor cell-specific drug release. The drug can be released from the polymer conjugate by specific enzymatic cleavage[18,19] or by pH-controlled chemical hydrolysis[20–22] (*e.g.*, a hydrazone bond or *cis*-aconityl spacer). To improve the tumor accumulation of HPMA copolymer-drug conjugates, the molecular size of the polymer carrier should be increased, either by branching or grafting HPMA copolymers or by their self-assembly to form micellar structures. However, the synthesis of branched polymer chains or graft polymers in a comb-like structure is relatively difficult to control; a high polydispersity index and lower reproducibility become a concern. In designing our drug carrier system we decided to use a dendrimer. Dendrimers are nearly monodisperse and their surface can be freely and explicitly modified, *e.g.*, by attaching semitelechelic PHPMA. Grafting of the dendrimer by PHPMA decreases the toxicity of the dendrimer as well.

[a]*Institute of Macromolecular Chemistry, Academy of Sciences of the Czech Republic, v.v.i., Heyrovský Sq. 2, 162 06 Prague 6, Czech Republic. E-mail: etrych@imc.cas.cz; Fax: +420-296 809 410; Tel: +420-296 809 224*
[b]*Institute of Microbiology ASCR v.v.i, Vídeňská 1083, 142 20 Prague 4, Czech Republic*

Similarly, we previously reported that a PHPMA-modified PAMAM dendrimer conjugated with doxorubicin (DOX) showed superior tumor accumulation and anti-tumor activity compared to that of linear HPMA copolymer conjugates of DOX.[23,24]

Taxanes such as paclitaxel and its semisynthetic analog docetaxel (DTX) are potent anti-cancer agents frequently used in treatment regimens for patients with breast, ovarian, prostate, lung, and other cancers. They interfere with microtubule disassembly, thereby inhibiting cell division and inducing cell death.[25] As with many other chemotherapeutic agents, metronomic dosing schedules with taxanes have been shown to exert anti-angiogenic activity in solid tumors.[26,27] One of the major disadvantages of taxanes is their prominent hydrophobic character. They must be administered in oily formulations using emulsifiers, such as mixtures of ethanol and Cremophor EL or polysorbate 80. The solvents were shown to induce serious adverse reactions in a considerable proportion of patients. A significant decrease in the drug effectiveness due to the presence of Cremophor EL was reported in several tumor models.[28] Thus, new strategies for improving the dosage form of taxanes remain highly desirable. In addition, achievement of more favorable pharmacokinetics, better bioavailability, and targeting of the drug to the tumor is required for improvement of the therapeutic effect and a reduction of systemic toxicity. In the literature, there have been described numerous attempts to prepare a drug delivery system for paclitaxel or docetaxel, including nanoparticles, liposomes, micelles or polymer conjugates. Various nanocarriers of paclitaxel are in different stages of clinical evaluation, with some having been commercialized, including Abraxane®, Lipusu, and Genexol PM®.[29] Previously, we described conjugates of paclitaxel and docetaxel with a linear HPMA copolymer carrier representing water-soluble prodrugs with tunable drug content and a clear anti-cancer effect in treating experimental murine tumors, such as EL4 T-cell lymphoma and 4T1 breast carcinoma.[30]

Here we describe the synthesis and physico-chemical properties of HMW star polymer-DTX conjugates designed for efficient tumor accumulation *via* the EPR effect and macromolecular nature of the star polymer-drug carrier, and present results from the biological evaluation of these new DTX conjugates. The star polymer carriers were prepared by grafting semitelechelic HPMA copolymers (M_w ~ 27–30 000 g mol^{-1}) onto poly(amido amine) (PAMAM) dendrimer cores, which formed HMW star-like structures with a narrow distribution of molecular weights. With the aim of attaching DTX to the polymer carrier *via* a hydrazone bond, DTX was modified by three different keto acids prior to attachment; thus keto groups suitable for hydrazone bond formation were introduced. Our intention was to keep the hydrodynamic diameter of the star conjugates below 30 nm, as Kataoka's group recently demonstrated that polymer micelles exceeding 30 nm poorly penetrated some types of tumor tissue.[31] *In vitro* cytotoxic/cytostatic activity of the polymer DTX conjugates was determined using several murine tumor cell lines. Very good results with the star DTX conjugates were obtained *in vivo*, including remarkably high maximum tolerated dose (MTD) and an excellent anti-tumor effect demonstrated in mice using the experimental murine EL4 T-cell lymphoma.

Materials and methods

Chemicals

1-Aminopropan-2-ol, methacryloyl chloride, 2,2′-azobis(isobutyronitrile) (AIBN), 4,4′-azobis(4-cyanovaleric acid) (ABIC), 6-aminohexanoic acid (ah), *N*,*N*′-dimethylformamide (DMF), *N*,*N*′-dicyclohexylcarbodiimide (DCC), *N*,*N*′-diisopropylcarbodiimide (DIPC), 1-hydroxy benzotriazole (HOBT), leucylglycine, levulinic acid (LEV), 6-oxohept-2-enoic acid (OHT), glycylphenylalanine, phthalaldehyde (OPA), *N*-ethyldiisopropylamine (EDPA), dimethyl sulfoxide (DMSO), *tert*-butyl carbazate, 4,5-dihydrothiazole-2-thiol, ethylenediaminetetraacetic acid (EDTA), ethylenediamine (EDA), cathepsin B and trifluoroacetic acid (TFA) were purchased from Fluka. 5-Cyclohexyl-5-oxovaleric acid (COV) was purchased from Rieke Chemicals. Docetaxel (DTX) was purchased from Aurisco, China and 2,4,6-trinitrobenzene-1-sulfonic acid (TNBSA) from Serva, Heidelberg, Germany. Poly(amido amine) (PAMAM) dendrimers were purchased from Dendritic Nanotechnologies, Inc., USA.

Synthesis of monomers and oligopeptide

N-(2-Hydroxypropyl)methacrylamide (HPMA) was synthesized as described in ref. 10 using K_2CO_3 as a base. M.p. 70 °C; purity > 99.8% (HPLC); elemental analysis: calcd, C 58.72%, H 9.15%, N 9.78%; found, C 58.98%, H 9.18%, N 9.82%.

N-(*tert*-Butoxycarbonyl)-*N*′-(6-methacrylamidohexanoyl)-hydrazine (Ma-ah-NHNH-Boc) was prepared in two-step synthesis as described in ref. 32. M.p. 110–114 °C; purity (HPLC) > 99.5%; elemental analysis: calcd C 57.70, H 8.33, N 13.46; found C 57.96, H 8.64, N 13.25.

The linear tetrapeptide H-Gly-Phe-Leu-Gly-OH (H-GFLG-OH) was prepared as described.[30] The product was characterized by MALDI-TOF MS (392.5 M + H) and reverse-phase high-performance liquid chromatography (HPLC) showing a single peak with a retention time of 18.0 min.

The derivative of DTX with levulinic acid (DTX-LEV, see Fig. 1) was synthesized as described in ref. 30. Briefly, LEV (38.1 mg, 0.33 mmol) and DCC (100 mg, 0.51 mmol) were dissolved in 0.5 mL DMF and left at −18 °C for 20 min. Then DTX (200 mg, 0.25 mmol) and DMAP (30 mg, 0.25 mmol) dissolved in 0.5 mL DMF were added, and the reaction mixture was left at 4 °C for 24 h. The reaction mixture was purified by gel filtration on a column filled with silica gel 60 (column 2 × 30 cm, eluent ethyl acetate) using a UV detector (240 nm). DTX-LEV was obtained after evaporation of the solvent, washing with diethyl ether, filtration and drying under vacuum. The yield was 74 mg (68%). HPLC showed 95.3% purity (peak maximum at 12.58 min). MS (APCI): *m*/*z*: 904.25 [M − H]$^-$.

The derivatives of DTX with OHT or COV (DTX-OHT and DTX-COV, see Fig. 1) were synthesized by the same procedure

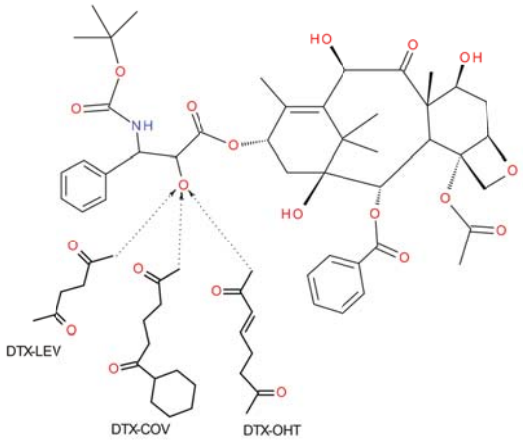

Fig. 1 Schematic description of DTX derivatives.

as that described for DTX-LEV. DTX-OHT: the yield was 81 mg (73%). HPLC showed 94.1% purity (peak maximum at 12.78 min). MS (APCI): *m/z*: 931.30 [M − H] . DTX-COV: the yield was 84 mg (77%). HPLC showed 92.1% purity (peak maximum at 13.12 min). MS (APCI): *m/z*: 987.12 $[M - H]^-$.

Purity of all the monomers, oligopeptides and derivatives mentioned above was examined by HPLC (Shimadzu, Japan) using a reverse-phase column (Chromolith Performance RP-18e; 100 × 4.6 mm) with UV detection at 230 nm, the eluent water–acetonitrile with an acetonitrile gradient of 0–100 vol.%, and a flow rate of 0.5 mL min^{-1}.

Synthesis of polymer precursors and polymer-drug conjugates

A semitelechelic HPMA copolymer terminated in the thiazolidine-2-thione (TT) groups containing hydrazide groups protected with *tert*-butoxycarbonyl groups (Boc) (polymer 1, Table 1) was prepared by radical copolymerization of HPMA (1.0 g, 0.007 mol) with Ma-ah-NHNH-Boc (189 mg, 0.6 mmol) in DMSO (7.4 mL) initiated with the azo-initiator 3,3′-[azobis-(4-cyano-4-methyl-1-oxobutane-4,1-diyl)]bis(thiazolidine-2-thione) (ABIC-TT, 0.38 g, 0.76 mmol). Polymerization was carried out in a sealed ampoule at 60 °C (6 h). The polymer was isolated by precipitation in an acetone–diethyl ether mixture (1 : 1) and purified by re-precipitation from a methanol solution into the same mixture. The polymer was filtered off, washed with diethyl ether, and dried under vacuum. The yield was 850 mg (72.8%). The content of end-chain TT groups was determined spectrophotometrically on a Helios Alfa (Thermochrom) spectrophotometer using ε_{305} = 10 700 L mol^{-1} cm^{-1} (methanol).

The semitelechelic polymer precursor 2 (Table 1), a HPMA copolymer with chain-terminating carboxyl group of the GFLG oligopeptide, was prepared by the reaction of terminal TT groups of polymer 1 with the amino group of the H-GFLG-OH oligopeptide in DMF as described in ref. 23. The content of end chain GFLG sequences was determined by amino acid analysis (Shimadzu, Japan, pre-column OPA derivatization).

Statistical copolymers of HPMA with Ma-ah-$NHNH_2$ (polymer 3, Table 1) and polymer conjugate **4** (Table 2) bearing DTX-LEV attached *via* a pH-sensitive hydrazone bond were prepared by the reaction described in detail recently.[30]

Synthesis of star precursors and polymer conjugates

The star polymer precursors were prepared by grafting the reactive semitelechelic HPMA copolymer precursors 1 or 2 onto the 2nd generation (G2) PAMAM dendrimers containing 16 terminal amino groups and a diaminobutan core.

Star polymer precursor 5 containing Boc-protected hydrazide groups was prepared by aminolysis of the TT groups of copolymer 1 with amino groups of the PAMAM dendrimer in methanol. Briefly, polymer 1 (654 mg; 0.06 mmol TT groups) was dissolved in 16 mL of methanol and added into a stirred solution of 16 mg of PAMAM dendrimer in 6.1 mL of methanol. After 2 h, the reaction was completed by adding 5 μL of 1-aminopropan-2-ol. Low molecular weight (LMW) impurities were removed by gel filtration (Sephadex LH-20, methanol

Table 2 Characteristics of the star polymer precursors and the polymer-DTX conjugates

Polymer or conjugate	Derivative of DTX	M_w (g mol^{-1})	M_w/M_n	R_h (nm)	DTX (wt%)
4	DTX-LEV	32 000	1.65	4.3	8.9
5	—	192 000	1.72	12.6	—
6	DTX-LEV	240 000	1.76	13.8	7.7
7	DTX-COV	222 000	1.72	13.1	7.5
8	DTX-OHT	238 000	1.80	13.6	7.9
9[a]	—	201 000	1.71	12.9	—
10[a]	DTX-LEV	265 000	1.68	15.2	7.6

[a] Biodegradable polymer with GFLG sequence cleavable by lysosomal enzymes.

Table 1 Characteristics of polymer precursors

Polymer	M_w (g mol^{-1})	M_w/M_n	Hydrazide (Hy) content (mol%)	Chain end-group	$M_{n,T}$[a] (g mol^{-1})	$M_n/M_{n,T}$[b]
1[d]	26 900	1.81	5.3	TT	11 400	1.31
2[d]	27 500	1.82	5.3	COOH	14 500	1.06
3[c]	26 900	1.77	5.8	—	—	—

[a] $M_{n,T}$ is the number-average molecular weight calculated from the GFLG-OH or TT group content. [b] $M_n/M_{n,T}$ is the functionality of a polymer. [c] Statistical copolymers of HPMA with Ma-ah-$NHNH_2$. [d] Semitelechelic copolymers containing the main chain-end reactive group.

solvent). The polymer-modified dendrimer was isolated by precipitation in ethyl acetate.

Star polymer precursor 9 (Table 2) was prepared by the reaction of the carboxyl group of the GFLG-OH terminal sequence of polymer 2 with amino groups of PAMAM dendrimer in DMF using the carbodiimide coupling method. Polymer 2 (200 mg; 12.2 μmol COOH groups) was dissolved in 4 mL of DMF and mixed with 13 μL of DIPC (11.4 mg, 84.7 μmol). After 5 min of stirring, a solution of 4.3 mg PAMAM dendrimer in 550 μL of DMF was added to the reaction mixture. After 20 h of stirring at room temperature, the reaction mixture was diluted with 13 mL of methanol, and LMW impurities were removed by gel filtration (Sephadex LH-20, methanol solvent). The star polymer was isolated by precipitation by acetone.

Free hydrazide groups needed for DTX derivative attachment were obtained in polymer precursors 5 and 9 by removing the protecting Boc groups from the hydrazides with concentrated TFA. Polymer conjugates 6, 7, 8 and 10 (Table 2), which had DTX derivatives attached *via* a pH-sensitive hydrazone bond, were prepared by the reaction of the precursors 5 or 9 with an appropriate DTX derivative for 2 h in methanol in the dark. The polymer-drug conjugates were purified from LMW impurities (DTX or its degradation products) by gel filtration on a Sephadex LH-20 column using methanol as the eluent.

Characterization of polymers and polymer-DTX conjugates

All the conjugates were characterized and tested for the content of free polymer or free drug using an HPLC (Shimadzu, Japan) equipped with GPC columns Superose™ 6 or TSKgel G3000SWxl and TLC (Kieselgel 60 F254). In addition, the content of free DTX or its derivatives was determined by HPLC after extraction of the respective drug from the aqueous solution of the conjugate by chloroform.

The total content of DTX derivatives in the polymer conjugates was determined by HPLC after complete hydrolysis of the polymer conjugates in an HCl solution (pH 2) for 1 h at 37 °C and extraction of derivatives by chloroform. No evidence of by-product formation during analysis was detected.

Determination of the molecular weight and polydispersity of the conjugates was carried out with an HPLC equipped with RI, UV and multiangle light scattering DAWN EOS (Wyatt Co., USA) detectors using a mobile phase of 20% of 0.3 M acetate buffer (CH_3COONa/CH_3COOH; pH = 6.5; 0.5 g L^{-1} NaN_3) and 80% of methanol and a TSKgel G3000SWxl column.

The content of hydrazide groups in polymer precursors was determined by a modified TNBSA assay as described earlier.[33] A molar absorption coefficient ε_{500} = 17 200 L mol^{-1} cm^{-1} (λ = 500 nm), estimated for the model reaction of MA-ah-$NHNH_2$ with TNBSA, was used.

The dynamic light scattering (DLS) of aqueous conjugate solutions was measured at a scattering angle of 173° on a Nano-ZS, Model ZEN3600 (Malvern, UK) zetasizer. The hydrodynamic radius (R_h) was determined using the DTS (Nano) program. MS spectra were measured using an LCQ Fleet spectrometer (Thermofisher Scientific).

In vitro release of DTX

The release rate of free or ester-DTX derivatives from the polymer conjugates was investigated by incubation of the conjugate in phosphate buffers at pH 5.0 or 7.4 (0.1 M phosphate buffer with 0.05 M NaCl) or in human plasma at 37 °C. The concentration of the conjugate in solution was equivalent to 1.10–4 mM DTX. The amount of released drugs and their ester derivatives was determined by HPLC analysis after their extraction into an organic solvent. Analysis was performed on an HPLC instrument using a reverse-phase column (Chromolith Performance RP-18e; 100 × 4.6 mm) with UV detection at 230 nm, the eluent water–acetonitrile with an acetonitrile gradient of 0–100%, and a flow rate of 0.5 mL min^{-1}. All drug-release data are expressed as the amounts of free drug relative to the total drug content in the conjugates. All experiments were carried out in triplicate.

In vitro degradation of the HMW star polymer conjugates

Polymer precursor 10 was incubated in sodium phosphate buffer (0.05 M sodium phosphate, 0.1 M NaCl, 1 mM EDTA, 3 mM GSH, pH 6) containing 0.5 μM cathepsin B at 37 °C at a final polymer concentration of 15 mg mL^{-1}. The activity of the cysteine proteinase cathepsin B was determined every 24 h using Bz-Arg-NAp as the substrate. The enzyme concentration of cathepsin B was maintained at 5 × 10^{-7} M, and the decreased enzyme activity was compensated by the addition of a fresh stock solution of cathepsin B. In predetermined time intervals, the molecular weight of the polymers was tested using HPLC.

In vitro cytotoxicity

Four murine cancer cell lines were used: EL4 T-cell lymphoma (ATCC TIB-39), 4T1 breast carcinoma (ATCC CRL-2539), CT26 colon carcinoma (ATCC CRL-2638), and LL2 lung carcinoma (ATCC CRL-1642). All cell lines were purchased from ATCC and maintained as recommended by the provider. The cells were cultivated in 96-well flat bottomed culture plates (Nunclon, Denmark) with various concentrations of conjugates and free DTX or DTX-LEV for 3 days. Cell counts at the beginning of cultivation were: 5000 per well for EL4, CT26, and LL2 cells, with 2500 per well for the 4T1 cell line. Cell proliferation was estimated by the standard ^{3}H-thymidine incorporation assay. Alternatively, determination of overall metabolic activity using an MTT assay was used as a parameter of EL4 lymphoma cell proliferation. The IC_{50} values were calculated as the drug concentrations that inhibit the cell proliferation or metabolic activity by 50% during the 3 day cultivation.

Maximum tolerated dose of linear and star polymer-DTX conjugates

Inbred C57BL/6 (*H-2b*) and BALB/c (*H-2d*) were obtained from the Institute of Physiology, ASCR, Prague, Czech Republic. The mice were i.v. injected with linear or star polymer-DTX conjugates in 300–400 μL of PBS at doses of 100, 125, 150 and 200 mg kg^{-1} of DTX eq. of linear conjugate, and 20, 40, 60, 80,

90, 100, 120, 140 and 180 mg kg^{-1} of DTX eq. of star conjugate. Mice injected with PBS were used as the controls. The number of mice per group ranged between three and nine. Injected mice were monitored daily or every other day until day 21 post administration. We defined the MTD, according to the recent publications, as the highest dose that should elicit minimal signs of toxicity (*e.g.*, ruffled fur, cachexy, and neurotoxicity), no deaths, and the weight loss of less than 15% of body mass.

Histology

Three random mice from the groups injected with PBS (control), 200 mg kg^{-1} of DTX eq. of linear conjugate, or 100, 120 and 140 mg kg^{-1} of DTX eq. of star polymer-DTX conjugate were sacrificed for the histological analysis on day 7 post injection. Mice injected with free DTX at its MTD (*i.e.*, 40 mg kg^{-1}) were used as a positive control. Tissue samples of spleen, liver, vertebral bone marrow and kidney were collected, fixed in 5% formalin, embedded in paraffin, and stained with hematoxylin/eosin (H&E). The vertebral column had been decalcified in 10% formic acid. Cryostat sections of selected samples were stained with Oil Red O, Sudan Black B and Luxol Fast Blue.

Tumor treatment

C57BL/6 mice were transplanted subcutaneously (s.c.) on day 0 with 1×10^5 EL4 cells and treated when palpable tumors (approx. 5–8 mm diameter) developed. The polymer-DTX conjugates were injected i.v. *via* the tail vein on days 8 and 12, each dose equivalent of 20 mg DTX per kg. For the administration, the conjugates were dissolved in 0.2 mL of PBS. Tumor growth, body weight, and survival of mice were regularly monitored. The tumor volume was calculated as $V = a \times b^2/2$, where a = longer diameter and b = smaller diameter. Analysis of statistical significance of the survival times was conducted using the log-rank (Mantel–Cox) test and GraphPad Prism software.

In all animal experiments, institutional guidelines for the care and use of laboratory animals were strictly followed under a protocol approved by the Institutional Animal Care and Use Committee of the Academy of Sciences of the Czech Republic, and conducted in compliance with local and European guidelines.

Results and discussion

We have already demonstrated the high efficacy of HMW star HPMA copolymer carriers containing doxorubicin in the treatment of tumors in mice (EL4 T-cell lymphoma).[23] We have used the EPR effect as the prime principle of tumor drug targeting in designing anti-tumor nanomedicines. Tumor-specific features causing the EPR effect led to the accumulation of biocompatible macromolecules in tumor tissue, which result in a superior anti-tumor effect with decreased adverse effects. In this study, we focused on improving the properties of the HMW drug carrier system, explored here for DTX delivery, using a new synthesis strategy of the HMW HPMA copolymer-

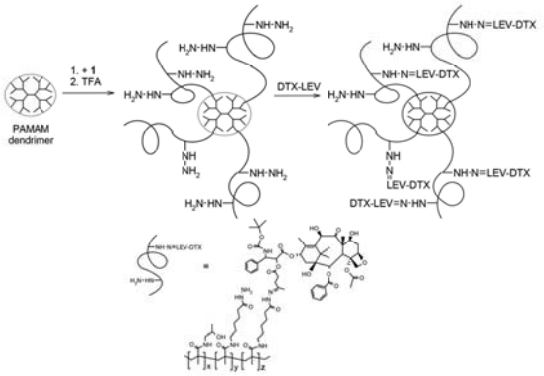

Fig. 2 Schematic representation of the synthesis and structures of the star polymer conjugates.

DTX conjugates with well-defined architecture, proper control of molecular weight and with low polydispersity. The HMW polymer carriers were prepared by grafting the semitelechelic HPMA copolymers onto a PAMAM dendrimer core to form the star-like structures depicted in Fig. 2. Molecular weight of the copolymer grafts bearing hydrazide groups enabling subsequent DTX derivative attachment was below the renal threshold and the copolymers were grafted onto the PAMAM dendrimer *via* a stable amide bond or enzymatically degradable linkages containing GFLG oligopeptide sequences. The molecular weight of the star polymer carrier exceeded the size limit for glomerular filtration of HPMA-based polymers, but the carrier structure allowed elimination of the polymer from the organism after its intracellular degradation.

Synthesis of polymer precursors and ester derivatives of DTX

Radical solution copolymerization of HPMA with a monomer bearing Boc-protected hydrazide groups (Ma-ah-NHNH-Boc) was initiated with ABIC-TT. This bifunctional azo-initiator, which contained reactive TT groups, was used for the synthesis of HPMA copolymer precursors terminating with the TT group, here termed semitelechelic copolymers. A previous study has shown that radical HPMA copolymerization can be precisely controlled by the initiator and monomer concentrations and polymerization temperature.[34] Therefore, radical polymerization using ABIC-TT was employed here in the synthesis of copolymer 1 (Table 1). The polymerization conditions were chosen to keep the molecular weights of the copolymer under the renal threshold, which was a prerequisite for subsequent elimination of the polymer from the body *via* glomerular filtration. Despite the preference for a disproportionation termination reaction, the functionality (number of chain-terminating TT functional groups per polymer chain) of the copolymer was higher than 1 ($M_n/M_{n,T} \sim 1.3$).

The semitelechelic copolymer bearing an end-chain biodegradable oligopeptide (copolymer 2) was prepared by aminolysis of the copolymer 1 with an oligopeptide H-GFLG-OH. The lower yield of the reaction resulted in a decreased functionality

of the copolymer 2 (close to 1) without observed changes in molecular weight and polydispersity.

We have developed and published the strategy for the synthesis of polymer-drug conjugates based on DTX derivatives containing the keto group.[30] Introduction of the keto group by DTX esterification with keto acids enabled DTX attachment to the polymer carrier *via* pH-sensitive hydrazone bonds together with more slowly hydrolyzable ester bonds. Three keto acids (levulinic acid, 6-oxohept-2-enoic acid and 5-cyclohexyl-5-oxovaleric acid) were selected as promising candidates for DTX derivatization.

The DTX acid derivatives, DTX-LEV, DTX-OHT and DTX-COV, were prepared by esterification of the primary hydroxyl group at C2′ of DTX with the carboxyl group of the above mentioned acids. The lower yield of the reaction (~70%) was caused by a competing reaction, *i.e.*, formation of diester derivatives of the acylated drug on the hydroxyls at both the C2′ and C7 positions. The products were purified from free DTX, keto acid diester and other components by preparative chromatography on silica. Approximately 95% product purity was determined by HPLC analysis with UV detection.

Synthesis of star polymer precursors and DTX conjugates

The star polymer conjugates were prepared by grafting semitelechelic copolymers 1 or 2 onto the second generation of PAMAM dendrimer containing 16 amino groups. Two structurally different types of the star polymer conjugates were synthesized. One type contained a stable, non-degradable amide bond between the polymer grafts and the central dendrimer (polymers 5–8). The second type was a biodegradable polymer construct containing the enzymatically degradable oligopeptide GFLG sequence (polymers 9 and 10). In both types, the products of the grafting reactions were HMW polymers with a star structure and a relatively narrow distribution of molecular weights ($M_w \sim 200\,000$ g mol^{-1}; $M_w/M_n \sim 1.7$), which made them applicable as drug carriers with passive targeting to solid tumors. Molecular characteristics of all the star copolymers were comparable and the method of synthesis and degradable or non-degradable structure did not significantly influence the molecular weight, polydispersity or Rh of the dendritic polymers derived from the PAMAM dendrimer.

Removing the protective Boc groups from the copolymer hydrazides (precursors 5 and 9) with TFA did not change the molecular weight or polydispersity of the copolymers. Star polymer-DTX conjugates 6, 7, 8 and 10, which contained DTX derivatives bound by a pH-sensitive hydrazone bond, were prepared by the reaction of keto groups of DTX derivatives with hydrazide groups of the polymer precursors 5 or 9 in methanol in the presence of a catalytic amount of acetic acid. In all cases, conversion was nearly complete and attachment of DTX derivatives had no significant influence on molecular weight, polydispersity, or Rh of the polymer conjugates.

The Rh of the polymer coil of the dendritic polymer conjugates in aqueous solution was much higher than that of the linear polymer-drug conjugate 4. Star polymer conjugates showed approximately three times higher Rh than the linear conjugate 4. This fulfilled the prerequisite criteria for enhanced accumulation of polymers in solid tumors due to the EPR effect. The scheme of the grafting reaction is given in Fig. 2.

In vitro drug release

The results of the *in vitro* release of DTX and its ester derivatives from polymer conjugates 4, 6, 7 and 8 showed that the release rate of the DTX esters or free drug at pH 7.4 (37 °C) was much lower than that at pH 5 (Fig. 3). After 2 h of incubation of the copolymer conjugates at pH 7.4, 7–24% of total DTX and DTX esters were released, while at pH 5, depending on the DTX ester structure, 50% to almost 92% of liberated DTX ester was found.

The rate of release at both pHs strongly depended on the specific structure of the DTX ester, with the highest release for the OHT ester, a moderate release for the LEV ester and the lowest release for the COV ester. No significant difference in the rate of release for linear conjugate 4 or HMW star polymer conjugate 6 containing DTX-LEV was found. No effect of the size of the copolymer-drug conjugates or steric hindrance to hydrolysis was observed in this case. At pH 7.4, the hydrazone bond was cleaved faster within the first 8 h of incubation, with the rate decreasing in parallel with the decreasing concentration of hydrazone bonds in the solution. Subsequently, in the case of DTX-LEV, free DTX was slowly released by spon-

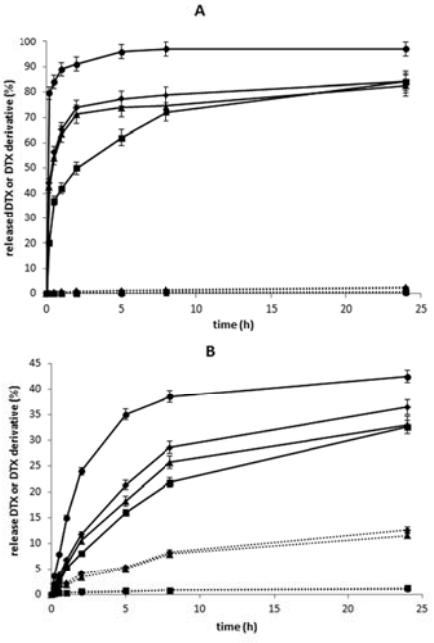

Fig. 3 Release of DTX and DTX derivatives from polymer conjugates 4, 6, 7 and 8 incubated in phosphate buffers at pH 5 (A) and pH 7.4 (B) at 37 °C. (◆ —) conjugate 4, DTX-LEV and DTX; (▲—) conjugate 6, DTX-LEV and DTX; (■ —) conjugate 7, DTX-COV and DTX; (● —) conjugate 8, DTX-OHT and DTX; (◆ ----) conjugate 4, DTX; (▲ ----) conjugate 6, DTX; (■ ----) conjugate 7, DTX; (● ----) conjugate 8, DTX; $n = 3$.

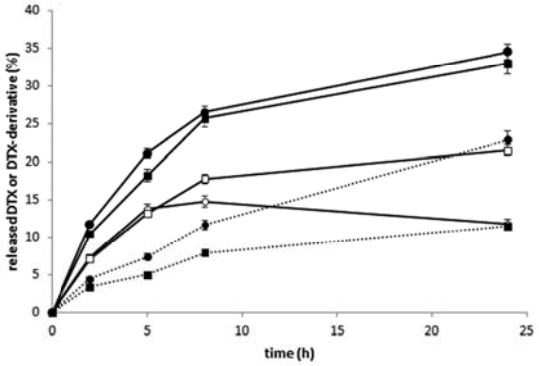

Fig. 4 Release of DTX and DTX derivatives from polymer conjugate 6 incubated in phosphate buffer at pH 7.4 or in human plasma at 37 °C. (■ —) buffer, total DTX released; (□ —) buffer, DTX-LEV; (■ ----) buffer, DTX; (● —) plasma, total DTX released; (○ —) plasma, DTX-LEV; (● ----) plasma, DTX; n = 3.

taneous hydrolysis of the ester bond; 10–12% DTX (~1/3 of total) was released within 24 h of incubation. Contrary to the spontaneous hydrolysis found with DTX-LEV, DTX-OHT and DTX-COV showed no evidence for release of free DTX within 24 h of incubation at pH 7.4. Similarly, no evidence of hydrolysis of the ester bond in all DTX esters was observed during 24 h of incubation at pH 5. Finally, the *in vitro* release experiment carried out with polymer conjugate 6 in human plasma showed almost the same release profile of total released DTX (free DTX and DTX-LEV) as observed in phosphate buffer at pH 7.4 (see Fig. 4).

The major difference in DTX release from polymer 6 in plasma and in a buffer with pH 7.4 was free DTX with a two-fold higher free DTX detected after 24 h of incubation of copolymer 6 in plasma. We suppose that the higher rate of hydrolysis of the ester bond in the released DTX-LEV in plasma was caused by the enzymatic activity of esterases present in human plasma. No evidence of enzymatic hydrolysis of the ester bond in DTX-LEV attached to the polymer was observed during 24 h of incubation in human plasma.

A basic criterion for effective drug delivery is the stability of the system during its transport in the blood and release of the drug at the site of action. Polymer conjugates 4, 6 and 10 containing DTX-LEV better fulfilled this criterion than the others, as demonstrated by the higher difference in the stability in model solutions at pH 5 and 7.4. That was why polymer conjugates 4, 6 and 10 were selected for further *in vitro* and *in vivo* biological evaluation.

In vitro degradation of star polymer carriers

Recently, we have shown that accumulation of the copolymers in solid tumors *via* the EPR effect[24,35] significantly depends on the molecular weight of the polymer conjugate. Linear HPMA-based copolymers are non-biodegradable polymers with a limited potential to be removed from the organism by glomerular filtration when the molecular weight exceeds the renal

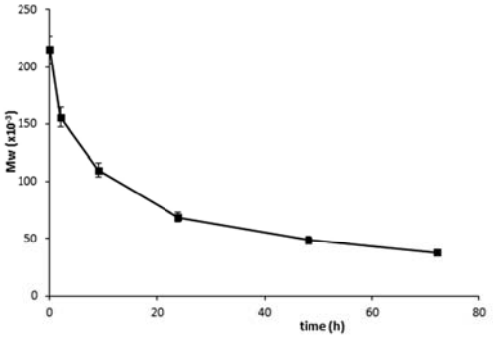

Fig. 5 Decrease in M_w during degradation of polymer 10 in phosphate buffer (pH 6) containing 0.5 μM cathepsin B at 37 °C.

threshold (approx. 50 000 g mol^{-1}).[35] The biodegradable star HPMA-based copolymer 10 consisted of a polymer precursor 2 grafted onto small rigid dendrimer cores *via* an enzymatically degradable oligopeptide sequence. The degradation of the conjugate was studied in phosphate buffer (pH 6) containing cathepsin B to simulate the intracellular environment (lysosomes).

Star polymer conjugate 10, which contained enzymatically degradable GFLG sequences, was hydrolyzed slowly within 72 h of incubation in the buffer containing 0.5 μM cathepsin B (Fig. 5). As expected, the hydrolysis products were polymers with molecular weights comparable with HPMA copolymers used for the synthesis (~35 000 g mol^{-1}). The stability of the star polymer conjugates in buffers mimicking blood circulation was tested by incubation in a phosphate buffer (pH 7.4) or in human plasma. No changes in molecular weight or polydispersity of the conjugates were observed.

The results of enzymatic degradation demonstrated that the conjugate 10 was stable under conditions modeling the blood stream, but underwent degradation after incubation in an intracellular environment-mimicking media. Thus, the HMW polymer-DTX conjugate derived from the PAMAM dendrimer and HPMA copolymers is expected to accumulate in solid tumors, release DTX and degrade inside tumor cells to form polymer fragments excretable from the body by glomerular filtration.

In vitro cytotoxicity of selected conjugates

Cytostatic/cytotoxic activity of star conjugates, either consisting of a non-degradable carrier (conjugate 6) or of a degradable carrier containing GFLG sequences (conjugate 10), was tested using several murine tumor cell lines and compared with the activity of linear conjugates containing DTX-LEV (conjugate 4), free DTX, and the DTX-LEV derivative. As an alternative to the standard measurement of the proliferative capacity of cells by thymidine incorporation, metabolic activity was used as a relevant parameter because the EL4 cell line is characterized by a very low capacity for thymidine incorporation. The DTX-LEV derivative showed pharmacological activity moderately lower than that of the parent drug in all the tested cell lines

Table 3 Cytotoxic/cytostatic activity of polymer-DTX-conjugates expressed as IC_{50}[a]

Cell line	EL4		4T1		LL2		CT26	
Drug/conjugate	IC_{50}[b]	SD	IC_{50}[c]	SD	IC_{50}[c]	SD	IC_{50}[c]	SD
DTX	2.5	0.6	1.7	0.4	5.5	1.5	23	6.9
DTX-LEV	4.3	1.2	3.0	0.5	9.9	3.4	32	10.1
Conjugate 4	6.6	1.6	3.8	1.3	11.1	3.3	36	7.6
Conjugate 6	5.0	2.6	3.6	0.5	9.4	3.0	26	3.5
Conjugate 10	4.9	1.1	2.8	0.8	7.8	2.6	26	8.5

[a] IC_{50} value is expressed as ng of DTX or DTX eq. mL^{-1}. Each IC_{50} value is the mean of data obtained from several independent experiments. [b] Cytotoxic activity detected using the MTT assay [c] Cytostatic activity detected by ^{3}H-TdR incorporation.

(Table 3). Cytostatic/cytotoxic activity of the star polymer conjugates was almost comparable to the activity of DTX-LEV, while the activity of the linear conjugate 4 was slightly lower than that observed in star conjugates. A similar activity relationship between the free drug and the polymer conjugate was observed in cell lines more sensitive to DTX (EL4, 4T1, and LL2), and in less DTX-sensitive cells (CT26). We conclude from these data that the derivatization of DTX by levulinic acid followed by binding of the derivative to the polymer carrier led to the preparation of a conjugate possessing cytotoxic/cytostatic activity in various tumor cell lines *in vitro*. The shape of the polymer carrier only slightly influenced the pharmacological activity of the conjugates *in vitro*, as the star-shaped polymer carriers linking DTX-LEV induced merely higher cytostatic activity than the linear one.

MTD determination of linear and star docetaxel-loaded HPMA copolymers in healthy mice

To determine the *in vivo* maximum tolerated dose (MTD) of linear and star polymer-DTX conjugates, we injected them i.v. into mice at titrated doses up to 200 mg kg^{-1} of DTX eq. of linear conjugate and up to 180 mg kg^{-1} of DTX eq. of star conjugate.

Initially, we determined the approximate MTD on smaller groups of C57BL/6 mice. In these preliminary experiments, we found that MTD of the linear conjugate (conjugate 4) is much higher than 150 mg kg^{-1} of DTX eq. as we observed no signs of toxicity and minimum weight loss (data not shown). In the case of the star conjugate (conjugate 6), we assumed its MTD to lie higher than 100 mg kg^{-1} of DTX eq. because all experimental mice appeared healthy and no morbidity or mortality was observed among groups (data not shown). Simultaneously, we tested the MTD also on BALB/c mice with no differences observed between strains (data not shown).

In accordance with the above mentioned preliminary testing, we injected larger groups of C57BL/6 mice (9 mice per group; 3 random mice were used for histological analysis) with titrated doses of the linear or star conjugate. The linear conjugate (conjugate 4) was administered at a dose of 200 mg kg^{-1} of DTX eq., which was the highest dose that we was able to solubilize and inject into mice as a bolus. Nevertheless, it still appeared to be safe with minimum weight loss and no signs of toxicity (Fig. 6A).

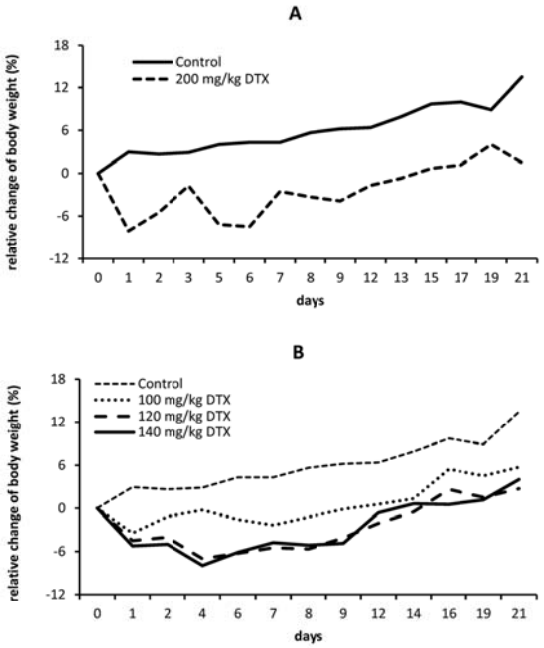

Fig. 6 Determination of MTD of linear polymer-DTX and star polymer-DTX. C57BL/6 mice were i.v. injected with 200 mg kg^{-1} of DTX eq. of linear polymer-DTX conjugate (A); 100, 120 and 140 mg kg^{-1} of DTX eq. of star polymer-DTX conjugate (B) and their body weight was monitored until day 21 post administration. Mice i.v. injected with PBS were used as controls. Each experimental group contained 6 mice.

Thus we suspect that the MTD is much higher and unreachable in a single dose injection (due to the high viscosity of the polymer solution) leaving a wide therapeutic window for this application of the conjugates. In the case of the star conjugate (conjugate 6), it was injected at doses of 100, 120 and 140 mg kg^{-1} of DTX eq. We observed no pathology or weight loss (Fig. 6B); therefore, we injected a small group of mice (3 mice per group) with 180 mg kg^{-1} of DTX eq., *i.e.*, the highest dose that we were able to solubilize. Mice showed an approx. 15% weight reduction with mild signs of toxicity (data not shown), which led us to the assumption that MTD of the star conjugate

lies between 140 and 180 mg kg^{-1} of DTX eq. In comparison with free DTX, which has an MTD of approximately 40 mg kg^{-1},[36] both conjugates have significantly lowered toxicity and a wide therapeutic window.

Histological analysis of selected organs

Histology of selected organs from 3 random experimental mice was performed on day 7 post injection. Spleen, kidney, liver and vertebral bone marrow were analysed, and no pathological differences or anomalies were observed compared with naïve control mice. Similar results were observed in mice injected with free DTX at its MTD. Therefore, we assume that the tested conjugates cause no observable damage to tissues and organs including bone marrow and are safe up to the maximum dose applicable in a bolus.

In vivo anti-tumor activity

The HMW star conjugates were designed to achieve enhanced tumor accumulation, leading to an improved anti-tumor effect for the treatment of solid tumors. In an EL4 lymphoma model, we observed an anti-tumor effect of conjugate 6 that was significantly better than the effect of the linear polymer-DTX conjugate (conjugate 4) or free DTX-LEV derivative, even at low dosing. Administration of 20 mg DTX eq. per kg on days 8 and 12 post tumor transplantation significantly reduced the tumor growth, prolonged survival time (median survival 100.5 days *vs.* 26 days in untreated controls), and finally led to complete cure in 50% of the mice treated with the star conjugate (conjugate 6). The linear polymer-DTX conjugate (conjugate 4) also significantly reduced the tumor growth (Fig. 7A) and prolonged survival when compared with untreated controls (median 39 days *vs.* 26 days), but only 25% of the mice remained tumor-free (Fig. 7B).

Indeed, treatment with free DTX-LEV led only to a slightly prolonged survival (median 34 days *vs.* 26 days in untreated controls) and only 1 of 8 mice was alive after the treatment. The body weight of the treated mice remained stable at least until day 25, documenting that the treatment with the conjugates was not associated with systemic toxicity (data not shown). Upon the second tumor challenge, the animals cured with the polymer conjugates (conjugates 4 and 6) showed tumor resistance, manifested by the absence of tumor growth even without any treatment. In contrast, the resistance was not apparent in the DTX-LEV-cured animal (Fig. 7B).

The enhanced anti-tumor activity of the HMW star conjugate could be directly related to increased accumulation of the drug in the tumor tissue due to the EPR effect. This is concordant with our previous data concerning a similar star conjugate containing doxorubicin.[23,35] This star DOX conjugate caused larger drug accumulation in the tumor than a linear one, peaking at 24 hours post administration. The enhanced drug accumulation is predominantly dependent on the size of the polymer carrier.[35] We hypothesize that similar to DOX conjugates, enhanced accumulation of DTX could be achieved with the star conjugate, leading to an increased anti-tumor effect. It should be noted that the size of the star DTX conjugate is approximately 26 to 30 nm (Table 2); thus, we assume that these conjugates would have a good ability to penetrate into the tissue.

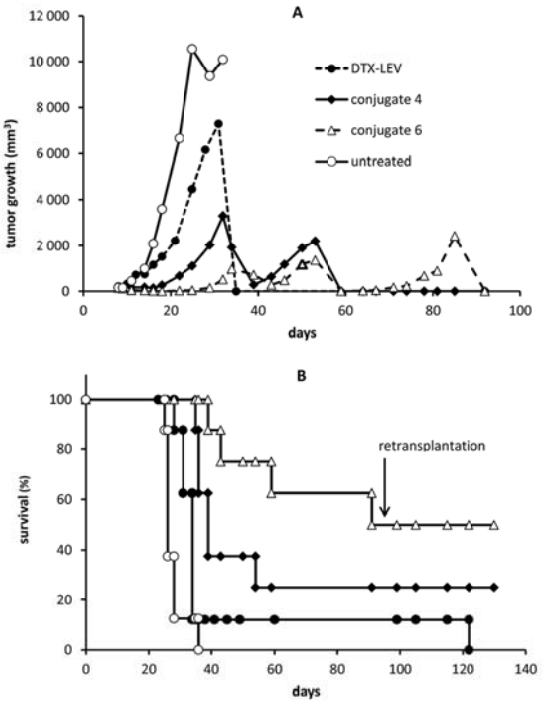

Fig. 7 Comparison of anti-tumor activities of linear DTX conjugate (conjugate 4), star non-degradable DTX conjugate (conjugate 6) and free DTX-LEV derivative in the murine EL4 lymphoma model. C57BL/6 mice were transplanted with 1 × 10^5 EL4 cells s.c. and treated with 20 mg DTX eq. per kg or DTX-LEV injected i.v. on days 8 and 12. The long-term survivors, in which the tumors completely regressed, were challenged with 1 × 10^5 EL4 cells s.c. on day 95 after the first tumor transplantation and left without any treatment. Tumor growth (A) and survival time (B) were monitored.

Combined, the high MTD and the low dose anti-tumor effects of the DTX star demonstrate their considerable therapeutic potential and low/undetectable systemic toxicity. We have already shown that reduced toxicity of drug conjugates toward the immune system is a prerequisite for obtaining safe cancer treatments, which may lead to immunologically mediated tumor resistance, which has been observed in experimental tumor treatments and even in patients.[30,37,38] The cancer resistance resulting from the treatment with HPMA copolymer conjugates serves as a safeguard against the cancer recurrence. Currently, consensus exists that modern cancer therapy not only kills the cancer but also initiates anti-cancer immune responses. The way the cancer cells die upon treatment is essential for initiating anti-cancer immune responses that support the therapy and is responsible for the final outcome of therapy. Cancer cell killing and anti-cancer immune responses are inseparable components of successful

cancer therapy.[39,40] Intact immune mechanisms were shown to be a prerequisite for the complete experimental tumor regression induced by HPMA-based polymer therapeutics.[41] In DOX-containing HPMA conjugates, induction of immunogenic cancer cell death was documented.[37,41–43] Some modulatory effects at low concentrations were also observed in DTX treatment, such as a reduction in immunosuppressive capacity of myeloid-derived suppressor cells that dampen the anti-cancer immune responses of the host organism in tumor-bearing animals and patients.[44] We speculate that a similar activity could manifest also in treatment with DTX bound to the HPMA copolymer carrier. In addition to the previously described star polymer-DOX conjugates,[23,35] we can summarise that HMW star polymer carriers could be used not only for enhanced drug delivery of soluble drugs as DOX, but also for solubilisation, elimination of systemic toxicity, controlled drug delivery and the related increase in the anti-tumor effect of highly hydrophobic, non-water soluble drugs such as DTX.

Conclusions

In the present study we described the synthesis, physicochemical characterization, *in vitro* drug release, biodegradation and *in vivo* anti-cancer activity of high-molecular-weight DTX conjugates based on star HPMA copolymer carriers. The increased size of the star conjugates as compared with the linear conjugates makes them excellent candidates for solid tumor treatment based on the enhanced passive accumulation driven by the EPR effect. Three types of star conjugates were synthesized with different hydrazone-containing spacers between the DTX and HPMA copolymer to enable controlled drug release in solutions modeling intracellular or intratumoral environments. The rate of release of DTX and/or its ester derivative is strongly dependent on the specific structure in the vicinity of the hydrazone bond, being the highest for the spacer containing the OHT ester of DTX, moderate for the LEV ester and the lowest for the COV ester. No significant difference was found in the rate of release when a linear conjugate or HMW star polymer conjugate was studied. *In vivo* evaluation of the MTD and anti-cancer activity of the star DTX-polymer conjugates confirmed their very low toxicity and superior activity over the linear polymer conjugate or free DTX in the treatment of EL4 T-cell lymphoma in mice. We have found that the star DTX conjugate had a remarkably higher MTD compared with DTX (single dose 140–180 mg DTX eq. kg^{-1} *vs.* 40 mg kg^{-1} stated for DTX), thus the conjugation of DTX to the HMW polymer carriers led to a significant decrease in systemic toxicity and opened a wide therapeutic window for the treatment of selected solid tumors. A remarkably high anti-tumor effect was induced in treating experimental murine EL4 lymphoma even at suboptimal doses of the star DTX conjugate (20 mg kg^{-1} DTX eq., below 14% of MTD) resulting in a 50% cure rate, significantly exceeding the effect induced by the linear DTX conjugate or free DTX-LEV. In conclusion, we illustrated that the star pH-sensitive polymer-DTX conjugates have the potential to induce an excellent *in vivo* anti-tumor effect without apparent adverse effects.

Acknowledgements

This work was supported by the Czech Science Foundation (project no. P301/11/0325 and P207/12/J030) and the Ministry of Education, Youth and Sports of the Czech Republic (project CZ.1.07/2.3.00/20.0055), and Institutional Research Concept RVO 61388971. The authors thank Pavlina Jungrova and Helena Misurcova for technical assistance.

Notes and references

1 R. Haag and F. Kratz, *Angew. Chem., Int. Ed.*, 2006, **45**, 1198–1215.
2 J. Kopecek, P. Kopeckova, T. Minko, Z. R. Lu and C. M. Peterson, *J. Controlled Release*, 2001, **74**, 147–158.
3 Y. Matsumura and H. Maeda, *Cancer Res.*, 1986, **46**, 6387–6392.
4 J. Fang, H. Nakamura and H. Maeda, *Adv. Drug Delivery Rev.*, 2011, **63**, 136–151.
5 H. Maeda, *Proc. Jpn. Acad. B: Phys.*, 2012, **88**, 53–71.
6 T. Lammers, *J. Controlled Release*, 2012, **161**, 151–151.
7 V. Torchilin, *Adv. Drug Delivery Rev.*, 2011, **63**, 131–135.
8 R. Duncan, *Nat. Rev. Drug Discovery*, 2003, **2**, 347–360.
9 J. Kopecek, P. Kopeckova, T. Minko and Z. R. Lu, *Eur. J. Pharm. Biopharm.*, 2000, **50**, 61–81.
10 K. Ulbrich, V. Subr, J. Strohalm, D. Plocova, M. Jelinkova and B. Rihova, *J. Controlled Release*, 2000, **64**, 63–79.
11 T. Etrych, P. Chytil, T. Mrkvan, M. Sirova, B. Rihova and K. Ulbrich, *J. Controlled Release*, 2008, **132**, 184–192.
12 K. Ulbrich, T. Etrych, P. Chytil, M. Jelinkova and B. Rihova, *J. Controlled Release*, 2003, **87**, 33–47.
13 D. Wang, P. Kopeckova, T. Minko, V. Nanayakkara and J. Kopecek, *Biomacromolecules*, 2000, **1**, 313–319.
14 Y. Noguchi, J. Wu, R. Duncan, J. Strohalm, K. Ulbrich, T. Akaike and H. Maeda, *Jpn. J. Cancer Res.*, 1998, **89**, 307–314.
15 L. W. Seymour, Y. Miyamoto, H. Maeda, M. Brereton, J. Strohalm, K. Ulbrich and R. Duncan, *Eur. J. Cancer*, 1995, **31A**, 766–770.
16 T. Etrych, T. Mrkvan, P. Chytil, C. Konak, B. Rihova and K. Ulbrich, *J. Appl. Polym. Sci.*, 2008, **109**, 3050–3061.
17 P. S. Steyger, D. F. Baban, M. Brereton, K. Ulbrich and L. W. Seymour, *J. Controlled Release*, 1996, **39**, 35–46.
18 D. Putnam and J. Kopecek, *Adv. Polym. Sci.*, 1995, **122**, 55–123.
19 K. Ulbrich, J. Strohalm, V. Subr, D. Plocova, R. Duncan and B. Rihova, *Macromol. Symp.*, 1996, **103**, 177–192.
20 F. Kratz, U. Beyer and M. T. Schutte, *Crit. Rev. Ther. Drug*, 1999, **16**, 245–288.

21 P. C. A. Rodrigues, T. Roth, H. H. Fiebig, C. Unger, R. Mulhaupt and F. Kratz, *Bioorgan Med. Chem.*, 2006, **14**, 4110–4117.

22 K. Ulbrich and V. Subr, *Adv. Drug Delivery Rev.*, 2004, **56**, 1023–1050.

23 T. Etrych, L. Kovar, J. Strohalm, P. Chytil, B. Rihova and K. Ulbrich, *J. Controlled Release*, 2011, **154**, 241–248.

24 T. Etrych, J. Strohalm, P. Chytil, P. Cernoch, L. Starovoytova, M. Pechar and K. Ulbrich, *Eur. J. Pharm. Sci.*, 2011, **42**, 527–539.

25 J. F. Diaz and J. M. Andreu, *Biochemistry*, 1993, **32**, 2747–2755.

26 D. Belotti, V. Vergani, T. Drudis, P. Borsotti, M. R. Pitelli, G. Viale, R. Giavazzi and G. Taraboletti, *Clin. Cancer Res.*, 1996, **2**, 1843–1849.

27 D. S. Grant, T. L. Williams, M. Zahaczewsky and A. P. Dicker, *Int. J. Cancer.*, 2003, **104**, 121–129.

28 S. S. W. Ng, A. Sparreboom, Y. Shaked, C. Lee, S. Man, N. Desai, P. Soon-Shiong, W. D. Figg and R. S. Kerbel, *Clin. Cancer Res.*, 2006, **12**, 4331–4338.

29 P. M. Ma and R. J. Mumper, *J. Nanomed. Nanotechnol.*, 2013, **4**, 1–16.

30 T. Etrych, M. Sirova, L. Starovoytova, B. Rihova and K. Ulbrich, *Mol. Pharmaceutics*, 2010, **7**, 1015–1026.

31 H. Cabral, Y. Matsumoto, K. Mizuno, Q. Chen, M. Murakami, M. Kimura, Y. Terada, M. R. Kano, K. Miyazono, M. Uesaka, N. Nishiyama and K. Kataoka, *Nat. Nanotechnol.*, 2011, **6**, 815–823.

32 K. Ulbrich, T. Etrych, P. Chytil, M. Jelinkova and B. Rihova, *J. Drug Targeting*, 2004, **12**, 477–489.

33 T. Etrych, P. Chytil, M. Jelinkova, B. Rihova and K. Ulbrich, *Macromol. Biosci.*, 2002, **2**, 43–52.

34 V. Subr and K. Ulbrich, *React. Funct. Polym.*, 2006, **66**, 1525–1538.

35 T. Etrych, V. Subr, J. Strohalm, M. Sirova, B. Rihova and K. Ulbrich, *J. Controlled Release*, 2012, **164**, 346–354.

36 U. Vanhoefer, S. Cao, A. Harstrick, S. Seeber and Y. M. Rustum, *Ann. Oncol.*, 1997, **8**, 1221–1228.

37 M. Sirova, M. Kabesova, L. Kovar, T. Etrych, J. Strohalm, K. Ulbrich and B. Rihova, *Curr. Med. Chem.*, 2013, **20**, 4815–4826.

38 M. Sirova, J. Strohalm, V. Subr, D. Plocova, P. Rossmann, T. Mrkvan, K. Ulbrich and B. Rihova, *Cancer Immunol. Immun.*, 2007, **56**, 35–47.

39 A. M. M. Eggermont, G. Kroemer and L. Zitvogel, *Eur. J. Cancer*, 2013, **49**, 2965–2967.

40 A. J. M. Thomas, *Expert Opin. Biol. Ther.*, 2014, **14**, 1–4.

41 B. Rihova and M. Kovar, *Adv. Drug Delivery Rev.*, 2010, **62**, 184–191.

42 B. Rihova, J. Strohalm, K. Hoste, M. Jelinkova, O. Hovorka, M. Kovar, D. Plocova, M. Sirova, M. Stastny, E. Schacht and K. Ulbrich, *Macromol. Symp.*, 2001, **172**, 21–28.

43 B. Rihova, J. Strohalm, J. Prausova, K. Kubackova, M. Jelinkova, L. Rozprimova, M. Sirova, D. Plocova, T. Etrych, V. Subr, T. Mrkvan, M. Kovar and K. Ulbrich, *J. Controlled Release*, 2003, **91**, 1–16.

44 K. N. Kodumudi, K. Woan, D. L. Gilvary, E. Sahakian, S. Wei and J. Y. Djeu, *Clin. Cancer Res.*, 2010, **16**, 4583–4594.

Journal of Controlled Release 223 (2016) 1–10

Contents lists available at ScienceDirect

Journal of Controlled Release

journal homepage: www.elsevier.com/locate/jconrel

The structure-dependent toxicity, pharmacokinetics and anti-tumour activity of HPMA copolymer conjugates in the treatment of solid tumours and leukaemia

Barbora Tomalova [a], Milada Sirova [a], Pavel Rossmann [a], Robert Pola [b], Jiri Strohalm [b], Petr Chytil [b], Viktor Cerny [a], Jakub Tomala [a], Martina Kabesova [a], Blanka Rihova [a], Karel Ulbrich [b], Tomas Etrych [b], Marek Kovar [a,*]

[a] Institute of Microbiology, Czech Academy of Sciences, Videnska 1083, 14220 Prague, Czech Republic
[b] Institute of Macromolecular Chemistry, Czech Academy of Sciences, Heyrovskeho nam. 2, 16206 Prague, Czech Republic

ARTICLE INFO

Article history:
Received 7 September 2015
Received in revised form 4 December 2015
Accepted 14 December 2015
Available online 18 December 2015

Keywords:
HPMA
Doxorubicin
Structure
Toxicity
Anti-tumour activity

ABSTRACT

Polymer drug carriers that are based on *N*-(2-hydroxypropyl)methacrylamide (HPMA) copolymers have been widely used in the development and synthesis of high-molecular-weight (HMW) drug delivery systems for cancer therapy. In this study, we compared linear (M_w ~27 kDa, R_h ~4 nm) and non-degradable star (M_w ~250 kDa, R_h ~13 nm) HPMA copolymer conjugates bearing anthracycline antibiotic doxorubicin (DOX) bound via pH-sensitive hydrazone bond. We determined the in vitro and in vivo toxicity of both conjugates and their maximum tolerated dose (MTD). We also compared their anti-tumour activity in mouse B-cell leukaemia (BCL1) and a mouse T-cell lymphoma (EL4) model. We found that MTD was higher for the linear conjugate (85 mg DOX/kg) and lower for the star conjugate (22.5 mg DOX/kg). An evaluation of the intestinal barrier integrity using FITC-dextran as a gut permeability tracer proved that no pathology was caused by the MTD of either conjugate. However, free DOX showed some damage to the gut barrier. The therapy of BCL1 leukaemia by both of the polymeric conjugates using the MTD or its fraction (i.e., equitoxic dosage) showed better results in the case of the star conjugate. On the other hand, treatment of EL4 lymphoma seemed to be more efficient when the linear conjugate was used. We suppose that the anti-cancer treatment of solid tumours and leukaemias requires different types of drug conjugates. We hypothesise that the most suitable HPMA copolymer-DOX conjugate for the treatment of solid tumours should have an HMW structure with increased R_h that would be stable for three to four days after the conjugate administration and then rapidly disintegrate in the short polymer chains, which are excretable from the body by glomerular filtration. On the other hand, the treatment of leukaemia requires a drug conjugate with a long circulation half-life. This would provide an active drug, whilst slowly degrading to excretable fragments.

1. Introduction

Anti-tumour chemotherapeutics are mostly small molecules with an extremely short circulation half-life. Their therapeutic window, i.e., the range of dosages that are effective for therapy while staying within the safety range, is usually quite narrow. Furthermore, treatment with these drugs is often accompanied with severe side toxicities.

The disadvantages of classical chemotherapy led to the development of high-molecular-weight (HMW) drug delivery systems that passively or actively accumulate in tumours where the drug is released. This lowers its systemic toxicity. In most types of solid tumours, the passive accumulation of macromolecules is described as the Enhanced Permeability and Retention effect (EPR) [1]. This principle is based on the abnormal architecture of tumour tissue. Capillaries are fenestrated with large pores of up to several hundreds of nanometres. This allows extravasation of the macromolecules from circulation [2–4]. Together with a limited lymphatic drainage, this results in the accumulation of macromolecules (≥40 kDa) in solid tumours. Theek et al. [5] reported a positive correlation between the degree of tumour vascularization and EPR-mediated tumour accumulation. Nevertheless, the EPR effect is highly variable. It varies significantly, not only between different types of tumours depending on the rate of their growth but also, within a single tumour where the structure of vessels can be quite diverse [1,6,7].

* Corresponding author at: Institute of Microbiology, Czech Academy of Sciences, Videnska 1083, 14220 Prague, Czech Republic.
E-mail addresses: barbora.tomalova@biomed.cas.cz (B. Tomalova), sirova@biomed.cas.cz (M. Sirova), rossmannp@seznam.cz (P. Rossmann), pola@imc.cas.cz (R. Pola), strohalm@imc.cas.cz (J. Strohalm), chytil@imc.cas.cz (P. Chytil), viktor.cerny@biomed.cas.cz (V. Cerny), tomala@biomed.cas.cz (J. Tomala), kabesova@biomed.cas.cz (M. Kabesova), rihova@biomed.cas.cz (B. Rihova), ulbrich@imc.cas.cz (K. Ulbrich), etrych@imc.cas.cz (T. Etrych), makovar@biomed.cas.cz (M. Kovar).

http://dx.doi.org/10.1016/j.jconrel.2015.12.023
0168-3659/

The EPR effect has been widely exploited in the design of HMW drug delivery systems, which employ large molecules or nanoparticles as drug carriers [8]. Different biodistribution, stability in circulation and the controlled release of the drug, together with the significantly lowered side toxicity, make these delivery systems promising tools for cancer therapy. Moreover, attachment of a targeting moiety (e.g., tumour antigen-specific antibody) to the drug carrier leads to specific and active accumulation of the drug(s) in the tumour site in addition to the EPR effect. However, recent data indicate that, over time, passive targeting could be superior to active targeting [9].

One of the most intensively studied HMW drug delivery system is based on *N*-(2-hydroxypropyl)methacrylamide (HPMA) copolymers, a water-soluble biocompatible drug carrier that is able to carry multiple pendant functional groups [8]. Attachment of the selected drug(s) – either via enzymatically degradable amide bond or via pH-sensitive hydrazone bond to HPMA copolymers – prolongs their circulation half-life and lowers toxicity in comparison to free drug(s) [10–14]. Furthermore, the hydrophilic character of the HPMA copolymer enables the solubilization of highly hydrophobic drug(s). The anthracycline drug, doxorubicin (DOX), is the most frequently used cytostatic drug for binding to HPMA copolymer carriers.

A wide variety of HPMA copolymer-based drug delivery systems have been designed. These range from simple linear conjugates, which are composed of a HPMA-copolymer chain with biologically active moieties, to complicated robust star-like systems with a dendrimer core bearing a number of HPMA-copolymer chains with the desired therapeutics. These systems differ in molecular weight, structure and other features. Thus, they show different biological properties, e.g., biodistribution, circulation half-life or anti-tumour activity [15].

In this study, we aimed to evaluate and compare the maximum tolerated dose (MTD), accumulation in tumour and anti-tumour activity of a linear (M_w ~27 kDa, R_h ~4 nm) and star-like HPMA-DOX conjugate with poly(amido amine) (PAMAM) dendrimer core (M_w ~250 kDa, R_h ~13 nm) in vivo. Both conjugates carried DOX bound via pH-sensitive hydrazone bond. We proved that they possess considerably lowered toxicity, wider therapeutic window, prolonged circulation half-life and higher anti-tumour activity than the free DOX. The conjugates significantly differed in maximum tolerated dose, with the linear conjugate having a wider therapeutic window than the star-like one.

2. Materials and methods

2.1. Synthesis of the polymer precursors and polymer-drug conjugates

Polymer precursors containing hydrazide groups were prepared, as previously described [16]. Briefly, linear L-Hy was prepared by a radical copolymerization of HPMA with a comonomer containing hydrazide groups. The star HMW polymer S-Hy and star enzymatically degradable polymer S(GFLG)-Hy were prepared by grafting semitelechelic linear HPMA-based polymers, which contained chain end reactive groups, onto second generations of PAMAM dendrimers. DOX was attached to the polymer precursors L-Hy, S-Hy and S(GFLG)-Hy by the reaction of the respective precursor with DOX.HCl in methanol in the dark.

The star polymer S-homo was prepared from HPMA homopolymer grafts, which were attached to the PAMAM dendrimer core by the same procedure that is described by Etrych et al. [16].

2.2. The polymer carriers and conjugates

In this study, we used a linear HPMA copolymer-DOX conjugate (conjugate 1), a non-degradable star HPMA copolymer-DOX conjugate (conjugate 2), a degradable star HPMA copolymer-DOX conjugate (conjugate 3), a star polyHPMA carrier with hydrazide groups (S-hy) and a star polyHPMA carrier (S-homo) based on HPMA homopolymer. Their schematic structures are depicted in Fig. 1 and specifications are listed in Table 1. DOX was bound to the polymer carrier via a pH sensitive hydrazone bond. The doses of the HPMA copolymer-DOX conjugates are referred to as DOX equivalent per kg (mg DOX/kg).

2.3. In vitro cytotoxicity

The employed murine cancer cell lines included: EL4.IL2 T-cell lymphoma (ATCC TIB-181; C57BL/6, *H-2*^{b}), LL2 lung carcinoma (ATCC CRL-1642; C57BL/6, *H-2*^{b}), and BCL1 B-cell leukaemia (ATCC TIB-197; BALB/c, *H-2*^{d}). All of the cell lines were purchased from ATCC, and maintained as recommended by the provider. The cells were cultivated in 96-well flat-bottomed culture plates (Nunclon, Denmark) with various concentrations of conjugates and free DOX for three days. At the beginning of cultivation, the cell counts were 5000 cells/well. Cell proliferation was estimated by a standard [^{3}H]-thymidine incorporation assay. The IC50 values were calculated as the drug concentrations that inhibit cell proliferation or metabolic activity by 50% during the three-day cultivation.

2.4. The mice

Inbred BALB/c (*H-2d*) and C57BL/6 (*H-2b*) mice were obtained from the animal breeding facility of the Institute of Physiology, Academy of Sciences of the Czech Republic, v.v.i. Mice were used at between nine and fifteen weeks of age, and food and water were given *ad libitum*. In all animal works, institutional guidelines for the care and use of laboratory animals were strictly followed under a protocol approved by the Institutional Animal Care and Use Committee of the Academy of Sciences of the Czech Republic, and conducted in compliance with local and European guidelines.

2.5. The maximum tolerated dose of the linear and non-degradable star HPMA copolymer-bound doxorubicin

BALB/c or C57BL/6 mice were i.v. injected with conjugate 1 or conjugate 2 in 300–400 μl of PBS at doses of 70, 85, 100, 120 and 140 mg DOX/kg for conjugate 1; 17.5, 20, 22.5, 27.5, 40 and 60 mg DOX/kg for conjugate 2. The mice that were injected with PBS, free DOX (10 mg/kg, i.e., MTD [17,18], S-Hy or S-homo (dose equivalent to conjugate 2, given at a dose of 22.5 mg DOX/kg) or conjugate 3 (22.5 mg DOX/kg) were used as controls. The number of mice per group ranged between three and nine. The injected mice were monitored daily or every other day until 21 days post-application. We defined the MTD as the highest dose that should elicit minimal signs of toxicity (i.e., ruffled fur, cachexy, muscle tremor and hunched posture), no deaths and the average weight loss should not exceed 15% of the body mass [19–21].

2.6. Histology

For the histological analysis, three random mice from the groups that were injected with 70, 85 and 100 mg DOX/kg of conjugate 1; 17.5, 22.5 and 27.5 mg DOX/kg of conjugate 2 were sacrificed on day seven post-injection. Three random mice selected from the groups that were injected with PBS, free DOX (10 mg/kg), conjugate 3 (22.5 mg DOX/kg), and S-Hy or S-homo (at dose eq. to conjugate 2, given at 22.5 mg DOX/kg) were used as controls. Moreover, for a further histological analysis, three random mice from the groups that were injected with conjugate 2 and conjugate 3 (22.5 mg DOX/kg), and S-Hy or S-homo (at dose eq. to conjugate 2, given at 22.5 mg DOX/kg) were sacrificed on day 18 post-injection. Tissue samples of the spleen, liver, vertebral bone marrow and kidney were sampled, fixed in 5% formalin, embedded in paraffin and stained with haematoxylin/eosin (H&E). The vertebral column had been decalcified in 10% formic acid. The cryostat sections of the selected samples (liver and spleens) were stained with Oil Red O, Sudan Black B and Luxol Fast Blue.

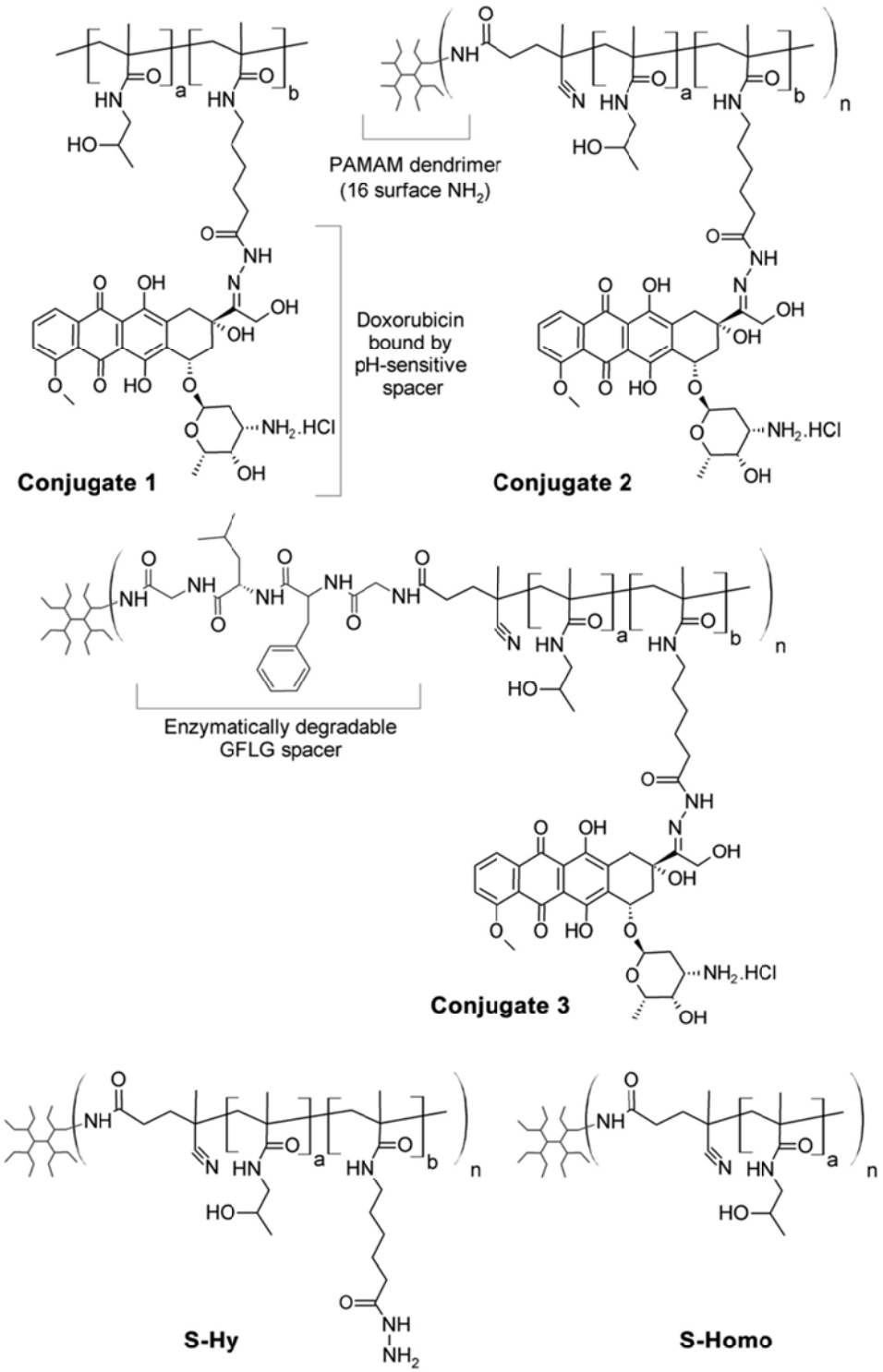

Fig. 1. Schematic structures of polymer carriers and DOX-conjugates.

Table 1
Characteristics of the star HPMA-based carriers and HPMA copolymer-DOX conjugates.

Polymer or conjugate	Polymer description	M_w (g·mol^{-1})	M_w/M_n	DOX (wt.%)	R_h (nm)
Conjugate 1	Linear conjugate	27 000	1.80	8.90[†]	4.3
Conjugate 2	Star nondegradable conjugate	280 000	1.50	10.02[‡]	12.8
Conjugate 3[*]	Star enzymatically degradadable conjugate	282 000	1.83	10.00[‡]	13.0
S-hy	Star polymer precursor with hydrazide groups	210 000	1.90	-	12.3
S-homo	Star polymer without reactive group	374 000	1.665	-	13.6

[*] Biodegradable polymer via GFLG sequence cleavable by lysosomal enzymes.
[†] Content of free Dox < 0.1% of total DOX content.
[‡] Content of free Dox < 0.2% of total DOX content.

2.7. Blood clearance and determination of DOX content in the tumour tissue

C57BL/6 mice were s.c. transplanted with 1×10^5 EL4 lymphoma cells into the right flank. When the tumour reached a diameter of 5–8 mm, the mice were i.v. injected with PBS (control), DOX (100% MTD; i.e., 10 mg/kg; Adriblastina, Teva), conjugate 1 (100% MTD; i.e., 85 mg DOX/kg) or conjugate 2 (100% MTD; i.e., 22.5 mg DOX/kg) in 300 μl of PBS. After the injection, samples of blood and tumour tissue were harvested at the following time intervals: 3 (only blood), 6, 12, 24, 48, 72 and 96 h (samples from three mice per each interval). Blood samples were collected from the tail vein (3 h interval only) or from the carotid artery (other time points) into heparinized tubes. The tissue samples were excised, weighted and homogenized in a glass homogenizer. All of the samples were stored at −20 °C. The total DOX content (free and polymer-bound DOX) was determined in each sample after quantitative acid hydrolysis in 1 M HCl (1 h, 50 °C). Doxorubicinone, an aglycon of DOX formed from free and polymer-bound DOX after hydrolysis, was extracted with chloroform. The organic phase was evaporated and the remaining solid phase was completely dissolved in methanol and analysed using a gradient-based HPLC Shimadzu system, which was equipped with a fluorescence detector (Shimadzu RF-10Axl; $\lambda_{exc} = 488$ nm, $\lambda_{em} = 560$ nm). The calibration curve was obtained by the injection of the exact doses of free DOX into heparinized blood.

2.8. Gut permeability assay

The integrity of the intestinal barrier was investigated as described in Viaud et al. 2013 [22]. Briefly, the C57BL/6 mice were i.v. injected with PBS (control), free DOX and conjugate 1 or conjugate 2 (100% MTD). Three days afterwards, the mice were fasted for 4 h and then fed with FITC-dextran (4 kDa, Sigma Aldrich) in 100 μl of PBS at dose of 0.44 mg/g. After 4 h, the mice were euthanized and exsanguinated from the carotid artery. Blood was collected and the plasma levels of FITC-dextran were determined on a fluorescence spectrophotometer (ex/em = 485/535 nm).

2.9. In vivo tumour treatment

The anti-tumour activity of the conjugates was tested in mice that were transplanted with a lethal dose of EL4 lymphoma (ATCC TIB-39; C57BL/6, *H-2*^{b}) or BCL1 leukaemia cells. On day zero, the C57BL/6 mice were s.c. injected with 1×10^5 EL4 T-cell lymphoma cells into the shaved right flank. The mice with palpable tumours that reached 5–8 mm in diameter within eight days were i.v. injected with titrated doses of conjugates, which were diluted in 300–400 μl of PBS. On day zero, the BALB/c female mice were i.p. injected with 5×10^5 BLC1 leukaemia cells. On day 11, titrated doses of conjugates that were diluted in 300–400 μl of PBS were i.v. injected. The mice that survived until day 60 (EL4 lymphoma) or day 180 (BCL1 leukaemia) without any signs of tumour were considered as long-term survivors (LTS). These mice were re-challenged with a lethal dose of tumour cells (1×10^5 EL4 or 5×10^4 BCL1 cells) and left untreated to determine their anti-tumour resistance.

The mice that were inoculated with the tumour cells and injected with PBS alone were used as controls. Tumour progression was checked every other day. Tumour size (in case of EL4 lymphoma), the body weight of the mice and survival (in both models) were monitored. Experimental groups were composed of eight animals. The EL4 tumour volume was calculated as $V = a \cdot b^2/2$, where a — the longer diameter and b = the smaller diameter.

2.10. Statistical analysis

Analysis used ANOVA followed by Tukey test for pairwise comparison of sub-groups; *, **, and *** represent p-value <0.05, 0.01 and 0.001, respectively. Data are representative of at least two experiments.

3. Results

3.1. The cytostatic activity of selected HPMA copolymer-DOX conjugates in vitro

The cytostatic activity of conjugates 1–3 was tested in three different cancer cell lines (EL4.IL2, BCL1 and LL2) in vitro and compared with the activity of free DOX. All of the conjugates had lower cytostatic activity than the free DOX in all of the tested cell lines (Table 2). The cytostatic activity of conjugates 2 and 3 was negligibly higher than the activity of conjugate 1. Thus, the cytostatic activity in various tumour cell lines *in vitro* was not significantly affected by the structure and size of the polymer carrier.

3.2. Determination of the maximum tolerated dose

In preliminary experiments, we evaluated the toxicity of both of the conjugates in small groups of BALB/c and C57BL/6 mice (three mice/group) to get the approximate values of MTD. Based on these data, we assumed that the MTD of conjugate 1 is a little bit lower than 100 mg DOX/kg (data not shown), since this dose showed a weight loss >25% and other signs of toxicity (cachexia, ruffled fur). The MTD of conjugate 2 was found to be between 20 and 30 mg DOX/kg (data not shown), as 20 mg DOX/kg appeared to be non-toxic and 30 mg DOX/kg led to mild toxicity (weight loss >15%). We observed no significant differences between the tested mice strains. Thus, to follow accurate studies, we only employed C57BL/6 mice.

Table 2
The cytostatic activity of HPMA copolymer-DOX conjugates as IC_{50}[a].

Cell line	EL4.IL2	LL2	BCL1
Drug/conjugate	$IC_{50} \pm SD$	$IC_{50} \pm SD$	$IC_{50} \pm SD$
DOX	11.5 ± 2.12	27.0 ± 2.83	0.7 ± 0.36
Conjugate 1	145.0 ± 7.07	165.0 ± 7.07	4.7 ± 0.58
Conjugate 2	115.0 ± 7.07	125.0 ± 7.07	2.9 ± 0.23
Conjugate 3	100.0 ± 14.14	100.0 ± 0.00	3.3 ± 0.58

[a] IC_{50} value is expressed as concentration of DOX (ng/ml) which inhibits cell proliferation to 50% of control cells. Mean IC50 values and standard deviations (SD) were calculated from two independent experiments. Cell proliferation was estimated by [^{3}H]-thymidine incorporation assay.

Next, we i.v. injected nine mice per group with titrated doses of either conjugate 1 or 2 to determine the MTD more precisely. Three mice from each group were sacrificed on day seven post-injection for histological analysis of the selected organs. The remaining mice were monitored until day 21. The administration of conjugate 1 at doses of 70, 85 and 100 mg DOX/kg showed that its MTD is approximately 85 mg DOX/kg, as we observed no mortality and only a marginal decrease in body weight (Fig. 2A). Conjugate 2 was given at doses of 17.5, 22.5 and 27.5 mg DOX/kg. We only observed a slight decrease in body weight in the group that was injected with the lowest dose, whereas the highest dose resulted in weight loss <15% and mild signs of toxicity (e.g., ruffled fur) (Fig. 2B). The dose of 22.5 mg DOX/kg appeared to lie on the threshold between a toxic and non-toxic dose. Thus, we claim it to be the MTD of this conjugate. Final MTDs of the conjugates and their fractions used in following *in vivo* experiments are presented in Table 3 together with widely accepted MTD of DOX.

Table 3
Relative MTD fractions of conjugates used in *in vivo* experiments and their translation into DOX eq. concentrations.

Drug/conjugate	MTD		
	100%	60%	30%
DOX	10 mg/kg	–	–
Conjugate 1	85 mg DOX/kg	51 mg DOX/kg	25.5 mg DOX/kg
Conjugate 2	22.5 mg DOX/kg	13.5 mg DOX/kg	6.75 mg DOX/kg

3.3. Histology of the selected organs

As mentioned above, organs from three mice randomly selected from each experimental group were used for a histological analysis, which was performed on day seven post-injection of the conjugates. We examined the spleen, kidney, liver and vertebral bone marrow of the experimental mice, which were treated as stated above. We compared them with those that were obtained from the control mice injected with PBS and the mice treated with free DOX (100% MTD, i.e., 10 mg/kg), conjugate 3 (dose eq. to conjugate 2, given at 100% MTD) and S-Hy or S-homo (dose eq. to conjugate 2, given at 100% MTD).

The histological findings in the mice that were injected with conjugates 1, 2 and 3 did not markedly differ (data not shown). The bone marrow had normal cellularity and composition. The only notable finding was hyperemia and dilatation of the capillaries that positively correlated with the dose of the conjugates. On the other hand, the spleens showed an apparent but non-destructive storage in the form of macrophages and large multinuclear cells with a translucent foamy cytoplasm (Supplement 1A). We used three staining methods in cryostat sections (i.e., Oil Red O, Sudan Black B and Luxol Fast Blue) in order to exclude lipid uptake. All of these yielded negative results in foamy elements (Supplement 2). This finding positively correlated with the dose of the conjugates and was associated with a decrease in red pulp haematopoiesis. The white pulp follicles displayed no germinal centres and were almost devoid of marginal zones. We also observed several abnormalities in the liver such as polymorphic nuclei and mitosis of

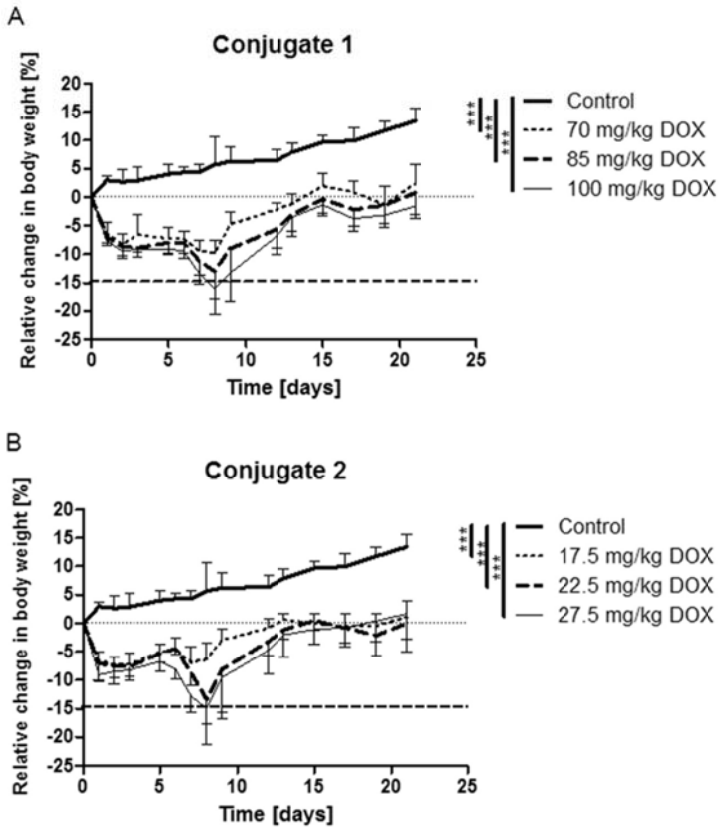

Fig. 2. Relative change in body weight of the mice i.v. injected with titrated doses of conjugate 1 (A) or conjugate 2 (B). The control mice were i.v. injected with the same volume of PBS. Six mice per group were used. Groups were compared using ANOVA followed by Tukey test for pairwise comparison of sub-groups; *** represents p-value <0.001. The experiment was repeated twice with similar results.

hepatocytes, sparse large multinuclear cells and inflammatory nodules (Supplement 1B). This finding positively correlated with the dose of the conjugates, similarly to the signs of storage that were seen in the spleen.

The application of free DOX at the dose 10 mg/kg (MTD) led to a mild inhibition of haematopoiesis in the spleen and rare mitosis of the hepatocytes (Supplement 3). No other anomalies were recorded. Together with the fact that the weight loss was on the threshold between toxic and non-toxic dosage, our findings are in accordance with other publications that mention this dose as the MTD of free DOX in mice [17,18].

Similarly to conjugates 1–3, we saw no differences between the mice that were treated with the S-Hy or S-homo. The samples of kidney, liver and vertebral bone marrow had normal cellularity and structure and no anomalies were detected. Nevertheless, we observed activation of the spleens with prominent germinal centres in the follicles (Supplement 4A), as well as occasionally in the central periarterial T zones (Supplement 4B). Otherwise, the spleens were of a normal structure with no signs of storage and a picture of a normal haematopoiesis.

Furthermore, we also compared the organs that were isolated from the mice that were injected with non-degradable conjugate 2 and enzymatically degradable conjugate 3 (100% MTD), and S-Hy or S-homo (dose eq. to conjugate 2) on day 18 post-administration. We did this so as to document the potential differences between the histological findings in early and late post-injection periods. As above, we observed no differences between conjugates 2 and 3 or between S-Hy or S-homo. The overall findings were similar to those seen in the samples that were collected on day seven post-application. We observed less intensive structures of storage, together with the usual extent of haematopoiesis in spleens (data not shown) and rare mitosis of hepatocytes of the mice that were injected with conjugate 2 or 3. Analogically, signs of splenic white pulp activation in the mice that were injected with S-Hy or S-homo were very mild or close to normal (data not shown).

3.4. Evaluation of intestinal barrier permeability

We employed FITC-labelled dextran to investigate the function of the intestinal barrier. The mice were i.v. injected with conjugate 1, 2 or free DOX. On day three, the mice were p.o. fed with a gut permeability tracer (FITC-dextran). The mice were euthanized 4 h after being fed with FITC-dextran and their sera were collected to determine the concentration of FITC-dextran. Sera from the mice that were injected with conjugates 1 and 2 showed FITC-dextran levels, which were comparable to the control mice, while sera from the mice that were injected with free DOX had significantly higher levels of FITC-dextran. Thus, the MTD of conjugates 1 and 2 does not damage the gut barrier, while the MTD of free DOX does (Fig. 3).

3.5. Blood clearance and tumour accumulation

We evaluated the blood clearance and tumour accumulation of conjugate 1, 2 and free DOX after their administration to the mice bearing EL4 T-cell lymphoma. Surprisingly, the collected data show comparable accumulation and persistence of DOX in the tumours from the mice that were injected with conjugate 1 or 2 (Fig. 4A) at equitoxic dose (100% MTD). On the other hand, conjugate 2 had significantly longer persistence in circulation than the much smaller and more easily excretable conjugate 1 (Fig. 4B). The peak concentration of DOX in tumour was reached within 24 h post-administration of either conjugate and began to drop 72 h post-administration of either conjugate. The injection of the free DOX only caused a very poor accumulation of DOX in the tumour tissue and it was extremely low in comparison to both of the polymer conjugates. The favourable profile of tumour to blood ratio was found for both of the polymer conjugates, and was more profound for conjugate 1 (Fig. 4C).

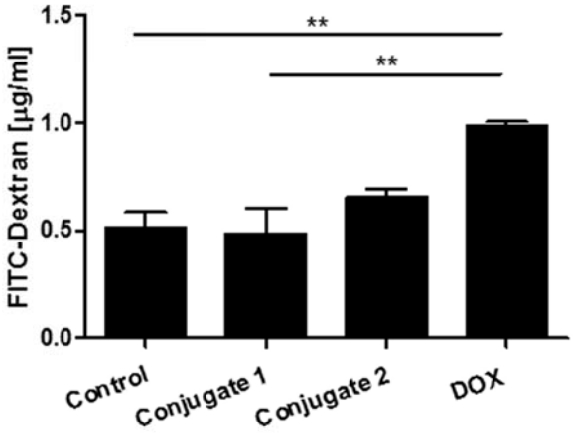

Fig. 3. Disruption of intestinal barrier. Mice were i.v. injected with PBS (control), free DOX and conjugate 1 or 2 (100% MTD). Three days afterwards, mice were fasted for 4 h and fed with 0.44 mg FITC-dextran/g. The plasma levels of FITC-dextran were measured 4 h after FITC-dextran administration. Three mice per group were used. Groups were compared using ANOVA followed by Tukey test for pairwise comparison of sub-groups; ** represents p-value <0.01. The experiment was repeated twice with comparable results.

3.6. Anti-tumour activity of conjugates

We evaluated and compared the anti-tumour activity of conjugates 1 and 2 in two selected mouse tumour models: EL4 T-cell lymphoma and BCL1 B-cell leukaemia. EL4 lymphoma is a model of solid vascularized tumour in which EPR effect plays an important role. On the contrary, BCL1 leukaemia is a model of diffuse malignancy, which does not form solid tumours. Thus, accumulation of polymers due to the EPR effect is not possible. Therefore, therapy of BCL1 leukaemia should only benefit from the long-term persistence of the conjugate acting as a drug depot in the organism.

In the case of EL4 lymphoma, the mice were i.v. injected with conjugates at doses of 100, 60 and 30% of MTD eight days after tumour cell inoculation. We observed a significant inhibition of tumour growth and prolonged survival of the experimental mice in all of the groups (Fig. 5A, B). However, the treatment with conjugate 1 appeared to be more efficient than with conjugate 2.

The dose corresponding to 100% of MTD of each conjugate cured six out of eight mice. However, the non-surviving mice showed longer average survival in the case of conjugate 1 (the mean survival for conjugates 1 and 2 was 47.5 ± 10.5 and 40.5 ± 1.5 days, respectively). Conjugate 1, given at 60% of the MTD, cured all mice, whereas 60% of the MTD of conjugate 2 cured five out of eight mice (the mean survival 47.0 ± 4.6 days). The lowest dose used, 30% of the MTD, cured six out of eight mice in the case of treatment with conjugate 1 (the mean survival 41.5 ± 2.5 days) in contrast to one out of eight mice cured with conjugate 2 (the mean survival 39.7 ± 6.7 days). Tumour-free mice that survived until day 60 (long-term survivors, LTS) were re-challenged with a lethal dose of EL4 lymphoma cells (1×10^5 cells/dose) s.c. into the left flank and were left untreated. The mean survival of the mice that were previously cured with conjugate 1 was 38.2 ± 5.5 days (100% MTD), 36.1 ± 11.4 days (60% MTD), 35.5 ± 7.5 days (30% MTD). The mean survival of the mice that were cured with conjugate 2 was 31.0 ± 7.1 days (100% MTD) and 39.5 ± 3.5 days (60% MTD). Only one mouse was cured with 30% MTD of conjugate 2 and died on day 36 after the re-challenge. The mice that were cured with conjugate 2 developed a slightly higher anti-tumour resistance (Fig. 6B) than those that were treated with conjugate 1 (Fig. 6A). Despite the limited number of the re-challenged animals, the data confirm the previously described phenomenon [23] that more successful treatment induces weaker anti-tumour resistance and vice versa.

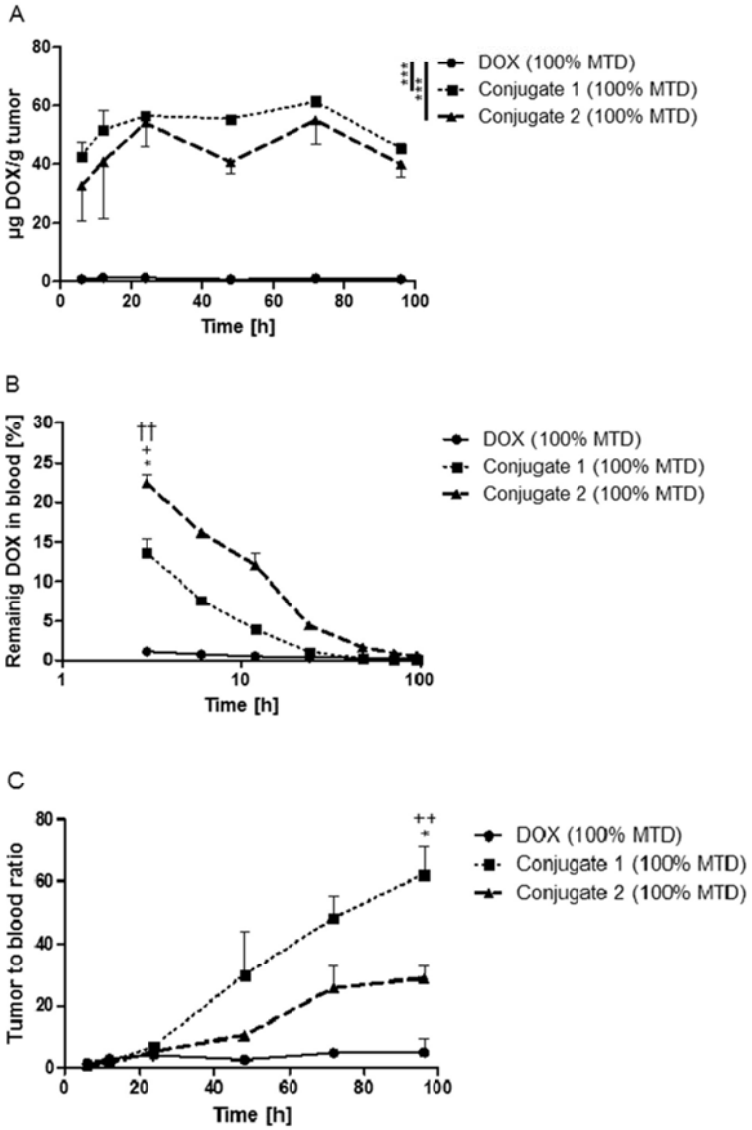

Fig. 4. Kinetics of DOX in the blood and tumour after i.v. administration of HPMA copolymer-DOX conjugates. The C57BL/6 mice were s.c. injected with 1×10^5 EL4 cells. Eight days afterwards, the mice were i.v. injected with PBS (control), DOX, conjugate 1 or 2 (100% MTD each). Samples of blood and tumour tissue were harvested at selected time intervals and the total DOX content was determined. Groups were compared using ANOVA followed by Tukey test for pairwise comparison of sub-groups. A) Accumulation of DOX in tumour tissue; *** represents p-value <0.001. B) Blood clearance of DOX. * indicates the level of statistical significance between groups injected with DOX and Conjugate 1 ($P < 0.05$); + indicates the level of statistical significance between groups injected with conjugates 1 and 2 ($P < 0.05$); †† indicates the level of statistical significance between groups injected with DOX and conjugate 2 ($P < 0.01$). C) Tumour to blood ratio. * indicates the level of statistical significance between groups injected with conjugates 1 and 2 ($P < 0.05$); ++ indicates the level of statistical significance between groups injected with DOX and conjugate 1 ($P < 0.01$). Three mice per one time interval were used. The control had no detectable level of DOX and was omitted for clarity.

In parallel, we i.p. inoculated mice with BCL1 leukaemia cells and 11 days afterwards, we i.v. injected them with 100 or 60% of the MTD of conjugate 1 or 2. As in the EL4 lymphoma treatment, we saw significantly prolonged survival. The application of conjugate 2 led to a complete cure of one out of eight mice that were injected with 100% MTD (mean survival 90.0 ± 19.0 days), and three of eight mice in the group injected with 60% MTD (mean survival 75.2 ± 19.6 days) (Fig. 7B). The treatment with conjugate 1 did not cure any of the mice at either dose, with the mean survival 105.9 ± 15.8 days for 100% MTD and 80.6 ± 20.9 days for 60% MTD (Fig. 7A).

4. Discussion

This study was focused on two types of HPMA copolymer-based conjugates bearing DOX attached via pH-sensitive hydrazone bond: linear conjugate (R_h ~4 nm) and star conjugate (R_h ~13 nm) with PAMAM dendrimer core. We investigated in detail their toxicity, tumour accumulation, blood clearance and anti-tumour activity *in vivo*.

Even though *in vitro* studies showed that the star conjugate has slightly higher cytostatic activity than the linear one, *in vivo* investigation of maximum tolerated dose (MTD) indicated that the linear

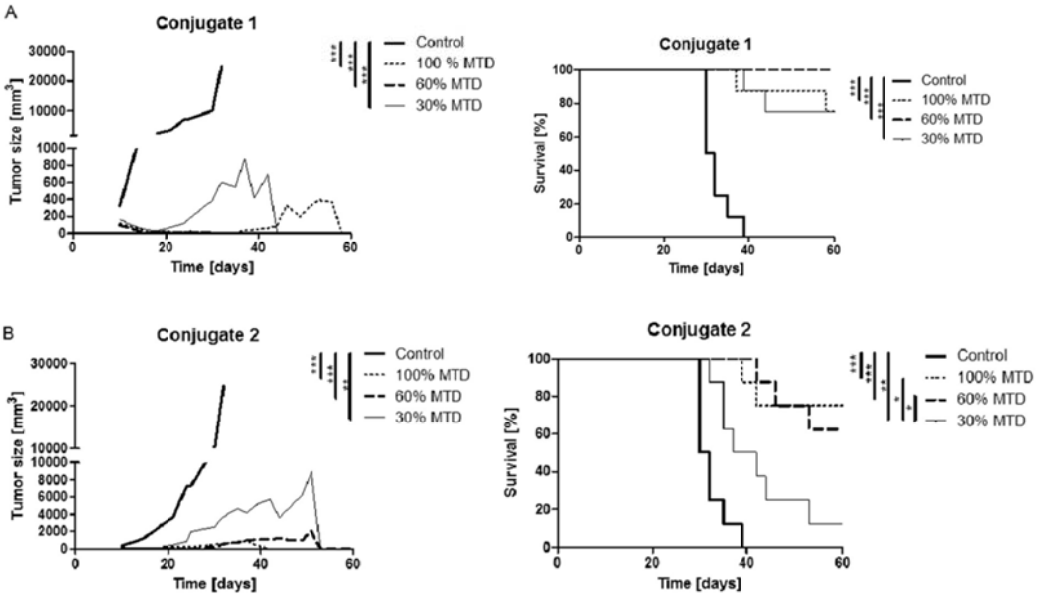

Fig. 5. Treatment of EL4 lymphoma by titrated doses of HPMA copolymer-DOX conjugates. The C57BL/6 mice were s.c. injected with 1×10^5 EL4 cells on day zero. Eight days afterwards, the mice were i.v. injected with titrated doses of conjugates. The untreated mice that were injected with tumour cells and PBS were used as controls. From day 32 onwards, we dropped out 2 deceased mice in control group. A) Tumour therapy with conjugate 1. B) Tumour therapy with conjugate 2. Eight mice per group were used. Groups were compared using ANOVA followed by Tukey test for pairwise comparison of sub-groups; *, **, *** represents p-value <0.05, 0.01 and 0.001, respectively. The experiment was repeated twice with similar results.

conjugate could be more effective in anti-tumour therapy. This is because it had a significantly wider therapeutic window in comparison to the star conjugate, as well as to the free DOX. We observed that the linear conjugate had an MTD that was 3.7 times higher than the MTD of the star conjugate and 8.5 times higher than the MTD of free DOX.

Further experiments revealed well-marked storage in the spleens of the mice that were injected with HPMA copolymer-DOX conjugates, irrespective of their structure, size and degradability. The accumulation of mononuclear elements and giant cells in the splenic and hepatic tissue of the mice that were injected with HPMA copolymer-DOX conjugates was a prominent and very unusual microscopic finding. The translucent, microvacuolar and foamy structure of the cytoplasm raised a suspicion of lipid storage, which is known, e.g., in Gaucher, Niemann–Pick and other diseases in humans. However, the three different staining methods for lipids that were used in the present experiments all remained completely negative. A possible explanation for this could be the storage of the polymers in the reticuloendothelial–histiomonocytic system. However, final proof would require the establishment of a specific histochemical detection.

Other data that were yielded from the histological sections led us to an assumption that the degradability (enzymatically driven) of a polymer carrier has no effect on the toxicity of a drug conjugate as we saw no differences between non-degradable and degradable star HPMA copolymer-DOX conjugates. These data are in accordance with the fact that biodegradable star carriers should be stable at pH 7.4 (i.e., blood circulation) and the degradation should only occur in a tumour in an intracellular environment of lysosomes in the presence of the lysosomal enzymes [24].

Unlike the above mentioned signs of storage that were seen in the spleen in the case of star HPMA copolymer-DOX conjugates, we observed a strong activation of the spleens that were isolated from the mice that were injected with star polymers S-Hy and S-Homo, both with or without hydrazide groups. The germinal centres in the follicles and, to our surprise, in some cases, even in the periarterial T zones of the follicles, were evident in all of the sections, regardless of the presence of hydrazide group on the polymer backbone. This observation supports various reports of immune-related activity of HPMA copolymers that contain oligopeptide sequences [23,25,26]. Nevertheless, we saw no more deviations from the naïve controls in other tested organs.

DOX therapy has many side-effects, including damage of the intestinal barrier function [22,27]. We saw no significant change in the gut permeability after administration of either conjugate. This proves that they are non-toxic to the gastrointestinal tract, compared to free DOX,

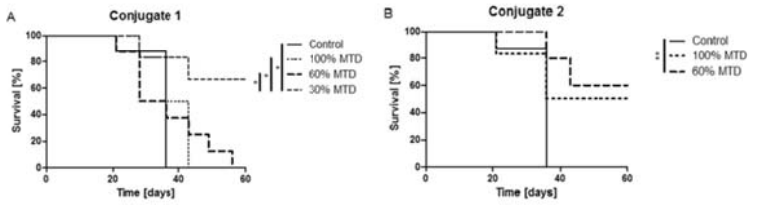

Fig. 6. The re-challenge of cured mice with a lethal dose of EL4. The completely cured C57BL/6 mice that survived challenge with EL4 T-lymphoma cells were re-challenged with a lethal dose of tumour cells (1×10^5) and left untreated. The mice that were injected with tumour cells and PBS were used as controls. A) The survival of mice that were cured with conjugate 1. B) The survival of mice that were cured with conjugate 2. Groups were compared using ANOVA followed by Tukey test for pairwise comparison of sub-groups; *, ** represents p-value <0.05 and 0.01, respectively. We show only groups of ≥4 cured mice.

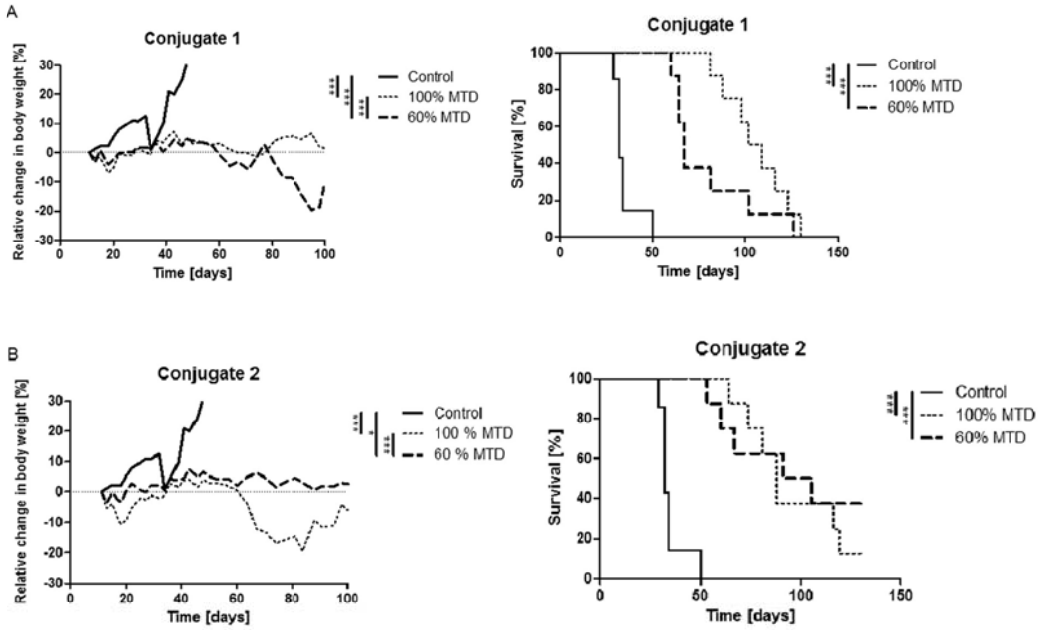

Fig. 7. Treatment of BCL1 leukaemia by titrated doses of HPMA copolymer-DOX conjugates. The BALB/c mice were i.p. injected with 5×10^5 BLC1 leukaemia cells on day zero. Eleven days afterwards, the mice were i.v. injected with titrated doses of conjugates. The untreated mice that were injected with tumour cells and PBS were used as controls. A) Tumour therapy with conjugate 1. B) Tumour therapy with conjugate 2. Eight mice per group were used. Groups were compared using ANOVA followed by Tukey test for pairwise comparison of sub-groups; *, **, *** represents p-value <0.05, 0.01 and 0.001, respectively. The experiment was repeated twice with similar results.

which, indeed, led to increased levels of gut permeability tracer in the sera of the experimental mice.

The biodistribution study of the conjugates at an equitoxic dose showed a similar accumulation in the tumour tissue of both of the studied polymer systems and higher tumour to blood ratio of the linear conjugate than the star conjugate. It seems like the outcome of the EPR effect of both of the conjugates given at equitoxic dose (100% MTD) was very similar. Thus, the potential of the star conjugate to be accumulated within a tumour in much higher levels than the linear conjugate (R_h ~13 nm versus R_h ~4 nm, respectively) is balanced by the significantly lower toxicity of the linear conjugate, enabling the injection of an approximately 3.5 times higher dose of the drug. The relatively small size of the linear conjugate facilitates its easier penetration through the highly dense tumour intersticium and quicker elimination from organism via the renal filtration in comparison to the robust star conjugate with more than three-times bigger size in solution [28–31].

Initially, we supposed that the star conjugate would be more efficient than the linear one due to its larger structure, which should lead to better accumulation in the solid tumour via the EPR effect and thus, lowered side toxicity. However, the very long persistence of the star polymer conjugate in the organism most likely increased the toxicity of the conjugate and thus, significantly reduced the MTD of the star conjugate in comparison to the linear one. Treatment of the EL4 lymphoma, the model of solid tumour, clearly showed that, even though the star conjugate should elicit a more intensive EPR effect than the linear conjugate, it appeared to be less efficient than the presumably therapeutically weaker linear conjugate. Even 5% MTD of the linear conjugate exerted a therapeutical effect in EL4 lymphoma-bearing mice (data not shown), which indicates, together with its remarkably wide therapeutic window, that it has vast potential for solid tumour therapy. On the other hand, we saw a slightly better development of anti-tumour resistance in the mice that were cured with the star conjugate and rechallenged with the lethal dose of EL4 lymphoma cells. We assume that the treatment with the star conjugate, which resulted in lower dose of immunosuppressive drug during the equitoxic dosage treatment in comparison to the linear conjugate (22.5 mg DOX/kg versus 85 mg DOX/kg, respectively), provides lower damage to the immune system.

The treatment with the star conjugate had higher therapeutic effects in BCL1 leukaemia, the model of a disseminated tumour, than the therapy with the linear conjugate. We assume that this is because the linear conjugate is excreted from the organism via a renal filtration relatively fast whereas the star conjugate is characteristic, with a long persistence in circulation due to the higher hydrodynamic size. This leads to prolonged exposure of the tumour to slowly decreasing low doses of DOX. DOX is released by slow hydrolysis of hydrazone bond in pH 7.4 (approx. 10% within 24 h). However, we suppose that this prolonged exposure of organism to DOX-bearing conjugate could be an explanation for the higher toxicity of the star conjugate, which would explain its lower MTD. This corresponds with the increased weight loss that we observed during the treatment with the star conjugate at a dose of 100% MTD from day 70 onwards.

It appears that the suitable drug delivery system (DDS) for solid tumour therapy would be a system that takes advantage of both of the studied DDS systems: i) HMW star system with profound accumulation in solid tumours; ii) the linear one, with the rapid elimination of polymer system from circulation after reaching the plato of tumour accumulation. We hypothesise that a suitable DDS should be a system with a "temporary" HMW structure. Thus, it would effectively accumulate in solid tumours and then rapidly disintegrate (preferably three to four days post-administration) into small linear polymer chains. Unfortunately, enzymatically degradable star polymer conjugates are degraded very slowly and do not fulfil the mentioned criteria. Another possibility, although less appealing, would be a HMW conjugate with R_h greater than 10 nm that is gradually degraded with selected kinetics and, thus, it reaches the Mw below the limit for a renal filtration (R_h ~4–5 nm) within three to four days post administration. On the contrary, the therapy of leukaemia would most probably benefit from the

application of a drug conjugate with a long circulation half-life, which would create a drug depot in the organism. However, the dose of such a conjugate would need to be carefully determined due to the possible high toxicity.

5. Conclusion

In this study, we investigated the *in vitro* and *in vivo* biological activity of two HPMA copolymer-based drug delivery systems, which differed in size and structure. The data indicate that different type of tumour requires different type of drug conjugate. The star-like conjugate with high R_h (~13 nm) and a long circulation half-life appears to be efficient for the treatment of disseminated leukaemia as it benefits from the prolonged exposure of leukaemic cells to the cytostatic drug. However, a lower dose of drug needs to be used to minimize damage to the immune system. In the case of therapy of solid tumours, the ideal drug conjugate would be of a higher R_h (~higher than 10 nm) with a time-controlled decomposition to excretable fragments (<40 kDa) to lower its toxicity.

Acknowledgements

This work was supported by the GACR (project P301/11/0325), by the Project BIOCEV of the European Regional Development Fund (project CZ.1.05/1.1.00/02.0109) and Institutional Research Concept RVO 61388971. The authors thank Albert Koválik, Pavlina Jungrova and Helena Misurcova for their excellent technical assistance.

Appendix A. Supplementary data

Supplementary data to this article can be found online at http://dx.doi.org/10.1016/j.jconrel.2015.12.023.

References

[1] Y. Matsumura, H. Maeda, A new concept for macromolecular therapeutics in cancer-chemotherapy — mechanism of tumoritropic accumulation of proteins and the antitumor agent smancs, Cancer Res. 46 (1986) 6387–6392.
[2] H. Hashizume, P. Baluk, S. Morikawa, J.W. McLean, G. Thurston, S. Roberge, R.K. Jain, D.M. McDonald, Openings between defective endothelial cells explain tumor vessel leakiness, Am. J. Pathol. 156 (2000) 1363–1380.
[3] S. Taurin, H. Nehoff, K. Greish, Anticancer nanomedicine and tumor vascular permeability; where is the missing link? J. Control. Release 164 (2012) 265–275.
[4] H. Kobayashi, R. Watanabe, P.L. Choyke, Improving conventional enhanced permeability and retention (EPR) effects; what is the appropriate target? Theranostics 4 (2014) 81–89.
[5] B. Theek, F. Gremse, S. Kunjachan, S. Fokong, R. Pola, M. Pechar, R. Deckers, G. Storm, J. Ehling, F. Kiessling, T. Lammers, Characterizing EPR-mediated passive drug targeting using contrast-enhanced functional ultrasound imaging, J. Control. Release 182 (2014) 83–89.
[6] U. Prabhakar, H. Maeda, R.K. Jain, E.M. Sevick-Muraca, W. Zamboni, O.C. Farokhzad, S.T. Barry, A. Gabizon, P. Grodzinski, D.C. Blakey, Challenges and key considerations of the enhanced permeability and retention effect for nanomedicine drug delivery in oncology, Cancer Res. 73 (2013) 2412–2417.
[7] H. Maeda, Toward a full understanding of the EPR effect in primary and metastatic tumors as well as issues related to its heterogeneity, Adv. Drug Deliv. Rev. (2015).
[8] J. Kopecek, P. Kopeckova, HPMA copolymers: origins, early developments, present, and future, Adv. Drug Deliv. Rev. 62 (2010) 122–149.
[9] S. Kunjachan, R. Pola, F. Gremse, B. Theek, J. Ehling, D. Moeckel, B. Hermanns-Sachweh, M. Pechar, K. Ulbrich, W.E. Hennink, G. Storm, W. Lederle, F. Kiessling, T. Lammers, Passive versus active tumor targeting using RGD- and NGR-modified polymeric nanomedicines, Nano Lett. 14 (2014) 972–981.
[10] J. Kopecek, I. Cifkova, P. Rejmanova, J. Strohalm, B. Obereigner, K. Ulbrich, Polymers containing enzymatically degradable bonds .4. Preliminary experiments in vivo, Makromol. Chem. 182 (1981) 2941–2949.
[11] P. Rejmanova, J. Kopecek, R. Duncan, J.B. Lloyd, Stability in rat plasma and serum of lysosomally degradable oligopeptide sequences in N-(2-hydroxypropyl) methacrylamide copolymers, Biomaterials 6 (1985) 45–48.
[12] T. Etrych, M. Jelinkova, B. Rihova, K. Ulbrich, New HPMA copolymers containing doxorubicin bound via pH-sensitive linkage: synthesis and preliminary in vitro and in vivo biological properties, J. Control. Release 73 (2001) 89–102.
[13] K. Ulbrich, T. Etrych, P. Chytil, M. Jelinkova, B. Rihova, HPMA copolymers with pH-controlled release of doxorubicin — in vitro cytotoxicity and in vivo antitumor activity, J. Control. Release 87 (2003) 33–47.
[14] B. Rihova, T. Etrych, M. Pechar, M. Jelinkova, M. Stastny, O. Hovorka, M. Kovar, K. Ulbrich, Doxorubicin bound to a HPMA copolymer carrier through hydrazone bond is effective also in a cancer cell line with a limited content of lysosomes, J. Control. Release 74 (2001) 225–232.
[15] T. Etrych, V. Subr, J. Strohalm, M. Sirova, B. Rihova, K. Ulbrich, HPMA copolymer-doxorubicin conjugates: the effects of molecular weight and architecture on biodistribution and in vivo activity, J. Control. Release 164 (2012) 346–354.
[16] T. Etrych, J. Strohalm, P. Chytil, P. Cernoch, L. Starovoytova, M. Pechar, K. Ulbrich, Biodegradable star HPMA polymer conjugates of doxorubicin for passive tumor targeting, Eur. J. Pharm. Sci. 42 (2011) 527–539.
[17] J.Q. Lu, W.C. Zhao, H. Liu, R. Marquez, Y.X. Huang, Y.F. Zhang, J. Li, W. Xie, R. Venkataramanan, L. Xu, S. Li, An improved D-alpha-tocopherol-based nanocarrier for targeted delivery of doxorubicin with reversal of multidrug resistance, J. Control. Release 196 (2014) 272–286.
[18] U. Vanhoefer, S. Cao, A. Harstrick, S. Seeber, Y.M. Rustum, Comparative antitumor efficacy of docetaxel and paclitaxel in nude mice bearing human tumor xenografts that overexpress the multidrug resistance protein (MRP), Ann. Oncol. 8 (1997) 1221–1228.
[19] S. Van, S.K. Das, X.H. Wang, Z.L. Feng, Y. Jin, Z. Hou, F. Chen, A. Pham, N. Jiang, S.B. Howell, L. Yu, Synthesis, characterization, and biological evaluation of poly(L-gamma-glutamyl-glutamine)-paclitaxel nanoconjugate, Int. J. Nanomedicine 5 (2010) 825–837.
[20] T.K. Stutchbury, F. Al-Ejeh, G.E. Stillfried, D.R. Croucher, J. Andrews, D. Irving, M. Links, M. Ranson, Preclinical evaluation of Bi-213-labeled plasminogen activator inhibitor type 2 in an orthotopic murine xenogenic model of human breast carcinoma, Mol. Cancer Ther. 6 (2007) 203–212.
[21] R.W.H.M. Staffhorst, K. van der Born, C.A.M. Erkelens, I.H.L. Hamelers, G.J. Peters, E. Boven, A.I.P.M. de Kroon, Antitumor activity and biodistribution of cisplatin nanocapsules in nude mice bearing human ovarian carcinoma xenografts, Anti-Cancer Drugs 19 (2008) 721–727.
[22] S. Viaud, F. Saccheri, G. Mignot, T. Yamazaki, R. Daillere, D. Hannani, D.P. Enot, C. Pfirschke, C. Engblom, M.J. Pittet, A. Schlitzer, F. Ginhoux, L. Apetoh, E. Chachaty, P.L. Woerther, G. Eberl, M. Berard, C. Ecobichon, D. Clermont, C. Bizet, V. Gaboriau-Routhiau, N. Cerf-Bensussan, P. Opolon, N. Yessaad, E. Vivier, B. Ryffel, C.O. Elson, J. Dore, G. Kroemer, P. Lepage, L.G. Boneca, F. Ghiringhelli, L. Zitvogel, The intestinal microbiota modulates the anticancer immune effects of cyclophosphamide, Science 342 (2013) 971–976.
[23] B. Rihova, M. Kovar, Immunogenicity and immunomodulatory properties of HPMA-based polymers, Adv. Drug Deliv. Rev. 62 (2010) 184–191.
[24] T. Etrych, V. Subr, R. Laga, B. Rihova, K. Ulbrich, Polymer conjugates of doxorubicin bound through an amide and hydrazone bond: impact of the carrier structure onto synergistic action in the treatment of solid tumours, Eur. J. Pharm. Sci. 58 (2014) 1–12.
[25] B. Rihova, M. Bilej, V. Vetvicka, K. Ulbrich, J. Strohalm, J. Kopecek, R. Duncan, Biocompatibility of N-(2-hydroxypropyl) methacrylamide copolymers containing adriamycin - immunogenicity, and effect on hematopoietic stem-cells in bone-marrow invivo and mouse splenocytes and human peripheral-blood lymphocytes in vitro, Biomaterials 10 (1989) 335–342.
[26] B. Rihova, J. Kopecek, K. Ulbrich, M. Pospisil, P. Mancal, Effect of the chemical-structure of N-(2-hydroxypropyl)methacrylamide copolymers on their ability to induce antibody-formation in inbred strains of mice, Biomaterials 5 (1984) 143–148.
[27] O. Tacar, P. Sriamornsak, C.R. Dass, Doxorubicin: an update on anticancer molecular action, toxicity and novel drug delivery systems, J. Pharm. Pharmacol. 65 (2013) 157–170.
[28] T. Lammers, F. Kiessling, W.E. Hennink, G. Storm, Drug targeting to tumors: principles, pitfalls and (pre-) clinical progress, J. Control. Release 161 (2012) 175–187.
[29] C. Wong, T. Stylianopoulos, J.A. Cui, J. Martin, V.P. Chauhan, W. Jiang, Z. Popovic, R.K. Jain, M.G. Bawendi, D. Fukumura, Multistage nanoparticle delivery system for deep penetration into tumor tissue, Proc. Natl. Acad. Sci. U. S. A. 108 (2011) 2426–2431.
[30] M.R. Dreher, W.G. Liu, C.R. Michelich, M.W. Dewhirst, F. Yuan, A. Chilkoti, Tumor vascular permeability, accumulation, and penetration of macromolecular drug carriers, J. Natl. Cancer Inst. 98 (2006) 335–344.
[31] Z. Popovic, W.H. Liu, V.P. Chauhan, J. Lee, C. Wong, A.B. Greytak, N. Insin, D.G. Nocera, D. Fukumura, R.K. Jain, M.G. Bawendi, A nanoparticle size series for in vivo fluorescence imaging, Angew. Chem. Int. Ed. 49 (2010) 8649–8652.

Macromolecular Bioscience
www.mbs-journal.de

Polymer Cancerostatics Targeted with an Antibody Fragment Bound via a Coiled Coil Motif: In Vivo Therapeutic Efficacy against Murine BCL1 Leukemia

Michal Pechar, Robert Pola, Olga Janoušková, Irena Sieglová, Vlastimil Král, Milan Fábry, Barbora Tomalová, and Marek Kovář*

Dedicated to Professor Karel Ulbrich on the occasion of his 70th birthday.

A BCL1 leukemia-cell-targeted polymer–drug conjugate with a narrow molecular weight distribution consisting of an *N*-(2-hydroxypropyl)methacrylamide copolymer carrier and the anticancer drug pirarubicin is prepared by controlled radical copolymerization followed by metal-free click chemistry. A targeting recombinant single chain antibody fragment (scFv) derived from a B1 monoclonal antibody is attached noncovalently to the polymer carrier via a coiled coil interaction between two complementary peptides. Two pairs of coiled coil forming peptides (abbreviated KEK/EKE and KSK/ESE) are used as linkers between the polymer–pirarubicin conjugate and the targeting protein. The targeted polymer conjugate with the coiled coil linker KSK/ESE exhibits 4× better cell binding activity and 2× higher cytotoxicity in vitro compared with the other conjugate. Treatment of mice with established BCL1 leukemia using the scFv-targeted polymer conjugate leads to a markedly prolonged survival time of the experimental animals compared with the treatment using the free drug and the nontargeted polymer–pirarubicin conjugate.

1. Introduction

The application of polymer–cancerostatic conjugates for neoplastic treatment provides several significant advantages compared with conventional chemotherapy. The polymer therapeutics usually exhibit much lower nonspecific toxicity against healthy cells and tissues as the biologically active molecules are preferentially released from the conjugates into the target tumor tissue or cells. The increased accumulation of the polymer conjugates in solid tumors resulting from the enhanced permeation and retention (EPR) effect further improves the tumor selectivity of the polymer therapeutics.[1] Additionally, the polymer carrier enables the attachment of various targeting ligands that actively target cancer cells.[2–6]

Unfortunately, the EPR effect can be utilized only in the treatment of solid vascularized tumors. In other cases, such as the treatment of blood malignancies or metastases in early stages, the active targeting of the polymer therapeutics is highly desirable to improve the overall therapeutic efficiency. Among the various ligands that have been described to actively target cancer cells, antibodies and their fragments thus far appear to be the most efficient.[2,7–9] However, the well-defined covalent conjugation of proteins to polymers is not easily accomplished. The reaction between proteins and reactive polymer precursors often results in a mixture of poorly defined products with a compromised biological activity. Therefore, there is an urgent need for conjugation methods that provide well-defined products with fully preserved biological activities.

Although several sophisticated methods to achieve the site-specific covalent modification of proteins have been recently described,[10–14] the formation of a specific noncovalent bond between two peptide tags is an equally attractive approach. Among the various noncovalent methods, the utilization of coiled coil heterodimers,[15–20] the hybridization of complementary morpholino oligonucleotides[21–23] and the formation of a complex between bungarotoxin and a bungarotoxin-binding peptide[24] for the attachment of biologically active proteins to polymer carriers are particularly notable.

The use of coiled coil heterodimers for preparation of polymer–drug conjugates containing either a biologically active protein (FosW$_C$ peptide)[16] or a low molecular weight cytostatic drug (methotrexate)[18] emerged in the literature after 2010.

Recently, we have reported the synthesis and in vitro evaluation of an *N*-(2-hydroxypropyl)methacrylamide (HPMA)-based polymer conjugate with an anticancer drug doxorubicin (Dox) targeted to murine leukemia BCL1 via a recombinant single

Dr. M. Pechar, Dr. R. Pola, Dr. O. Janoušková
Institute of Macromolecular Chemistry
Czech Academy of Sciences
Heyrovského nám. 2, 162 06 Prague 6, Czech Republic
E-mail: pechar@imc.cas.cz
I. Sieglová, Dr. V. Král, Dr. M. Fábry
Institute of Molecular Genetics
Czech Academy of Sciences
Flemingovo nám. 2, 166 10 Prague 6, Czech Republic
B. Tomalová, Dr. M. Kovář
Institute of Microbiology
Czech Academy of Sciences
Vídeňská 1083, 142 20 Prague 4, Czech Republic

DOI: 10.1002/mabi.201700173

chain fragment (scFv) of the monoclonal antibody B1.[25] The targeting protein was attached to the polymer–drug conjugate via a noncovalent interaction between two peptides that formed a coiled coil heterodimer. The scFv-targeted polymer conjugate exhibited almost 100 times higher cytotoxicity against BCL1 cells compared with the corresponding nontargeted polymer conjugate.

We have further optimized the structure of the targeted macromolecular therapeutic using a modified method to synthesize the polymer carrier, employing an improved structure of the coiled coil heterodimer between the polymer and the targeting protein[26] and introducing pirarubicin (Pir) instead of doxorubicin as a cytostatic drug.[27] In this paper, we describe the synthesis, results of physicochemical characterization and both in vitro and in vivo biological evaluations of the optimized HPMA-based polymer system using a BCL1 leukemia model.

2. Experimental Section

2.1. Materials and Methods

3-[2-[2-[2-(2-Azidoethoxy)ethoxy]ethoxy]ethoxy]propanoic acid (N_3-PEG_4-COOH) and *N*-[2-[2-[2-(2-azidoethoxy)ethoxy]-ethoxy]ethyl]-biotinamide (N_3-PEG_3-biotin) were purchased from Click Chemistry Tools, USA. (*RS*)-1-Aminopropan-2-ol, 2,2′-azobis(2-methylpropionitrile) (AIBN), 4-cyano-4-thiobenzoylsulfanylpentanoic acid (CTP), 1-ethyl-3-(3-dimethylamino-propyl)carbodiimide (EDC), *N*,*N*-dimethylacetamide (DMA), 4-dimethylaminopyridine (DMAP), dimethyl sulfoxide (DMSO), methacryloyl chloride, *tert*-butanol, triisopropylsilane (TIPS), and trifluoroacetic acid (TFA) were purchased from Sigma-Aldrich (Sigma-Aldrich, Czech Republic). 3-Amino-1-(11,12-didehydrodibenzo[b,f]azocin-5(6H)-yl)propan-1-one (DBCO-NH_2) was purchased from Click Chemistry Tools (AZ, USA). Pirarubicin (Pir) was obtained from Meiji Seika Pharma Co., Ltd. (Japan). All other chemicals and solvents were of analytical grade. Solvents were dried and purified by conventional procedures and distilled before use.

2.2. HPLC Monitoring of Polymer–Analogous Reactions

Monitoring of the conjugation reactions of DBCO-NH_2, pirarubicin, biotin, and peptides to the reactive polymer precursors was performed by HPLC using a 100 × 4.6 mm Chromolith Performance RP-18e column (Merck, Germany) and a linear gradient of water–acetonitrile (0–100% acetonitrile) in the presence of 0.1% TFA with a UV–vis diode array detector (Shimadzu, Japan).

2.3. Cell Lines

BCL1 cell line was obtained from Prof. Blanka Říhová (Institute of Microbiology, Czech Academy of Sciences). The cells were cultivated in RPMI medium (Thermo Scientific, Czech Republic) supplemented with heat inactivated 10% fetal bovine serum (FCS), 100 U mL^{-1} penicillin, 100 µg mL^{-1} streptomycin, and 0.05×10^{-3} M 2-sulfanylethanol.

Table 1. Basic characteristics of the copolymers.

Copolymer	M_w[a]	M_w/M_n[a]	TT [mol%][b]	Pir [wt%][c]	Peptide [wt%][d]	Biotin [wt%][d]
P_{TT}	46 300	1.28	6.8	–	–	–
P_{Pir}	59 700	1.19	–	9.6	–	–
P_{EKE}	61 500	1.15	–	8.0	14.2	2.0
P_{ESE}	62 000	1.13	–	8.1	13.8	2.1

[a]Molecular weights determined by SEC using RI and LS detection; [b]TT determined by UV–vis spectrophotometry in methanol (ε_{305} = 10 300 L·mol^{-1}·cm^{-1}); [c]Pir determined by UV–vis spectrophotometry in methanol (ε_{488} = 11 300 L·mol^{-1}·cm^{-1}); [d]Determined by HPLC analysis.

2.4. Size-Exclusion Chromatography (SEC)

The molecular weights and dispersity values of the polymers and polymer–Pir conjugates were determined by SEC on a Shimadzu HPLC system equipped with UV–vis diode array detector (Shimadzu, Japan), refractive index Optilab-rEX, and multi-angle light scattering DAWN EOS detectors (Wyatt Technology Corp., Santa Barbara, CA). TSK-Gel SuperAW3000 column and 80% methanol/20% sodium acetate buffer (0.3 M, pH 6.5) as an eluent at a flow rate of 0.6 mL min^{-1} were used in all experiments. A method based on the known total injected mass with an assumption of 100% recovery was used to calculate of the molecular weights from the light scattering data. The number- and weight-average molecular weights for the polymer precursors and the polymer–Pir conjugates are summarized in Table 1.

2.5. UV–Vis Spectrophotometry

The spectrophotometric analyses were carried out in quartz glass cuvettes on a Helios Alpha UV–vis spectrophotometer (Thermospectronic, UK). The content of dithiobenzoate (DTB) end groups in the polymers were determined at 302 nm in methanol using the molar absorption coefficient ε_{DTB} = 12 100 L mol^{-1} cm^{-1}. The results are summarized in Table 1. The determination of the Pir content in the polymer–Pir conjugates (without fluorophore) was performed at 488 nm in methanol using the molar absorption coefficient ε_{Pir} = 11 300 L mol^{-1} cm^{-1}. The Pir contents are summarized in Table 2. The contents of carbonylthiazolidine-2-thione (TT) reactive groups in the polymer precursors were determined at 305 nm in methanol using the molar absorption

Table 2. Cytostatic activity of the scFv-targeted and nontargeted polymer–Pir conjugates and free Pir.

Sample	IC_{50} (±SD)[a]
P_{ESE}/$scFv_{KSK}$	9 ± 2
P_{EKE}/$scFv_{KEK}$	18 ± 3
P_{ESE}/$scFv_0$	89 ± 2
P_{EKE}/$scFv_0$	146 ± 2
Pir	1 ± 0.2

[a]IC_{50} (µg L^{-1}), concentration of Pir equivalent in the sample inhibiting growth of the 50% cells compared with the untreated control.

coefficient $\varepsilon_{TT} = 10\,300$ L mol^{-1} cm^{-1}. The contents of aza-dibenzocyclooctyne (DBCO) groups in the copolymers were determined at 292 nm using the absorption coefficient for DBCO in methanol, $\varepsilon_{292} = 13\,000$ L mol^{-1} cm^{-1}.

2.6. Dynamic Light Scattering (DLS)

The hydrodynamic radii and scattering intensities of the polymer precursors and polymer conjugates were measured using the DLS technique at a scattering angle of $\theta = 173°$ on a Nano-ZS instrument (Model ZEN3600, Malvern Instruments, UK) equipped with a 632.8 nm laser. The measurements were performed in 0.012 M phosphate buffer with 0.138 M NaCl (PBS) (1.0 mg mL^{-1}, pH 7.4) solutions. For the evaluation of the dynamic light scattering data, the DTS (Nano) program was used. The mean of at least three independent measurements was calculated.

2.7. Synthesis of Peptides EKE and ESE

The EKE and ESE peptides were prepared as described previously.[26]

2.8. Synthesis of Monomers

HPMA and Ma-GFLG-OH were prepared as described earlier.[28,25] Ma-GFLG-TT was prepared by reacting Ma-GFLG-OH (92 mg, 0.2 mmol) with 4,5-dihydrothiazole-2-thiol (29 mg, 0.24 mmol) using 1-ethyl-3-(3-dimethylaminopropyl)carbodiimide hydrochloride (57.5 mg, 0.3 mmol) in DMF in the presence of 4-dimethylaminopyridine at 4 °C overnight. After DMF was evaporated, the reaction mixture was dissolved in DCM and the water-soluble urea derivative was removed by subsequent washing of the organic solution with an aqueous solution of $KHSO_4$, with a solution of NaCl and with water. After DCM was evaporated, the product was dried to yield 80 mg of the monomer, which was then characterized by HPLC (single peak) and MS ESI (calculated 561.7, found 562.9 M+H).

2.9. Synthesis of Polymer Precursor

Reversible addition-fragmentation chain transfer (RAFT) polymerization was performed as described earlier.[29] A monomer/CTA/initiator molar ratio of 1000:2:1 was used. HPMA (90 mol%, 100 mg), Ma-GFLG-TT (10 mol%, 43.6 mg) treated with the initiator ABIN (1.3 mg), and the chain transfer agent 4-cyano-4-thiobenzoylsulfanylpentanoic acid (1.06 mg) were mixed in DMA and tert-butyl alcohol (50/50 v/v). After removal of dithiobenzoate (DTB) ω-end groups,[30] the polymer precursor $\mathbf{P_{TT}}$ was characterized by SEC ($M_W = 46\,300$, $M_W/M_n = 1.28$) and the content of TT groups (6.8 mol%) was determined by UV–vis.

2.10. Synthesis of Polymer Conjugates

The polymer precursor $\mathbf{P_{TT}}$ (90 mg, 0.033 mmol TT, i.e., 6.3 mol%) was dissolved in 1.5 mL of DMA and mixed with pirarubicin (10 mg, 0.016 mmol) in 0.5 mL DMA. After 2 h, no remaining free drug was detected by HPLC. DBCO-NH_2 (5.8 mg, 0.021 mmol) was added and the reaction was left overnight. HPLC revealed a small amount of remaining DBCO-NH_2 and no TT groups on the polymer. The reaction mixture was precipitated into ethyl acetate; the crude polymer was dissolved in methanol and re-precipitated into ethyl acetate to yield the polymer–drug conjugate $\mathbf{P_{Pir}}$. The polymer was characterized using UV–vis to determine the amount of Pir (9.6 wt%).

The conjugation of the EKE or ESE peptide (1 mol%) to $\mathbf{P_{Pir}}$ in DMA was monitored by HPLC, and the reaction was completed in 5 min. Then, N_3-PEG_3-biotin (1 mol%) was attached to the polymer and the remaining DBCO groups were end-capped with two molar excesses of N_3-PEG_4-COOH. The mixture was precipitated into acetone; the crude product was dissolved in methanol and re-precipitated into acetone to yield the polymer–drug–peptide conjugates $\mathbf{P_{EKE}}$ and $\mathbf{P_{ESE}}$.

The contents of unbound Pir and peptides in the polymer conjugates (measured by HPLC analysis) were below 0.2% and 0.4% w/w of their total amount, respectively.

2.11. Preparation of Recombinant Proteins and Scfv-Targeted Polymer Conjugates

The scFv B1 fragment with a C-terminal KSK tag was obtained using a similar method as that used previously[17,25] for scFv B1 tagged with KEK. The difference between the KEK and KSK tags was that the design of KSK was improved; namely, IAALKSKIAALKSE-$(IAALKSK)_2$ ensured the formation of an antiparallel coiled coil with a suitable polymer-bound counterpart.[26] Briefly, the 90 bp oligonucleotide duplex was prepared from four oligonucleotides:

SK1 = 5′-gtactatcgcagcgctgaaatctaagattgcggccttgaaa,
SK2 = 5′-tccgagatcgcggcactgaaatctaagatcgccgctctgaaaagcaagg,
SK3 = 5′-tgccgcgatctcggatttcaaggccgcaatcttagatttcagcgctgcgata, and
SK4 = 5′-gtacccttgcttttcagagcggcgatcttagatttcag,

where SK2 and SK3 partly overlapped and had their 5′ ends phosphorylated, and where the 5′ ends of SK1 and SK4 contained four-base overhangs to allow for cloning into the Acc65I site. The oligonucleotides SK1 + SK3 and SK2 + SK4 were annealed, the resulting duplexes were ligated, and the 90 bp KSK oligonucleotide duplex was gel-purified and used to replace the KEK tag in scFv B1. The final construct thus encoded scFv B1 in the format of VH-(gly4ser)4-VL-myc-KSK tag-His5.

2.12. Expression and Purification of the Fusion Protein scFv B1-KSK

For expression in *E. coli* BL21(DE3) cells, a modified pET-22(b) vector was used. In this vector, the scFv coding sequence is preceded by the PelB signal sequence, which allows for translocation of the product into the periplasmic space. The His5 tag at the C-terminus of the polypeptide was used for product isolation and purification by IMAC chromatography on

Ni-CAM (Sigma). The final purification was achieved by ion exchange chromatography on a MonoS column.[17,25]

2.13. In Vitro Cytotoxic Activity of the Polymer Conjugates

The cells (5×10^3) were seeded into 100 µL of media in 96-well flat-bottom plates 24 h before the addition of free Pir or before the polymer conjugates P_{ESE} or P_{EKE} were dissolved in the solution of recombinant scFv fragments of the B1 antibody. These antibody fragments varied based on the presence of the coiled coil tags (KEK or KSK) or the absence of the tags ($scFv_{KEK}$, $scFv_{ksk}$, and $scFv_0$, respectively, concentration 3.16 mg mL^{-1}). The polymer/protein weight ratio of 2:1, which corresponded to an ESE/KSK (or EKE/KEK) molar ratio of 3:1, was used. The concentrations of the P_{ESE} and P_{EKE} conjugates dissolved in the solutions of scFv fragments for the cytotoxicity testing varied from 0.02 to 100 µg mL^{-1}. The drug concentrations of free Pir varied from 0.001 to 5 µg mL^{-1} for the cytotoxicity testing. The cells were subsequently cultivated for 72 h in 5% CO_2 at 37 °C. Then, 10 µL of Alamar Blue cell viability reagent was added to each well, and the plates were incubated for 4 h at 37 °C. The metabolic activity was measured according to the protocol for the Synergy Neo plate reader (Bio-Tek, Czech Republic) using an excitation wavelength of 570 nm and an emission wavelength of 600 nm. As a control, the cells cultivated in medium without any treatment were employed. The assay was conducted in triplicate and repeated three times independently.

2.14. In Vitro Cell Binding Studies

To determine the binding of the $scFv_{KEK/KSK}$-targeted $P_{EKE/ESE}$ conjugates to the cell membrane, the cells were washed with 0.5% bovine serum albumin in PBS (BSA–PBS) and ≈2.5×10^5 of cells in a 50 µL volume were incubated for 30 min at 25 °C with $P_{ESE}/scFv_{KSK}$, $P_{EkE}/scFv_{KEK}$ or $P_{ESE}/scFv_0$, $P_{EkE}/scFv_0$ (as a control). The conjugates with scFv were prepared as described above using a polymer/protein weight ratio of 2:1. The final concentration of scFv for the binding studies was 50 µg mL^{-1}. Then, the cells were washed with 0.5% BSA–PBS, diluted in 50 µL, and labeled for 30 min in the dark at 25 °C with streptavidin-Alexa 405 (Thermo Scientific, Czech Republic), which recognizes biotin on conjugates, and anti-c-Myc-fluorescein (Exbio, Czech Republic), which recognizes the Myc tag sequence in scFv. Afterward, the cells were washed with 0.5% BSA–PBS and diluted in 0.5 mL of 0.5% BSA–PBS containing 1 µg mL^{-1} 7-AAD to detect dead cells. The median fluorescence intensity of the polymer conjugates labeled with streptavidin-Alexa fluor 405 and scFv labeled with anti-c-Myc-fluorescein was determined. The samples were analyzed by FACS Verse (Becton Dickinson) and FlowJo software (TreeStar). The FACS analysis of the cell binding of the polymer conjugates was performed five times in triplicates.

2.15. Mice

Inbred BALB/c (*H-2*^{d}) mice (females) were obtained from the animal breeding facility of the Institute of Physiology, Czech Academy of Sciences. Mice were used at 9–15 weeks of age, and food and water were given ad libitum. In all animal works, institutional guidelines for the care and use of laboratory animals were strictly followed under a protocol approved by the Institutional Animal Care and Use Committee of the Czech Academy of Sciences and compliant with local and European guidelines.

2.16. Monoclonal Antibodies

The following monoclonal antibodies were used to stain surface antigens: anti-Myc-fluorescein (ExBio), CD3-biotin, CD3-eF450, CD4-PE, CD4-APC, CD4-FITC, CD80-APC, MHC II-PE, and STP-eF450 (eBiosciences). Live and dead cells were distinguished by propidium iodide staining.

2.17. Blood Clearance of the Polymer Conjugates

BALB/c mice were i.v. injected with the polymer–pirarubicin conjugate $P_{ESE}/scFv_{KSK}$, the polymer–pirarubicin conjugate $P_{ESE}/scFv_0$, or the same volume of PBS (220 µL). The dose of the conjugate corresponded to a dose of 75 µg Pir per mouse. Samples of blood were taken from experimental mice at 1 min, 1, 6, 12, 24, and 48 h postinjection. Samples taken at 1 min, 12, and 48 h were taken from the carotid arteries and samples taken at 1, 6, and 24 h were taken from the tail vein. Blood samples were collected in heparinized microtubes and the plasma was separated. The concentration of Pir in the plasma samples was determined using HPLC analysis. The amount of Pir released from the polymer conjugate was determined after its extraction from the plasma into chloroform. Mixtures of 50 µL of blood plasma samples and 50 µL of 6 M HCl were heated to 50 °C for 1 h followed by extraction with 0.4 mL of chloroform for 15 min. The chloroform extract was evaporated to dryness and the residue was diluted with 0.5 mL of methanol. The Pir content was determined using an HPLC Shimadzu system equipped with a fluorescence detector with an excitation wavelength of 488 nm and an emission wavelength of 560 nm. The calibration was carried out using Pir standards dissolved in DMSO that were diluted with blood plasma, hydrolyzed with 6 M HCl and extracted with chloroform as described above.

2.18. In Vivo Binding Studies

BALB/c mice were i.p. inoculated with 5×10^5 BCL1 cells in 250 µL of PBS on day 0. The targeted polymer–pirarubicin conjugate $P_{ESE}/scFv_{KSK}$ and the nontargeted control polymer conjugate P_{ESE} dissolved in PBS at concentrations of 6.2 mg mL^{-1} (polymer conjugate) and 3.1 mg mL^{-1} (scFv). These treatments were i.v. administered on day 30, and one dose contained 5 mg kg^{-1} of polymer-bound Pir. The spleens were harvested 1, 2.5, 6, and 24 h after the administration of conjugates. Naïve mice, mice inoculated with BCL1 cells, and mice i.v. injected with PBS alone were used as controls. Each experimental group contained two mice.

2.19. Staining for Surface Antigens and Flow Cytometry

The spleens were harvested and homogenized using a gentleMACS Dissociator (Miltenyi Biotech) in flow cytometry buffer (PBS, 2% FCS, 2×10^{-3} M EDTA). The cell suspensions were filtered using a 70 µm cell strainer (BD Biosciences), resuspended in flow cytometry buffer after red blood cell lysis with ACK lysing buffer (GIBCO), and filtered again using a 30 µm cell strainer (BD Biosciences). The resultant cell suspensions were blocked by 20% mouse serum for 30 min on ice and stained with anti-c-Myc-fluorescein (Exbio, Czech Republic) for 30 min on ice in the dark. The cells were then washed twice in flow cytometry buffer, stained with streptavidin-eF450 (eBioscience, Czech Republic) for 20 min on ice in the dark and washed twice in flow cytometry buffer. Finally, the cells were stained with propidium iodide shortly before analysis on an LSR II flow cytometer (BD Biosciences). The data were analyzed using FlowJo software (Tree Star).

2.20. Treatment of Established BCL1 Leukemia In Vivo

BALB/c mice were i.p. inoculated with 5×10^5 BCL1 cells in 250 µL of PBS on day 0. The targeted polymer–Pir conjugate $\mathbf{P_{ESE}}$/scFv$_{KSK}$ and the nontargeted control polymer conjugate $\mathbf{P_{ESE}}$ were dissolved in PBS at concentrations of 6 mg mL^{-1} (polymer conjugate) and 3 mg mL^{-1} (scFv). The treatments were then i.v. administered in three doses on days 11, 14, and 17. One dose contained 5 mg kg^{-1} of polymer-bound Pir. Another group of BALB/c mice were inoculated with BCL1 cells and treated with free Pir on days 11, 14, and 17. One dose contained 3.5 mg kg^{-1} Pir (estimated as equitoxic to 5 mg kg^{-1} of polymer-bound Pir) in PBS with 2% of DMSO at a concentration of 0.34 mg mL^{-1}. BALB/c mice inoculated with BCL1 cells and injected with PBS on days 11, 14, and 17 were used as the control group. Tumor progression and general fitness of the mice were checked every second day, and the body weight and survival of the mice were recorded. Each experimental group included eight mice.

2.21. Statistical Analysis

Statistical analysis was performed using the Log-rank test (survival graphs) or ANOVA, followed by Tukey's multiple comparison test; *, ** and *** represent p-values <0.05, 0.01, and 0.001, respectively. The data were representative of at least two experiments.

3. Results and Discussion

3.1. Synthesis of the Peptides and Polymer Conjugates

In our previous work,[26] we compared the associative behavior of two pairs of coiled coil peptides: $(VAALEKE)_4$/$(VAALKEK)_4$ (EKE/KEK) formed coiled coil heterodimers with randomly oriented peptide chains, whereas $(IAALESE)_2$-IAALESKIAALESE/IAALKSKIAALKSE-$(IAALKSK)_2$ (ESE/KSK) formed higher heterooligomers with antiparallel orientations of the peptides and stronger binding activities. Though it is not possible to describe the formation of the coiled coil oligomers using a single binding constant due to the multi-step characteristics of the process, the higher stability of the latter pair was evident from the following observations. While the individual peptides EKE and KEK had random coil conformations and adopted the coiled coil conformation only upon mixing of the two peptides (α-helix melting T_m > 61 °C), the peptides ESE and KSK already exhibited high helical contents as individual peptides, and upon mixing of the two components, the stability of the coiled coil was further increased (T_m > 95 °C). We hypothesized that the latter pair of peptides would be more suitable for attachment of a targeting ligand to the polymer drug carrier due to the higher stability of the coiled coil and due to the antiparallel orientation of the peptide chains that would minimize eventual steric hindrance.

Compared with our previous work, we have improved the synthesis of the polymer precursors in order to obtain polymer carriers with low dispersity (<1.2). Specifically, we used RAFT copolymerization of HPMA with 3-(*N*-methacryloylglycylphenylalanylleucylglycyl)thiazolidine-2-thione (Ma-GFLG-TT). The resulting reactive copolymer $\mathbf{P_{TT}}$ was submitted to reaction with a cytostatic drug pirarubicin (Pir), and the remaining TT groups were aminolyzed with an amino derivative of dibenzoazacyclooctyne (DBCO-NH_2) to yield the polymer precursor $\mathbf{P_{Pir}}$ (**Scheme 1**).

The coiled coil-forming peptides with *N*-terminal azide groups were designed and synthesized as described in our previous publications.[17,25,26] The peptide azides (EKE and ESE) were bound to the polymer precursor $\mathbf{P_{Pir}}$ via metal-free azide-alkyne cycloaddition ("click" chemistry) utilizing the reaction between DBCO groups of the polymer precursor and the azide functions of the peptides. Another part of DBCO groups was modified with an azide derivative of biotin to enable monitoring of the fate of the polymer carrier both in vitro and in vivo. The remaining DBCO groups were end-capped with N_3-PEG_4-COOH to yield the polymer–drug–peptide conjugates $\mathbf{P_{EKE}}$ and $\mathbf{P_{ESE}}$, which contained the peptides EKE and ESE, respectively (Scheme 1).

The basic physicochemical characteristics of all of the prepared copolymers are summarized in Table 1. SEC chromatogram of the polymer–pirarubicin conjugate $\mathbf{P_{ESE}}$ is shown in Figure S2 (Supporting Information) as an example.

The low dispersity value of the copolymers is an important feature of the presented polymer drug delivery system. It has been repeatedly reported that the pharmacokinetic behavior of a polymer therapeutic is significantly influenced by both its molecular weight and dispersity. Polymers with a broad distribution of molecular weights contain a fraction of smaller macromolecules with shorter blood circulation times and lower levels of accumulation in solid tumors, whereas a fraction of larger macromolecules show longer blood circulation times and higher levels of tumor accumulation due to the EPR effect. If the molecular weight of the largest macromolecules exceeds the renal threshold, they cannot be eliminated via glomerular filtration and may remain in organism for extended periods of time, with unknown physiological effects.[31] Consequently, only a limited fraction of such polydispersed polymeric drugs

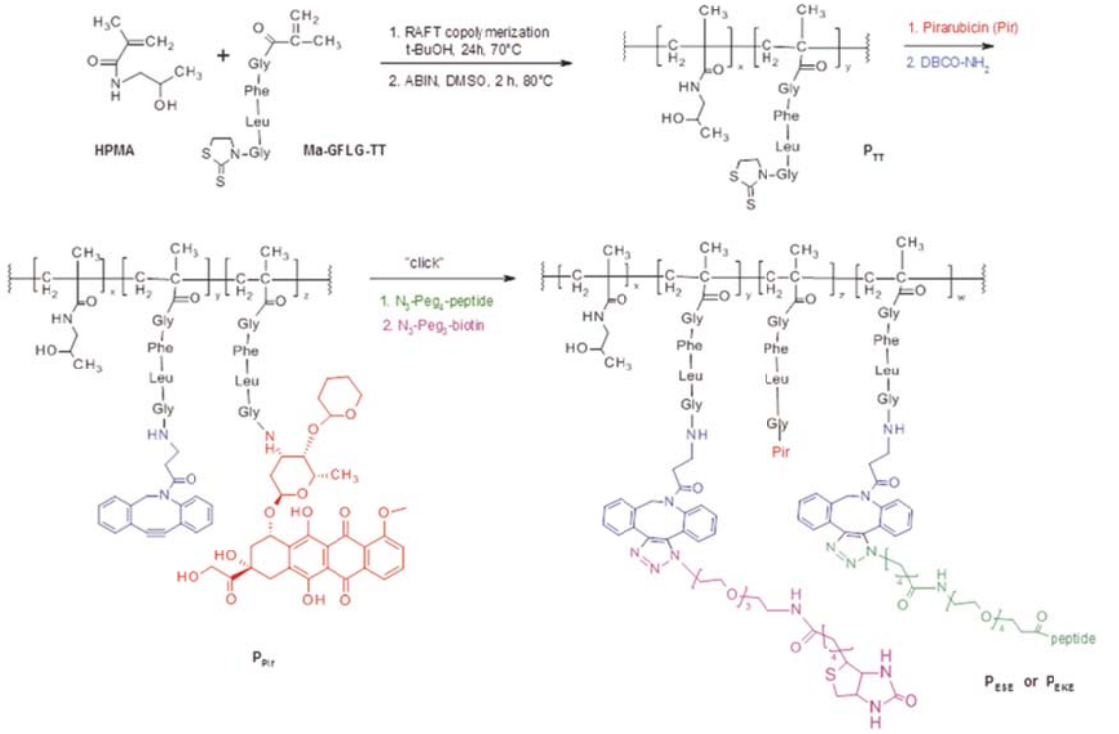

Scheme 1. Synthesis of the polymer–drug–peptide conjugates $\mathbf{P_{EKE}}$ and $\mathbf{P_{ESE}}$.

have the optimal pharmacokinetic and therapeutic profiles. In contrast, we can speculate that macromolecular therapeutics with low dispersity (e.g., originating from RAFT polymerization) should exhibit more uniform pharmacokinetics and, consequently, better therapeutic efficacy. Nevertheless, it should be noted that this is just a hypothesis, and there is not yet enough experimental in vivo data available in the literature to support this statement.

3.2. Preparation of Recombinant Proteins and scFv-Targeted Polymer Conjugates

The recombinant scFv fragments of the B1 antibody with either the KEK or KSK coiled coil tag or without the tag ($\mathbf{scFv_{KEK}}$, $\mathbf{scFv_{ESE}}$, and $\mathbf{scFv_0}$, respectively) were expressed and isolated from *E. coli*, as described earlier. The purified proteins in PBS buffer (pH 7.4) were mixed with the corresponding complementary polymer conjugates to yield the scFv-targeted supramolecular complexes $\mathbf{P_{EKE}/scFv_{KEK}}$ and $\mathbf{P_{ESE}/scFv_{KSK}}$. The molar ratio of EKE/KEK (and ESE/KSK) was set to 3:1, which corresponds to a polymer/protein weight ratio of 2:1. In addition to the physicochemical methods (size-exclusion chromatography and sedimentation analysis) described in our previous papers, the formation of the supramolecular complexes polymer–protein was also confirmed by dynamic light scattering (**Figure 1**).

3.3. In Vitro Binding Studies

The in vitro binding efficacy of the targeted polymer conjugates $\mathbf{P_{EKE}/scFv_{KEK}}$ and $\mathbf{P_{ESE}/scFv_{KSK}}$ or the polymer conjugate $\mathbf{P_{EKE}}$ or $\mathbf{P_{ESE}}$ mixed together with the targeting protein without the coiled coil-forming tag ($\mathbf{P_{EKE}/scFv_0}$; $\mathbf{P_{ESE}/scFv_0}$) was evaluated in BCL1 cells using flow cytometry. **Figure 2**A,B shows a representative example of the detection of scFv and the polymer backbone in the samples incubated with the targeted conjugates. We were able to detect similar anti-Myc-FITC signals originating from the targeting scFv in both targeted polymer conjugates ($\mathbf{P_{EKE}/scFv_{KEK}}$ and $\mathbf{P_{ESE}/scFv_{KSK}}$). The binding of streptavidin-Alexa fluor 405 to the biotin-labeled targeted $\mathbf{P_{ESE}/scFv_{KSK}}$ conjugate showed a significantly higher median fluorescence intensity (MFI) of Alexa 405 (MFI 16 306) than $\mathbf{P_{EKE}/scFv_{KEK}}$ (MFI 3967). Figure 2C shows quantitative difference in MFI of Alexa 405 after binding streptavidin-Alexa fluor 405 to the biotin-labeled targeted $\mathbf{P_{EKE}/scFv_{KEK}}$ and $\mathbf{P_{ESE}/scFv_{KSK}}$ conjugates. In accordance with our original hypothesis and previously published[26] results, we attributed this difference in cell binding efficiency to the formation of antiparallel coiled coil heterodimers and to the stronger interactions between ESE/KSK peptides compared with the weaker, randomly oriented EKE/KEK coiled coils.

The cells incubated with the nontargeted polymers mixed with the control protein without the coiled coil tag ($\mathbf{P_{EKE}}$+$\mathbf{scFv_0}$; $\mathbf{P_{ESE}}$+$\mathbf{scFv_0}$) exhibited only the signal of scFv binding to the

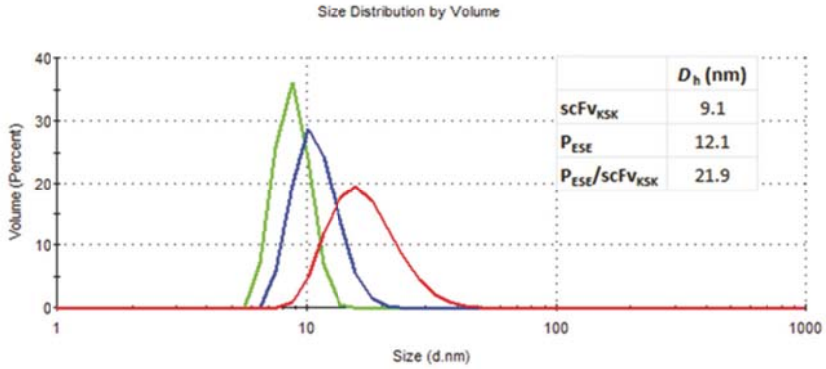

Figure 1. Particle size distribution and hydrodynamic diameters obtained by DLS analysis. Green line, $scFv_{KSK}$; blue line, P_{ESE}; red line, $P_{ESE}/scFv_{KSK}$ complex.

cells, and no signal corresponding to the polymer was detected (data not shown).

3.4. Cytostatic Activity of the Polymer Conjugates In Vitro

In accordance with the results of flow cytometry cell binding studies, the in vitro evaluation of the cytotoxicity of the targeted conjugates revealed that the cytotoxicity of $P_{ESE}/scFv_{KSK}$ was two times greater than that of $P_{EKE}/scFv_{KEK}$ (Table 2). The targeted polymer conjugates $P_{ESE}/scFv_{KSK}$ and $P_{EKE}/scFv_{KEK}$ exhibited cytotoxicities that were ten times and eight times higher, respectively, than those of the nontargeted conjugates $P_{ESE}/scFv_0$ and $P_{EKE}/scFv_0$.

In general, the targeted polymer conjugates show significantly higher cytotoxic effects in vitro than the corresponding nontargeted conjugates. The cytotoxicities of both the nontargeted polymer conjugates differed only slightly, as $P_{ESE}/scFv_0$ exhibited somewhat higher cytotoxic effects than $P_{EKE}/scFv_0$. We speculated that this difference might be explained by different interactions between the polymer-borne peptide sequences and the cell membrane. The dependence of the

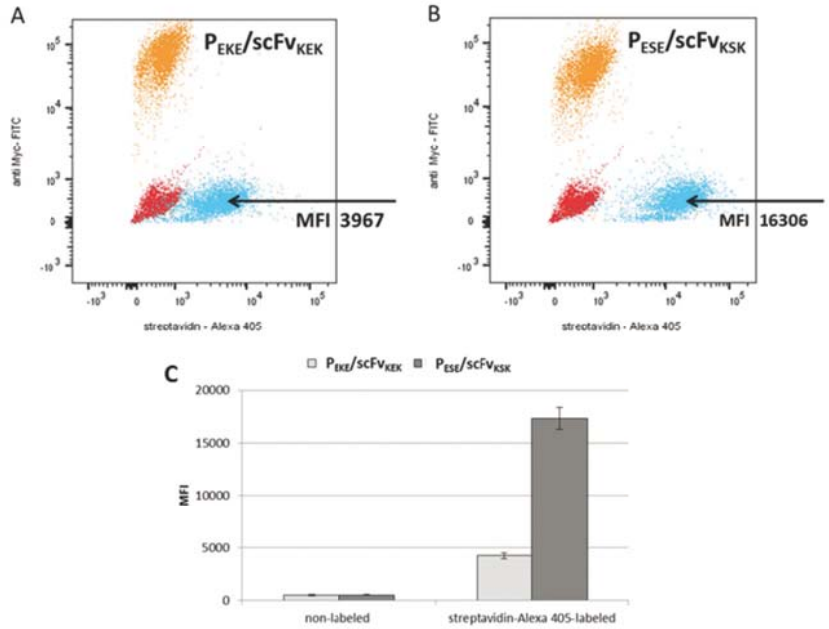

Figure 2. Flow cytometry analysis of BCL1 cell binding by the targeted conjugates A) $P_{EKE}/scFv_{KEK}$ and B) $P_{ESE}/scFv_{KSK}$. Along the *y*-axis, the dot plot shows anti-Myc-FITC signals (orange) indicating the binding of scFv to the cells; along the *x*-axis, the streptavidin-Alexa 405 signal (blue) indicates the binding of the polymer to the cells and nonlabeled population of cells (red). C) Quantification of MFI of the cell binding experiment.

cell viability on the concentration of the polymer conjugates is shown in Figure S1 (Supporting Information). Free pirarubicin shows the highest cytotoxicity, which is a well-known fact from in vitro studies.[25,32,33] The advantages of polymeric drugs become evident in vivo due to their longer circulation times, decreased side effects and the possible presence of targeting ligands.

Based on the results of both the cell binding and cytotoxicity studies, the following in vivo experiments were performed using only the most efficient targeted polymer conjugate, $\mathbf{P_{ESE}/scFv_{KSK}}$.

3.5. Blood Clearance of the Polymer Conjugates

The persistence of the conjugates in circulation was determined in BALB/c mice i.v. injected with the polymer–pirarubicin conjugate $\mathbf{P_{ESE}/scFv_{KSK}}$ or the polymer–pirarubicin conjugate $\mathbf{P_{ESE}}$ + $\mathbf{scFv_0}$. The data showed that the majority (≈90%) of injected Pir disappeared from circulation within 6 h after the administration of polymeric conjugates (**Figure 3**). However, a small fraction of injected Pir (about 1%) was still detectable in the blood even 48 h after administration. At the 6 h time point, a slightly slower elimination rate of Pir from the circulation was seen when the polymeric conjugate associated with the targeting scFv was used in comparison to the use of the conjugate without scFv; however, this effect was diminished at later time points. The slower elimination of the scFv-targeted polymer conjugate can be most likely attributed to its higher molecular weight (and hydrodynamic volume) compared with that of the nontargeted polymer. The corresponding half-times $T_{1/2\alpha}$ and $T_{1/2\beta}$ characterizing the absorption and elimination phases of the pharmacokinetics of the both polymer conjugates together with the biexponential functions used for the calculations are shown in Figure S3 (Supporting Information).

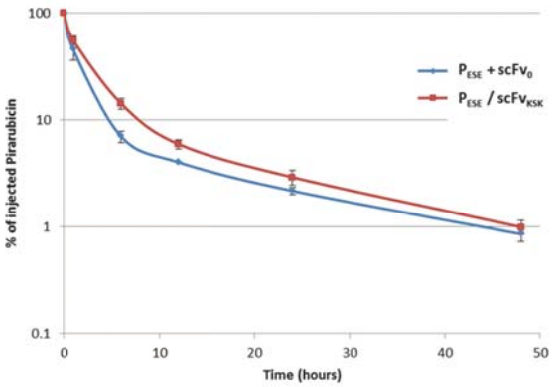

Figure 3. Pharmacokinetics of Pir in the blood of mice injected with targeted and nontargeted polymer–pirarubicin conjugates. BALB/c mice were i.v. injected with the targeted polymer–pirarubicin conjugate $\mathbf{P_{ESE}/scFv_{KSK}}$ (red line) or the nontargeted polymer conjugate $\mathbf{P_{ESE}}$ (blue line) mixed with $\mathbf{scFv_0}$ at doses equivalent to 75 μg of pirarubicin. Blood was collected 1 min, 1, 6, 12, 24, and 48 h postinjection and was analyzed using HPLC. The concentration of Pir in the blood determined at 1 min after administration was considered 100%. Each experimental group included three mice.

3.6. In Vivo Binding Studies

The ability of the targeted polymeric conjugate to bind to tumor cells in vivo was determined in BALB/c mice with developed BCL1 leukemia. Mice were i.v. injected with the targeted polymer–Pir conjugate $\mathbf{P_{ESE}/scFv_{KSK}}$ or the nontargeted polymer conjugate $\mathbf{P_{ESE}}$ mixed with scFv 30 d after inoculation with BCL1 cells, which ensured that the spleens of the experimental mice contained significant BCL1 tumor cell counts. BCL1 cells were identified by double positivity for MHC II and CD80, as BCL1 cells are known to strongly express these markers in vivo.[34] At selected time points after conjugate administration, the polymeric conjugates and scFv bound to the surface of BCL1 cells were detected in spleen cell suspensions using streptavidin-eF450 (as the polymer conjugates contained biotin) and anti-c-Myc mAb-FITC (as scFv contained the Myc tag), respectively. The BCL1 cells in mice injected with the polymer conjugate $\mathbf{P_{ESE}}$ mixed with $\mathbf{scFv_0}$ showed gradually increasing $\mathbf{scFv_0}$ binding for up to 6 h and much lower binding at 24 h (**Figure 4**). In contrast, the BCL1 cells in mice injected with the targeted polymer–Pir conjugate $\mathbf{P_{ESE}/scFv_{KSK}}$ showed very strong binding of both scFv and the polymer at 1 h postinjection. The binding was somewhat lower at 2.5 and 6 h postinjection and very low at 24 h postinjection (Figure 4). The sharp decrease in binding of the polymer conjugate targeted with scFv in comparison with free scFv after 24 h likely reflected the much stronger internalization of the multivalent polymer–Pir conjugate $\mathbf{P_{ESE}/scFv_{KSK}}$ complexes compared with that of monovalent scFv. Overall, we clearly demonstrated that $\mathbf{scFv_{KSK}}$ tightly binds to the polymer–Pir conjugate $\mathbf{P_{ESE}}$ and that the resulting targeted polymer–Pir conjugate $\mathbf{P_{ESE}/scFv_{KSK}}$ binds to the targeted BCL1 cells in vivo upon i.v. administration. Our targeted polymeric carrier bearing the cytostatic drug Pir is thus able to selectively deliver Pir to tumor cells in mice.

3.7. Treatment of Established BCL1 Leukemia In Vivo

The antitumor activities of the targeted polymer–pirarubicin conjugate $\mathbf{P_{ESE}/scFv_{KSK}}$ and the nontargeted control polymer conjugate $\mathbf{P_{ESE}}$ mixed with scFv was tested in a BCL1 leukemia mouse model with diffuse malignancy that did not form solid tumors. The mice were injected with tumor cells and the conjugates or free pirarubicin were administered in three separate doses on days 11, 14, and 17. Only the targeted polymeric conjugate therapy impeded the increase in body weight of the experimental mice, which is a sign of disease progression (**Figure 5**A). This result showed that only the targeted polymeric conjugate was capable of inhibiting the massive outbreak of the disease within the recorded time period (up to day 40). The median survival times were 36.5, 42.5, 45.5, and 66.5 d for the untreated mice, the mice treated with free pirarubicin, the mice injected with the nontargeted polymer and the mice injected with the targeted conjugate, respectively.

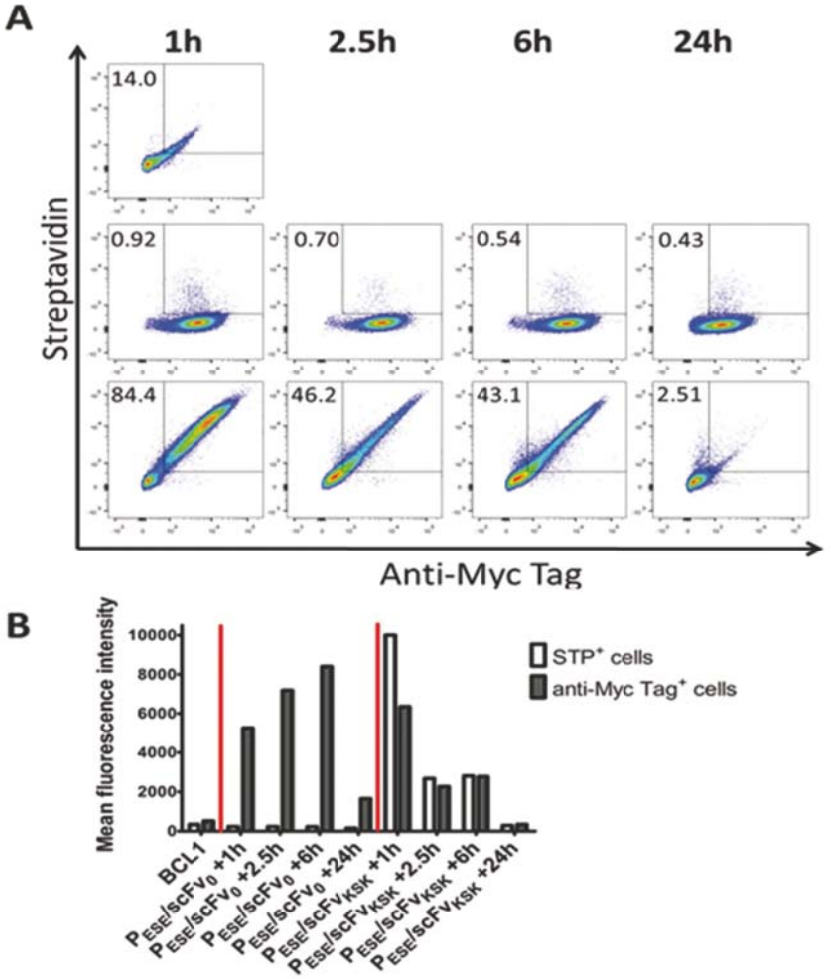

Figure 4. In vivo binding of targeted and nontargeted polymer–pirarubicin conjugates. BALB/c mice were i.p. injected with 5×10^5 BCL1 cells on day 0. Mice were i.v. injected with the targeted polymer–pirarubicin conjugate $\mathbf{P_{ESE}/scFv_{KSK}}$ ($\mathbf{P_{ESE}/scFv_{KSK}}$: 5 mg kg^{-1} of polymer-bound pirarubicin per dose) or the nontargeted control polymer conjugate $\mathbf{P_{ESE}}$ ($\mathbf{P_{ESE}}$: 5 mg kg^{-1} of polymer-bound pirarubicin per dose) mixed with scFv on day 30. BALB/c mice bearing BCL1 leukemia (BCL1) and i.v. injected with PBS were used as controls. Spleens were harvested 1, 2.5, 6, and 24 h after the injection of polymeric conjugates. BCL1 cells were gated as MHC II$^+$ CD80$^+$ double positive cells. A) Dot plots showing binding of scFv (anti-Myc labeling) and polymeric conjugate (streptavidin labeling) to BCL1 cells. Each dot plot shows one representative mouse. The upper row shows a control mouse, the middle row shows mice injected with the polymer conjugate $\mathbf{P_{ESE}}$ mixed with $\mathbf{scFv_0}$, and the lower row shows mice injected with the targeted polymer conjugate $\mathbf{P_{ESE}/scFv_{KSK}}$. B) Mean fluorescence intensities of scFv binding (dark columns) and polymer conjugate binding (empty columns); each column shows one representative mouse from the group.

Both conjugates significantly prolonged the survival times of the experimental mice (Figure 5B) compared with both mice treated with the free drug and the untreated control. Though there was a statistically nonsignificant difference in the survival times of mice treated with the nontargeted and targeted conjugates, therapy with the targeted conjugate led to a complete cure in one experimental mouse and markedly prolonged survival of another five animals. Thus, the targeted polymeric conjugate proved to be the most efficient treatment modality, and the results reflected the ability of the targeted polymeric conjugate to selectively deliver the cytostatic drug to the cancer cells.

4. Conclusions

We synthesized hydrophilic polymer conjugates with narrow molecular weight distributions containing the anticancer drug pirarubicin bound to the polymer backbone via an enzymatically cleavable tetrapeptide spacer. A recombinant antibody fragment

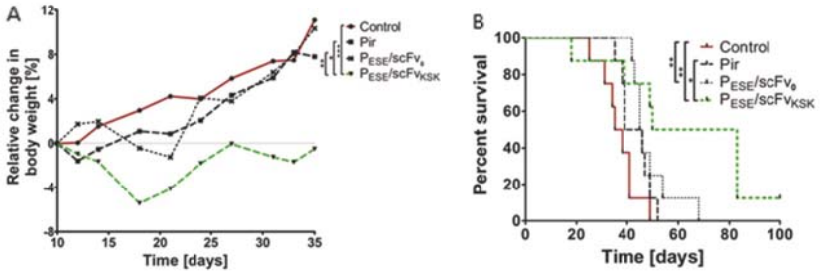

Figure 5. Treatment of BCL1 leukemia with polymer conjugates. BALB/c mice were i.p. injected with 5×10^5 BCL1 cells on day 0. Mice were i.v. injected with three doses of targeted polymer–pirarubicin conjugate $\mathbf{P_{ESE}/scFv_{KSK}}$ ($\mathbf{P_{ESE}/scFv_{KSK}}$; 5 mg kg^{-1} of polymer-bound pirarubicin per dose), nontargeted control polymer conjugate $\mathbf{P_{ESE}}$ ($\mathbf{P_{ESE}}$; 5 mg kg^{-1} of polymer-bound pirarubicin per dose) mixed with $\mathbf{scFv_0}$, or free pirarubicin (Pir; 3.5 mg kg^{-1}) on days 11, 14, and 17. BALB/c mice injected with BCL1 cells and treated with PBS were used as controls. A) Changes in relative body weights of experimental mice. B) Survival of experimental mice. Groups were compared using ANOVA followed by A) Tukey's multiple comparison test or B) Log-rank test; *, **, and *** represent *p*-values <0.05, 0.01, and 0.001, respectively. Eight mice per group were used. The experiment was repeated twice with similar results.

that specifically binds to leukemia cells was attached to the polymer–drug conjugate via a universal noncovalent coiled coil interaction. The major advantage of the coiled coil approach compared with traditional covalent conjugation methods lies in the well-defined and absolutely nondestructive preparation of the polymer–protein complex. It was demonstrated that the choice of the coiled coil linker between the protein and the polymer can significantly affect both the cell binding efficiency of the targeted polymer–drug conjugate and its cytotoxic activity against the target malignant cells. The superior therapeutic efficiency of the scFv-targeted polymer cancerostatic compared with the low-molecular weight drug and the nontargeted polymer–drug conjugate was demonstrated in vivo using a murine BCL1 leukemia model.

We believe that targeted polymer cancerostatics utilizing noncovalent interactions of the two complementary peptides between the polymer carrier and the targeting protein ligand represent a highly promising new type of nanomedicine. The approach used herein might help to overcome not only the drawbacks of current chemotherapies, such as the general nonspecific toxicity, but also frequent problems with the clinical approval of nanomedicines by regulatory authorities due to the low uniformity and poorly defined structures of polymer–protein conjugates prepared by more traditional covalent methods.

Supporting Information

Supporting Information is available from the Wiley Online Library or from the author.

Acknowledgements

This work was supported by the Ministry of Education, Youth and Sports of the Czech Republic within the National Sustainability Program I (project POLYMAT LO1507) and II (project BIOCEV-FAR LQ1604), by the Ministry of Health of the Czech Republic (project 16-28594A), and by the Czech Science Foundation (projects 16-17207S and 13-12885S).

Conflict of Interest

The authors declare no conflict of interest.

Keywords

cancer therapy, coiled coil, drug targeting, hydrophilic polymer, scFv

Received: May 16, 2017
Revised: July 17, 2017
Published online:

[1] H. Maeda, H. Nakamura, J. Fang, *Adv. Drug Delivery Rev.* **2013**, *65*, 71.
[2] J. Kopeček, Z.-R. Lu, P. Kopečková, *Nat. Biotechnol.* **1999**, *17*, 1101.
[3] C. M. Ward, M. Pechar, D. Oupický, K. Ulbrich, L. W. Seymour, *J. Gene Med.* **2002**, *4*, 536.
[4] R. Pola, M. Studenovský, M. Pechar, K. Ulbrich, O. Hovorka, D. Větvička, B. Říhová, *J. Drug Targeting* **2009**, *17*, 763.
[5] Z.-R. Lu, S.-Q. Gao, P. Kopečková, J. Kopeček, *Bioconjugate Chem.* **2000**, *11*, 3.
[6] J. Hongrapipat, P. Kopečková, J. Liu, S. Prakongpan, J. Kopeček, *Mol. Pharmaceutics* **2008**, *5*, 696.
[7] B. Říhová, P. Kopečková, J. Strohalm, P. Rossmann, V. Větvička, J. Kopeček, *Clin. Immunol. Immunopathol.* **1988**, *46*, 100.
[8] M. Kovář, T. Mrkvan, J. Strohalm, T. Etrych, K. Ulbrich, M. Šťastný, B. Říhová, *J. Controlled Release* **2003**, *92*, 315.
[9] T.-W. Chu, J. Kopeček, *Biomater. Sci.* **2015**, *3*, 908.
[10] K. S. Palla, L. S. Witus, K. J. Mackenzie, C. Netirojjanakul, M. B. Francis, *J. Am. Chem. Soc.* **2015**, *137*, 1123.
[11] F. Sun, W.-B. Zhang, A. Mahdavi, F. H. Arnold, D. A. Tirrell, *Proc. Natl. Acad. Sci. USA* **2014**, *111*, 11269.
[12] R. J. Spears, M. A. Fascione, *Org. Biomol. Chem.* **2016**, *14*, 7622.
[13] L. S. Witus, T. Moore, B. W. Thuronyi, A. P. Esser-Kahn, R. A. Scheck, A. T. Iavarone, M. B. Francis, *J. Am. Chem. Soc.* **2010**, *132*, 16812.
[14] S. Ulrich, D. Boturyn, A. Marra, O. Renaudet, P. Dumy, *Chem. – A Eur. J.* **2014**, *20*, 34.
[15] B. Apostolovic, M. Danial, H.-A. Klok, *Chem. Soc. Rev.* **2010**, *39*, 3541.
[16] S. P. E. Deacon, B. Apostolovic, R. J. Carbajo, A. Schott, K. Beck, M. J. Vicent, A. Pineda-Lucena, H. Klok, R. Duncan, *Biomacromolecules* **2011**, *12*, 19.
[17] M. Pechar, R. Pola, R. Laga, K. Ulbrich, L. Bednárová, P. Maloň, I. Sieglová, V. Král, M. Fábry, O. Vaněk, *Biomacromolecules* **2011**, *12*, 3645.
[18] B. Apostolovic, S. P. E. Deacon, R. Duncan, H.-A. Klok, *Macromol. Rapid Commun.* **2011**, *32*, 11.

[19] K. Wu, J. Yang, J. Liu, J. Kopeček, *J. Controlled Release* **2012**, *157*, 126.
[20] K. Wu, J. Liu, R. N. Johnson, J. Yang, J. Kopeček, *Angew. Chem., Int. Ed.* **2010**, *49*, 1451.
[21] T.-W. Chu, R. Zhang, J. Yang, M. P. Chao, P. J. Shami, J. Kopeček, J. Kopeček, *Theranostics* **2015**, *5*, 834.
[22] T.-W. Chu, K. M. Kosak, P. J. Shami, J. Kopeček, *Drug Delivery Transl. Res.* **2014**, *4*, 389.
[23] T.-W. Chu, J. Yang, R. Zhang, M. Sima, J. Kopeček, *ACS Nano* **2014**, *8*, 719.
[24] R. A. Willemsen, M. Pechar, R. C. Carlisle, E. Schooten, R. Pola, A. J. Thompson, L. W. Seymour, K. Ulbrich, *Pharm. Res.* **2010**, *27*, 2274.
[25] R. Pola, R. Laga, K. Ulbrich, I. Sieglová, V. Král, M. Fábry, M. Kabešová, M. Ková , M. Pechar, *Biomacromolecules* **2013**, *14*, 881.
[26] M. Pechar, R. Pola, R. Laga, A. Braunová, S. K. Filippov, A. Bogomolova, L. Bednárová, O. Vaněk, K. Ulbrich, *Biomacromolecules* **2014**, *15*, 2590.
[27] H. Nakamura, E. Koziolová, T. Etrych, P. Chytil, J. Fang, K. Ulbrich, H. Maeda, *Eur. J. Pharm. Biopharm.* **2014**, *90*, 90.
[28] K. Ulbrich, V. Šubr, J. Strohalm, D. Plocová, M. Jelínková, B. Říhová, *J. Controlled Release* **2000**, *64*, 63.
[29] R. Pola, O. Janoušková, T. Etrych, *Physiol. Res.* **2016**, *65*, 225.
[30] S. Perrier, P. Takolpuckdee, J. Westwood, D. M. Lewis, *Macromolecules* **2004**, *37*, 2709.
[31] T. Etrych, V. Šubr, J. Strohalm, M. Šírová, B. Říhová, K. Ulbrich, *J. Controlled Release* **2012**, *164*, 346.
[32] H. Nakamura, E. Koziolová, P. Chytil, K. Tsukigawa, J. Fang, M. Haratake, K. Ulbrich, T. Etrych, H. Maeda, *Mol. Pharmaceutics* **2016**, *13*, 4106.
[33] R. Laga, O. Janoušková, K. Ulbrich, R. Pola, J. Blažková, S. K. Filippov, T. Etrych, M. Pechar, *Biomacromolecules* **2015**, *16*, 2493.
[34] M. Kovář, J. Tomala, H. Chmelová, L. Kovář, T. Mrkvan, R. Josková, Z. Zákostelská, T. Etrych, J. Strohalm, K. Ulbrich, M. Šírová, B. Říhová, *Cancer Res.* **2008**, *68*, 9875.

IV. CONCLUSIONS

1. HPMA copolymer-bound DOX conjugate based on non-degradable polymeric carrier does not induce severe side toxicity.

2. Smaller and less complex linear conjugates exert higher MTD in comparison to larger complex conjugates with dendrimer core.

3. Effective therapy of solid tumors should employ HMW drug delivery system with increased R_h, it should be stable for at least 3 or 4 days following administration and, shortly afterwards, rapidly degraded and excreted from organism.

4. Effective therapy of leukemias should employ drug delivery system with prolonged circulation half-life (providing a depot of biologicaly active drug) and very slow degradation rate.

5. Attachment of BCL1 leukemia-targeting moiety (scFv fragment of B1 mAb) to the HPMA copolymer-bound drug conjugate via non-covalent coiled-coil interaction between complementary peptides show better therapeutic efficacy than non-targeted HPMA copolymer-drug conjugate counterpart or a free drug.

6. HPMA copolymer-bound drug conjugate bearing BCL1 leukemia-targeting moiety attached via non-covalent coiled-coil interaction between KSK and ESE complementary peptides exerts 4 times better binding activity and 2 times higher cytotoxicity *in vitro* than conjugate containing KEK and EKE complementary peptides.

V. REFERENCES

1. Duncan, R., et al., *Polymer-drug conjugates: towards a novel approach for the treatment of endrocine-related cancer.* Endocr Relat Cancer, 2005. **12 Suppl 1**: p. S189-99.
2. Rihova, B., *Biocompatibility and immunocompatibility of water-soluble polymers based on HPMA.* Composites Part B, 2007. **38**(3): p. 386-397.
3. P., E., *Studies in immunity.* New York: Plenum Press, 1906.
4. Ringsdorf, H., *Structure and properties of pharmacologically active polymers.* Journal of Polymer Science: Polymer Symposia, 1975. **51**(1): p. 135-153.
5. Kratz, F., et al., *Prodrug strategies in anticancer chemotherapy.* ChemMedChem, 2008. **3**(1): p. 20-53.
6. Kopecek, J., *Reactive copolymers of N-(2-hydroxypropyl)methacrylamide with N-methacryloylated derivatives of L-leucine and L-phenylalanine. I. Preparation, characterization, and reactions with diamines.* Macromol Chem, 1977. **178**: p. 2169-2183.
7. Rihova, B., et al., *Immunogenicity of N-(2-hydroxypropyl)methacrylamide copolymers.* Macromol Chem, 1985. **9**: p. 13-24.
8. Flanagan, P.E., et al., *Immunogenicity of protein-N-(2-hydroxypropyl)methacrylamide copolymer conjugates in A/J and B10 mice.* J Bioact Compat Polym, 1990. **5**: p. 151-166.
9. Zitvogel, L., et al., *Immunological aspects of cancer chemotherapy.* Nat Rev Immunol, 2008. **8**(1): p. 59-73.
10. Park, I.H., et al., *An Open-Label, Randomized, Parallel, Phase III Trial Evaluating the Efficacy and Safety of Polymeric Micelle-Formulated Paclitaxel Compared to Conventional Cremophor EL-Based Paclitaxel for Recurrent or Metastatic HER2-Negative Breast Cancer.* Cancer Res Treat, 2017. **49**(3): p. 569-577.
11. Liu, B., et al., *Use of solubilizers in preclinical formulations: Effect of Cremophor EL on the pharmacokinetic properties on early discovery compounds.* European Journal of Pharmaceutical Sciences, 2016. **87**: p. 52-57.
12. Farokhzad, O.C. and R. Langer, *Impact of nanotechnology on drug delivery.* ACS Nano, 2009. **3**(1): p. 16-20.
13. Yang, H. and W.J. Kao, *Dendrimers for pharmaceutical and biomedical applications.* J Biomater Sci Polym Ed, 2006. **17**(1-2): p. 3-19.

14. Pouton, C.W., *Lipid formulations for oral administration of drugs: non-emulsifying, self-emulsifying and 'self-microemulsifying' drug delivery systems.* Eur J Pharm Sci, 2000. **11 Suppl 2**: p. S93-8.
15. Yoo, H.S. and T.G. Park, *Biodegradable polymeric micelles composed of doxorubicin conjugated PLGA-PEG block copolymer.* J Control Release, 2001. **70**(1-2): p. 63-70.
16. Tang, Y., et al., *Efficient in vitro siRNA delivery and intramuscular gene silencing using PEG-modified PAMAM dendrimers.* Mol Pharm, 2012. **9**(6): p. 1812-21.
17. Whiteman, K.R., et al., *Poly(Hpma)-coated liposomes demonstrate prolonged circulation in mice.* J Liposome Res, 2001. **11**(2-3): p. 153-64.
18. Kudr, J., et al., *Magnetic Nanoparticles: From Design and Synthesis to Real World Applications.* Nanomaterials (Basel), 2017. **7**(9).
19. Soni, K.S., S.S. Desale, and T.K. Bronich, *Nanogels: An overview of properties, biomedical applications and obstacles to clinical translation.* J Control Release, 2016. **240**: p. 109-126.
20. Chytil, P., et al., *New HPMA copolymer-based drug carriers with covalently bound hydrophobic substituents for solid tumour targeting.* J Control Release, 2008. **127**(2): p. 121-30.
21. MacEwan, S.R., D.J. Callahan, and A. Chilkoti, *Stimulus-responsive macromolecules and nanoparticles for cancer drug delivery.* Nanomedicine (Lond), 2010. **5**(5): p. 793-806.
22. Kiessling, F., et al., *Synthesis and characterization of HE-24.8: a polymeric contrast agent for magnetic resonance angiography.* Bioconjug Chem, 2006. **17**(1): p. 42-51.
23. Li, W., et al., *Overcoming ABC transporter-mediated multidrug resistance: Molecular mechanisms and novel therapeutic drug strategies.* Drug Resist Updat, 2016. **27**: p. 14-29.
24. Matsumura, Y. and H. Maeda, *A new concept for macromolecular therapeutics in cancer chemotherapy: mechanism of tumoritropic accumulation of proteins and the antitumor agent smancs.* Cancer Res, 1986. **46**(12 Pt 1): p. 6387-92.
25. Seymour, L.W., et al., *Influence of molecular weight on passive tumour accumulation of a soluble macromolecular drug carrier.* Eur J Cancer, 1995. **31A**(5): p. 766-70.
26. Carmeliet, P., *Angiogenesis in life, disease and medicine.* Nature, 2005. **438**(7070): p. 932-6.
27. Kerbel, R.S., *Tumor angiogenesis.* N Engl J Med, 2008. **358**(19): p. 2039-49.

28. Hashizume, H., et al., *Openings between defective endothelial cells explain tumor vessel leakiness.* Am J Pathol, 2000. **156**(4): p. 1363-80.
29. Greish, K., *Enhanced permeability and retention of macromolecular drugs in solid tumors: a royal gate for targeted anticancer nanomedicines.* J Drug Target, 2007. **15**(7-8): p. 457-64.
30. Maeda, H., et al., *Vascular permeability enhancement in solid tumor: various factors, mechanisms involved and its implications.* Int Immunopharmacol, 2003. **3**(3): p. 319-28.
31. Cabral, H., et al., *Accumulation of sub-100 nm polymeric micelles in poorly permeable tumours depends on size.* Nat Nanotechnol, 2011. **6**(12): p. 815-23.
32. Noguchi, Y., et al., *Early phase tumor accumulation of macromolecules: a great difference in clearance rate between tumor and normal tissues.* Jpn J Cancer Res, 1998. **89**(3): p. 307-14.
33. Theek, B., et al., *Characterizing EPR-mediated passive drug targeting using contrast-enhanced functional ultrasound imaging.* J Control Release, 2014. **182**: p. 83-9.
34. Rihova, B., *Receptor-mediated targeted drug or toxin delivery.* Adv Drug Deliv Rev, 1998. **29**(3): p. 273-289.
35. Mahne, A.E., et al., *Dual Roles for Regulatory T-cell Depletion and Costimulatory Signaling in Agonistic GITR Targeting for Tumor Immunotherapy.* Cancer Res, 2017. **77**(5): p. 1108-1118.
36. Dadey, D.Y.A., et al., *Antibody Targeting GRP78 Enhances the Efficacy of Radiation Therapy in Human Glioblastoma and Non-Small Cell Lung Cancer Cell Lines and Tumor Models.* Clin Cancer Res, 2017. **23**(10): p. 2556-2564.
37. Glatt, D.M., et al., *The Interplay of Antigen Affinity, Internalization, and Pharmacokinetics on CD44-Positive Tumor Targeting of Monoclonal Antibodies.* Mol Pharm, 2016. **13**(6): p. 1894-903.
38. Gefen, T., et al., *A TIM-3 Oligonucleotide Aptamer Enhances T Cell Functions and Potentiates Tumor Immunity in Mice.* Mol Ther, 2017. **25**(10): p. 2280-2288.
39. Lopes, A.M., K.Y. Chen, and D.T. Kamei, *A transferrin variant as the targeting ligand for polymeric nanoparticles incorporated in 3-D PLGA porous scaffolds.* Mater Sci Eng C Mater Biol Appl, 2017. **73**: p. 373-380.
40. Lee, J.Y., et al., *Dual CD44 and folate receptor-targeted nanoparticles for cancer diagnosis and anticancer drug delivery.* J Control Release, 2016. **236**: p. 38-46.

41. Kopecek, J., L. Sprincl, and D. Lim, *New types of synthetic infusion solutions. I. Investigation of the effect of solutions of some hydrophilic polymers on blood.* J Biomed Mater Res, 1973. **7**(2): p. 179-91.
42. Duncan, R., J.B. Lloyd, and J. Kopecek, *Degradation of side chains of N-(2-hydroxypropyl) methacrylamide copolymers by lysosomal enzymes.* Biochem Biophys Res Commun, 1980. **94**(1): p. 284-90.
43. Etrych, T., et al., *Conjugates of doxorubicin with graft HPMA copolymers for passive tumor targeting.* J Control Release, 2008. **132**(3): p. 184-92.
44. Etrych, T., et al., *Biodegradable star HPMA polymer-drug conjugates: Biodegradability, distribution and anti-tumor efficacy.* J Control Release, 2011. **154**(3): p. 241-8.
45. Korcakova, L., et al., *Asimple test for immunogenicity of colloidal infusion solutions-the draining lymph node activation.* Z Immunitatsforsch Exp Klin Immunol, 1976. **151**(3): p. 219-23.
46. Rihova, B., et al., *Immunogenicity of N-(2-hydroxypropyl)-methacrylamide copolymers--potential hapten or drug carriers.* Folia Microbiol (Praha), 1983. **28**(3): p. 217-27.
47. Rihova, B., et al., *Effect of the chemical structure of N-(2-hydroxypropyl)methacrylamide copolymers on their ability to induce antibody formation in inbred strains of mice.* Biomaterials, 1984. **5**(3): p. 143-8.
48. Rihova, B., et al., *Biocompatibility of N-(2-hydroxypropyl) methacrylamide copolymers containing adriamycin. Immunogenicity, and effect on haematopoietic stem cells in bone marrow in vivo and mouse splenocytes and human peripheral blood lymphocytes in vitro.* Biomaterials, 1989. **10**(5): p. 335-42.
49. Volfova, I., et al., *Biocompatibility of Biopolymers.* J Bioact Compat Polym, 1992. **7**(175-190).
50. Kopecek, J., et al., *Controlled release of drug model from N-(2-hydroxypropyl)-methacrylamide copolymers.* Ann N Y Acad Sci, 1985. **446**: p. 93-104.
51. Kovar, M., et al., *In vitro and in vivo effect of HPMA copolymer-bound doxorubicin targeted to transferrin receptor of B-cell lymphoma 38C13.* J Drug Target, 2002. **10**(1): p. 23-30.
52. Duncan, R., et al., *Pinocytic uptake and intracellular degradation of N-(2-hydroxypropyl)methacrylamide copolymers. A potential drug delivery system.* Biochim Biophys Acta, 1981. **678**(1): p. 143-50.

53. Omelyanenko, V., et al., *Targetable HPMA copolymer-adriamycin conjugates. Recognition, internalization, and subcellular fate.* J Control Release, 1998. **53**(1-3): p. 25-37.
54. Hovorka, O., et al., *HPMA based macromolecular therapeutics: internalization, intracellular pathway and cell death depend on the character of covalent bond between the drug and the peptidic spacer and also on spacer composition.* J Drug Target, 2006. **14**(6): p. 391-403.
55. Warburg, O., *On respiratory impairment in cancer cells.* Science, 1956. **124**(3215): p. 269-70.
56. Tannock, I.F. and D. Rotin, *Acid pH in tumors and its potential for therapeutic exploitation.* Cancer Res, 1989. **49**(16): p. 4373-84.
57. Rihova, B., et al., *Induction of systemic antitumour resistance with targeted polymers.* Scand J Immunol, 2005. **62 Suppl 1**: p. 100-5.
58. Rihova, B., et al., *Cytotoxicity and immunostimulation: double attack on cancer cells with polymeric therapeutics.* Trends Biotechnol, 2009. **27**(1): p. 11-7.
59. Etrych, T., et al., *New HPMA copolymers containing doxorubicin bound via pH-sensitive linkage: synthesis and preliminary in vitro and in vivo biological properties.* J Control Release, 2001. **73**(1): p. 89-102.
60. Rihova, B., et al., *Doxorubicin bound to a HPMA copolymer carrier through hydrazone bond is effective also in a cancer cell line with a limited content of lysosomes.* J Control Release, 2001. **74**(1-3): p. 225-32.
61. Rihova, B., et al., *Doxorubicin release is not a prerequisite for the in vitro cytotoxicity of HPMA-based pharmaceuticals: in vitro effect of extra drug-free GlyPheLeuGly sequences.* J Control Release, 2008. **127**(2): p. 110-20.
62. Ulbrich, K., et al., *Synthesis of biodegradable polymers for controlled drug release.* Ann N Y Acad Sci, 1997. **831**: p. 47-56.
63. Duncan, R., et al., *Anticancer agents coupled to N-(2-hydroxypropyl)methacrylamide copolymers. II. Evaluation of daunomycin conjugates in vivo against L1210 leukaemia.* Br J Cancer, 1988. **57**(2): p. 147-56.
64. Jelinkova, M., et al., *Targeting of human and mouse T-lymphocytes by monoclonal antibody-HPMA copolymer-doxorubicin conjugates directed against different T-cell surface antigens.* J Control Release, 1998. **52**(3): p. 253-70.
65. Etrych, T., et al., *HPMA copolymer conjugates of paclitaxel and docetaxel with pH-controlled drug release.* Mol Pharm, 2010. **7**(4): p. 1015-26.

66. Ulbrich, K., et al., *Antibody-targeted polymer-doxorubicin conjugates with pH-controlled activation.* J Drug Target, 2004. **12**(8): p. 477-89.
67. Ulbrich, K., et al., *Targeted Drug Delivery with Polymers and Magnetic Nanoparticles: Covalent and Noncovalent Approaches, Release Control, and Clinical Studies.* Chem Rev, 2016. **116**(9): p. 5338-431.
68. Pechar, M., et al., *Coiled coil peptides and polymer-peptide conjugates: synthesis, self-assembly, characterization and potential in drug delivery systems.* Biomacromolecules, 2014. **15**(7): p. 2590-9.
69. Duncan, R., *Development of HPMA copolymer-anticancer conjugates: clinical experience and lessons learnt.* Adv Drug Deliv Rev, 2009. **61**(13): p. 1131-48.
70. Krinick, N.L., et al., *A polymeric drug delivery system for the simultaneous delivery of drugs activatable by enzymes and/or light.* J Biomater Sci Polym Ed, 1994. **5**(4): p. 303-24.
71. Krakovicova, H., T. Etrych, and K. Ulbrich, *HPMA-based polymer conjugates with drug combination.* Eur J Pharm Sci, 2009. **37**(3-4): p. 405-12.
72. Lammers, T., et al., *Simultaneous delivery of doxorubicin and gemcitabine to tumors in vivo using prototypic polymeric drug carriers.* Biomaterials, 2009. **30**(20): p. 3466-75.
73. Kostkova, H., et al., *HPMA copolymer conjugates of DOX and mitomycin C for combination therapy: physicochemical characterization, cytotoxic effects, combination index analysis, and anti-tumor efficacy.* Macromol Biosci, 2013. **13**(12): p. 1648-60.
74. Etrych, T., et al., *Polymer conjugates of doxorubicin bound through an amide and hydrazone bond: Impact of the carrier structure onto synergistic action in the treatment of solid tumours.* Eur J Pharm Sci, 2014. **58**: p. 1-12.
75. Rejmanova, P., et al., *Stability in rat plasma and serum of lysosomally degradable oligopeptide sequences in N-(2-hydroxypropyl) methacrylamide copolymers.* Biomaterials, 1985. **6**(1): p. 45-8.
76. Vasey, P.A., et al., *Phase I clinical and pharmacokinetic study of PK1 [N-(2-hydroxypropyl)methacrylamide copolymer doxorubicin]: first member of a new class of chemotherapeutic agents-drug-polymer conjugates. Cancer Research Campaign Phase I/II Committee.* Clin Cancer Res, 1999. **5**(1): p. 83-94.
77. Lammers, T., et al., *Effect of intratumoral injection on the biodistribution and the therapeutic potential of HPMA copolymer-based drug delivery systems.* Neoplasia, 2006. **8**(10): p. 788-95.

78. Sirova, M., et al., *Treatment with HPMA copolymer-based doxorubicin conjugate containing human immunoglobulin induces long-lasting systemic anti-tumour immunity in mice.* Cancer Immunol Immunother, 2007. **56**(1): p. 35-47.
79. Seymour, L.W., et al., *Phase II studies of polymer-doxorubicin (PK1, FCE28068) in the treatment of breast, lung and colorectal cancer.* Int J Oncol, 2009. **34**(6): p. 1629-36.
80. Sirova, M., et al., *Preclinical evaluation of linear HPMA-doxorubicin conjugates with pH-sensitive drug release: efficacy, safety, and immunomodulating activity in murine model.* Pharm Res, 2010. **27**(1): p. 200-8.
81. Choi, W.-M., et al., *Synthesis of HPMA Copolymer Containing Adriamycin Bound via an Acid-Labile Spacer and its Activity toward Human Ovarian Carcinoma Cells* J Bioact Compat Polym, 1999. **14**(6): p. 447-456.
82. DuPage, M., et al., *Expression of tumour-specific antigens underlies cancer immunoediting.* Nature, 2012. **482**(7385): p. 405-9.
83. Cheung, A.F., et al., *Regulated expression of a tumor-associated antigen reveals multiple levels of T-cell tolerance in a mouse model of lung cancer.* Cancer Res, 2008. **68**(22): p. 9459-68.
84. Smyth, M.J., N.Y. Crowe, and D.I. Godfrey, *NK cells and NKT cells collaborate in host protection from methylcholanthrene-induced fibrosarcoma.* Int Immunol, 2001. **13**(4): p. 459-63.
85. Street, S.E., E. Cretney, and M.J. Smyth, *Perforin and interferon-gamma activities independently control tumor initiation, growth, and metastasis.* Blood, 2001. **97**(1): p. 192-7.
86. Street, S.E., et al., *Suppression of lymphoma and epithelial malignancies effected by interferon gamma.* J Exp Med, 2002. **196**(1): p. 129-34.
87. Julyan, P.J., et al., *Preliminary clinical study of the distribution of HPMA copolymers bearing doxorubicin and galactosamine.* J Control Release, 1999. **57**(3): p. 281-90.
88. Seymour, L.W., et al., *Hepatic drug targeting: phase I evaluation of polymer-bound doxorubicin.* J Clin Oncol, 2002. **20**(6): p. 1668-76.
89. Rihova, B., et al., *Antiproliferative effect of a lectin- and anti-Thy-1.2 antibody-targeted HPMA copolymer-bound doxorubicin on primary and metastatic human colorectal carcinoma and on human colorectal carcinoma transfected with the mouse Thy-1.2 gene.* Bioconjug Chem, 2000. **11**(5): p. 664-73.
90. Wroblewski, S., et al., *Biorecognition of HPMA copolymer-lectin conjugates as an indicator of differentiation of cell-surface glycoproteins in development, maturation,*

and diseases of human and rodent gastrointestinal tissues. J Biomed Mater Res, 2000. **51**(3): p. 329-42.

91. Kunath, K., et al., *HPMA copolymer-anticancer drug-OV-TL16 antibody conjugates. 3. The effect of free and polymer-bound adriamycin on the expression of some genes in the OVCAR-3 human ovarian carcinoma cell line.* Eur J Pharm Biopharm, 2000. **49**(1): p. 11-5.
92. Jelinkova, M., et al., *Starlike vs. classic macromolecular prodrugs: two different antibody-targeted HPMA copolymers of doxorubicin studied in vitro and in vivo as potential anticancer drugs.* Pharm Res, 2003. **20**(10): p. 1558-64.
93. Etrych, T., et al., *Star-shaped immunoglobulin-containing HPMA-based conjugates with doxorubicin for cancer therapy.* J Control Release, 2007. **122**(1): p. 31-8.
94. Kovar, M., et al., *Star structure of antibody-targeted HPMA copolymer-bound doxorubicin: a novel type of polymeric conjugate for targeted drug delivery with potent antitumor effect.* Bioconjug Chem, 2002. **13**(2): p. 206-15.
95. Rihova, B., et al., *Cytostatic and immunomobilizing activities of polymer-bound drugs: experimental and first clinical data.* J Control Release, 2003. **91**(1-2): p. 1-16.